Novel Mouse Models for Use in IL-17A and Th17 Research

Dissertation
Zur Erlangung des Grades
Doktor der Naturwissenschaft

Am Fachbereich Biologie
Der Johannes Gutenberg-Universität Mainz

Andrew Lewis Croxford
Geb. am 1. Januar 1981 in New York, USA

Mainz, 2009

Abbreviations

Ab	antibody
APC	antigen presenting cell or allophycocyanin
approx.	approximately
BAC	bacterial artificial chromosome
Bio	biotinylated
b-ME	b-mercaptoethanol
bp	base pair
BSA	bovine serum albumin
°C	temperature in degrees celsius
CD	cluster of differentiation
CFA	Complete Freund's Adjuvant
cDNA	complementary DNA
CNS	central nervous system
cpm	counts per minute
Cre	site-specific recombinase (causes recombination)
d	day/s
DC	dendritic cell
DMEM	Dulbecco's modified Eagle medium
DNA	desoxyribonucleic acid
DNFB	Dinitroflorobenzene
dNTP	desoxynucleotide triphosphate
DTT	dithiothritole
Dtx	Diphtheria toxin
EAE	experimental autoimmune encephalomyelitis
EDTA	ethylene-diaminetetraacetic acid
ELISA	enzyme-linked immuno-sorbent assay
ES	embryonic stem
EtOH	ethanol
FACS	fluorescence activated cell sorting
FCS	fetal calf serum
Fig.	Figure
FITC	fluorescein isothiocyanate
Flp	site-specific recombinase, product of yeast *FLP1*-gene
FoxP3	forkhead box protein 3
FRT	Flp recombination target
g	gram
h	hour/s
HEPES	N-2-hydroxyethylpiperazine-N'-2-ethansulfonic acid
i.p.	intraperitoneally
i.v.	intravenously
IFN-γ	interferon-γ
Ig	immunoglobulin
IL	interleukin
kb	kilobase pair
l	liter
LN	lymph node/s
loxP	recognition sequence for Cre (locus of X-ing over of phage P1)
LPS	lipopolysaccharide

Ly6C	lymphocyte antigen 6 complex, locus C
M	molar
MACS	magnetic activated cell sorter
MFI	mean fluorescence intensity
$MgCl_2$	magnesium chloride
MHC	major histocompatibility complex
min	minute
ml	milliliter
mM	millimolar
MOG	myelin oligodendrocyte glycoprotein
mRNA	messenger RNA
MS	multiple sclerosis
MΦ	macrophage/s
NaCl	sodium chloride
n	nano
NaOH	sodium hydroxide
neo	neomycin resistance gene
o/n	over night
OD	optical density
PBS	phosphate buffered saline
PCR	polymerase chain reaction
PE	phycoerythrine
Ptx	Pertussis toxin
RAG	recombinase activating gene
RNA	ribonucleic acid
rpm	revolutions per minute
RT	room temperature
sec	seconds
SA	streptavidine
s.c.	subcutaneously
sc	spinal cord
SDS	sodium dodecyl sulfate
SN	supernatant
SSC	sodium chloride/sodium citrate buffer
TAE	Tris-acetic acid-EDTA buffer
TAM	Tamoxifen
Taq	polymerase from *Thermus aquaticus*
TCR	T cell receptor
TE	Tris-EDTA buffer
TEC	thymic epithelial cell
tg	transgenic
TGF-β	transforming growth factor-β
Tregs	regulatory T cells
Tris	2-amino-2-(hydroxymethyl-)1,3-propandiole
U	units
UV	ultraviolett
V	volts
vs	versus
v/v	volume per volume
w/v	weight per volume
WT	wild type

µl	microliter
µM	micromolar
3’	three prime end of DNA sequences
5’	five prime end of DNA sequences

1 Introduction

1.1 EAE, an animal model for MS

Experimental autoimmune encephalomyelitis (EAE) is one of the most intensively studied animal models focusing on autoimmune neuroinflammation. EAE has been established successfully in a number of model species, and is generally thought to share many physiological and pathological aspects with the human autoimmune condition, multiple sclerosis (MS). The most striking similarities are the destruction of myelin sheaths protecting nerve fibres, the distribution of CNS lesions throughout the CNS in both kinetic and location, the predominantly perivascular lesion development, partial remyelination and presence of immunoglobulins in the CNS and CSF (Baxter, 2007).

EAE is typically initiated by priming the immune response with mylein-derived antigens. Myelin-specific T cells must be activated in the periphery, migrate into the CNS and be reactivated by APCs presenting self-antigen. The anatomy of the CNS itself offers significant protection against this process, as cellular infiltration is strictly inhibited by the blood-brain-barrier (BBB), which surrounds the parenchymal venules. Also the blood cerebro-spinal fluid (CSF) barrier, which surrounds the choroid plexus and meningeal venules, blocks another potential route of entry for pathogenic cells (Reboldi et al., 2009). However, activated and/or memory T cells are able to gain access to the CNS based on expression of chemokine receptors and adhesion molecules such as CCR6 and VLA-4 (Ransohoff et al., 2003; Reboldi et al., 2009).

Infiltration in EAE is first detected in the subarachnoid space (SAS), where T cells were shown to re-engage self antigen on MHC-class II+ APCs, after which formations of T cell aggregates were shown to form (Kivisakk et al., 2009). This reactivation is followed by the activation of perivascular endothelial cells, which encourages T cell infiltration into the perivascular space. This process triggers microglial activation, axonal damage and upregulation of adhesion molecules on parenchymal vasculature in a CNS region morphologically distinct from the initial site of T cell infiltration (Brown and Sawchenko, 2007).

1.2 The T helper cell subset paradigm

T helper cells are essential mediators of immune responses. Their major function is to coordinate other branches of the immune system by the timely secretion of cell signaling molecules. Upon interaction with TCR cognate antigen presented by an activated antigen presenting cell (APC), $CD4^+$ T cells are able to differentiate into a selection of subsets including the well established Th1 and Th2 cells, and the more recently identified induced regulatory T cells (iTregs), follicular T helper cells (Tfh) and Th17 cells. This decision is made for the naive cell based on its surrounding cytokine environment at the point of priming. The process of initiating a T cell effector cascade must be tightly regulated for efficient control of infections, while simultaneously avoiding the development of autoimmunity and/or immunopathology.

Twenty years ago, an immunological dogma was put into place by Mosmann and Coffman who initially described the stable differentiation of naive T cells into distinct effector lineages defined by their cytokine secretion patterns (Mosmann et al., 1986). This specific cytokine secretion was hypothesized to be mutually exclusive, with cytokines from one subset inhibiting differentiation of another, thus propogating differentiation of its own species. Much of the current thinking surrounding T helper cell subsets is still derived from these landmark experiments, which imply that naive T cells can differentiate independently into each lineage, and that each lineage has a unique and transcriptionally-stable gene expression signature. Interleukin-17 (IL-17)-expressing T cells are now widely considered to have fulfilled the criteria for acceptance as a distinct T helper cell subset. These cells are now termed Th17 cells and have been the source of a recent burst of interest within the immunology community. Th17 cells do not only differ from other T helper subsets because of gene regulation and expression, but also diverge significantly with respect to biological function.

1.3 Differentiation of Th17 cells

Three independent laboratories identified a combination of TGF-β and IL-6 to be sufficient to induce IL-17A expression from naive T cells (Bettelli et al., 2006; Mangan et al., 2006; Veldhoen et al., 2006). The discovery was made somewhat unexpectedly while trying to identify soluble factors capable of inhibiting Foxp3 expression upon

activation in the presence of TGF-β (Thomas Korn, personal communication). This is an interesting paradigm, given that both TGF-β and IL-6 are thought to have largely opposing functions, but synergize to promote proinflammatory IL-17 production from T cells. This is also the case in human T cells, where TGF-β and IL-6 have also been shown to be crucial for the development of Th17 cells from naive T cells (Manel et al., 2008; Yang et al., 2008a). Indeed, disrupting the IL-6 signaling cascade, either at the receptor or ligand, will result in an inhibition of Th17 differentiation. Depletion of regulatory T cells, however, was able to overcome the resistance to EAE observed in both IL-$6^{-/-}$ and $gp130^{-/-}$ T cells, which was credited to a partial restoration in Th17 differentiation (Korn et al., 2007a; Korn et al., 2008). These findings implied that another factor was capable of inducing Th17 cells in combination with TGF-β. After returning to initial experiments to identify factors inhibiting Foxp3 expression, IL-21 in combination with TGF-β was identified as an alternative pathway to IL-6-mediated Th17 differentiation (Korn et al., 2007a), and was subsequently proposed to be the mechanism by which Th17 cells arise in the absence of IL-6 signaling (Korn et al., 2008).

1.4 Transcriptional control of Th17 cells

Regulatory cytokines modulate Th1 and Th2 differentiation via STAT family proteins that regulate target gene transcription and lineage-specific transcription factors. Th1 differentiation is known to be crucially dependent on STAT1 and STAT4, which are downstream of IFN-γ and IL-12 signaling, respectively, and upregulate the Th1 master regulator T-bet (Afkarian et al., 2002). During Th2 differentiation, IL-4 signals via STAT6, which regulates GATA-binding protein 3 (GATA-3). STAT1, STAT4 and STAT6 are all, however, dispensable for Th17 cells, strengthening the claim that Th17 cells represent a distinct T helper cell subset (Harrington et al., 2005).

In recent years, there has been swift progress in identifying the transcription factors that are necessary for Th17 differentiation. Like Th1 and Th2 cells, Th17 cells also have unique transcription factors, which regulate their differentiation. RORγ and RORα are both members of the retinoic-acid-receptor-related orphan nuclear hormone receptor family (Jetten, 2004). RORα-deficiency in T cells only resulted in a minimal decrease in IL-17A and IL-23R expression, and as such was considered to be a minor

player in Th17 generation (Yang et al., 2008d). An isoform of RORγ, termed RORγt, is solely expressed in immune cells (Eberl and Littman, 2003). Ivanov et al. were able to show that RORγt was the master regulator behind Th17 differentiation (Ivanov et al., 2006). In this study, RORγt was induced by TGF-β and IL-6, and overexpression of RORγt was able to induce *de novo* Th17 differentiation if both Th1 and Th2 polarizing cytokines were neutralized. RORγt-deficient T cells are also highly deficient in IL-17A and IL-17F production in response to TGF-β, IL-6 and IL-21 (Nurieva et al., 2007; Zhou et al., 2007). In addition to RORγt, interferon regulatory factor-4 (IRF4)-deficiency also completely abolishes Th17 differentiation. *Irf4*-/- T cells also show a significant decrease in RORγt expression in response to TGF-β and IL-6 (Brustle et al., 2007), and as such place IRF-4 function upstream of RORγt. Collectively these publications identified RORγt and IRF-4 as key regulators of Th17 cell differentiation.

1.5 Foxp3 and RORγt

$Foxp3^+$ regulatory T cells (T-regs) are essential for the maintenance of peripheral tolerance. Deletion of $Foxp3^+$ T-regs results in multiorgan autoimmunity (Kim et al., 2007). Naturally occurring $Foxp3^+$ T-regs are generated in the thymus (Fontenot et al., 2005) and are introduced into the peripheral immune compartment during early postnatal development. In the peripheral immune compartment, IL-2 is an essential cytokine for the proliferation of T-regs, whereas TGF-β is important for their maintenance (Knoechel et al., 2005). Apart from naturally occurring $CD4^+CD25^+Foxp3^+$ T-regs, several subsets of T-regs have been described that are induced from naïve conventional T cells in the peripheral immune compartment under specific circumstances (Bluestone and Abbas, 2003). However, under physiological conditions, it is believed that induced $Foxp3^+$ T-regs (iTregs) are generated mainly in the gut and possibly in diverse immunological niches that contain high local concentrations of TGF-β and are colonized by specialized types of antigen-presenting cells (Coombes et al., 2007; Kamanaka et al., 2006).

Recently, a reciprocal developmental relationship between $Foxp3^+$ T-regs and Th17 was discovered. TGF-β triggers the expression of Foxp3 in naïve T cells, whereas IL-6 inhibits the TGF-β-driven expression of Foxp3, and TGF-β plus IL-6 together induce RORγt, triggering the developmental program of Th17 cells (Bettelli et

al., 2006). In the absence of IL-6, IL-21, which is a member of the IL-2 family of cytokines, can 'stand in' for IL-6, and activation with TGF-β plus IL-21 might constitute an alternative pathway to induce Th17 cells (Korn et al., 2007a). Together, these findings suggested that IL-6 and IL-21 are switch factors between the induction of T-regs and Th17 cells.

IL-6 is a potent factor to switch immune responses from the induction of Foxp3 T-regs to pathogenic Th17 cells *in vivo*. There is accumulating molecular evidence that a single naïve T cell can develop into both a functional T-reg cell and an IL-17-producing T cell (Bettelli et al., 2006). TGF-β is necessary to induce the expression of both Foxp3, the master transcription factor of T-regs, and RORγt, the essential transcription factor of Th17 cells (Manel et al., 2008). Although necessary for the expression of both Foxp3 and RORγt, TGF-β enhances the function of Foxp3 but inhibits the function of RORγt (Manel et al., 2008). Only when additional signaling of pro-inflammatory cytokines such as IL-6 or IL-21 is operational, the TGF-β-mediated functional inhibition of RORγt is released, and Th17 cells are induced.

1.6 IL-23

After initial differentiation of Th17 cells in the presence of TGF-β and IL-6 and/or IL-21, signaling events take place in mature Th17 cells to ensure that the proinflammatory phenotype is maintained during an immune response. IL-23, an APC derived cytokine of the IL-12 cytokine family, was demonstrated to promote the production of IL-17 from primed T lymphocytes (Aggarwal et al., 2003). It was further reported that IL-23 was key to expanding IL-17-expressing $CD4^+$ T cells, and also that *il23a*-/- mice are fully resistant to EAE and also lack T cells capable of expressing IL-17 (Cua et al., 2003; Langrish et al., 2005; Murphy et al., 2003). It was then proposed that IL-23 was a factor capable of expanding Th17 cells. It was shown in these same publications that IL-23-polarized cells express high levels of IL-17A, IL-17F and TNF-α. Further evidence comes from the finding that transgenic expression of RORγt in naive T cells is sufficient to upregulate *il23r* expression (Ivanov et al., 2006), implying that IL-23R-signaling is a critical event downstream of initial Th17 differentiation. IL-23 also has

been shown to play a role in proliferation at inflammatory sites, and be essential for Th17 accumulation in the inflamed CNS (Gyulveszi et al., 2009).

1.7 IL-17A

IL-17A is a disulphide linked homodimeric glycoprotein consisting of 155 amino acids. It was orignally cloned in 1993 (Rouvier et al., 1993) and was termed CTLA-8, before being renamed IL-17. After homology-based cloning and the discovery of five additional family members (IL-17B-F), IL-17 was once again renamed to IL-17A. IL-17A binds it receptor and thus exerts its function as a homodimer, with a combined molecular weight of 35kDa. Yao et al. described expression of IL-17RA, an IL-17R family member, on epithelial and endothelial cells and other mesenchymal cells such as fibroblasts (Yao et al., 1995). IL-17RA can form heterodimeric signaling units with IL-17RC, which gives rise to a potentially complex IL-17 signaling mechanism with respect to binding affinity and diverging cascades. Indeed, IL-17A has been demonstrated more than a decade ago to activate both the nuclear factor-κB (NFκB) and mitogen-activated protein kinase (MAPK) pathways (Shalom-Barak et al., 1998). Dependance on the NFκB pathway is further demonstrated by the tumor-necrosis factor receptor (TNFR)-associated factor 6 (TRAF-6)-dependent expression of IL-6 in response to IL-17 signaling in mouse embryonic fibroblast cells (Schwander et al, 2000). In addition, the adaptor protein ACT1 was found to be essential for IL-17RA downstream signaling due to its involvement in NFκB activation (Chang et al., 2006). ACT1-deficient mice were also resistant to EAE, although this may not be due to IL-17 signaling deficiencies.

Park et al. were able to demonstrate that genes encoding numerous chemokines were upregulated after *in vitro* stimulation of mouse fibroblasts with IL-17A. These include CC-chemokine ligand 2 (CCL2), CCL7, CCL20 and CXC-chemokine ligand 1 (CXCL1), and also matrix metalloproteinases MMP3 and MMP13 (Park et al., 2005). Expression of these genes after IL-17A stimulation is further augmented by addition of TNF-α to culture conditions, and as such TNF-α and IL-17A were shown to synergise to induce expression of proinflammatory chemokines (Ruddy et al., 2004).

1.8 IL-17F

Of all the family members, IL-17F has the highest degree of peptide sequence homology with IL-17A at the amino acid level (55%). Interestingly, genes encoding

IL-17A and IL-17F are situated only 46kb apart on chorosome 1 in the mouse, and chromosome 6 in the human genome. Considering the similar expression profile of IL-17A and F from murine T cells (Croxford et al., 2009; Haak et al., 2009), some degree of mutual control of expression can be anticipated at these loci.

Although considerable knowledge has been generated surrounding IL-17A, relatively little is known about IL-17F. IL-17F was shown to be expressed by Th17 cells proliferating in the presence of IL-23 (Langrish et al, 2005). IL-17F is also known to be expressed by Th17 and Tc17 cells *in vitro* (Croxford et al., 2009; Veldhoen et al., 2006). Some limited data exists showing that T cells can express IL-17F and not IL-17A, although the role of these single expresser cells is unknown, and the relationship between IL-17A and IL-17F will need to be studied in further detail.

Like IL-17A, IL-17F expression has been linked to upregulation of cytokines, chemokines and adhesion molecules in human epithelial cells and fibroblasts. It is not clear why T cells would co-express molecules of such similar function. However, a heterodimeric cytokine consisting of IL-17A and IL-17F has been described in mouse and human Th17 cells (Chang and Dong, 2007; Wright et al., 2007). This adds another layer of complexity to the mechanisms and potential redundancies involved in IL-17F signaling. The receptor for IL-17F has also remained elusive. Recently IL-17RC was shown to receive IL-17F (Kuestner et al., 2007), though IL-17A was also shown to bind this receptor.

1.9 IL-17A Signaling and Tissue Inflammation

Neutrophils are produced in the bone marrow, circulate in the blood, and are rapidly recruited to sites of infection in response to a variety of chemoattractants produced by inflamed tissues (Baggiolini, 1998; Scapini et al., 2000). Neutrophils are the most abundant nucleated cell in the blood and play a crucial role in immune responses to pathogens. Neutrophils are best known for their role in phagocytosis and killing of extracellular bacteria; however, they can provide protection against a diverse set of pathogens, and do so by performing a variety of different functions (Appelberg, 2007; Nathan, 2006). These functions include tissue remodeling, antigen presentation, recruiting other blood cells, and polarizing T cell responses (Beauvillain et al., 2007; Megiovanni et al., 2006; Pesce et al., 2008; Tvinnereim et al., 2004). For example, neutrophils play an important protective role during infection with the intracellular

protozoan parasite Toxoplasma gondii (Bennouna et al., 2003; Bliss et al., 2001) (Denkers et al., 2004) in spite of the fact that the parasite is relatively resistant to killing by neutrophils (Channon et al., 2000).

The majority of available literature suggests a role for IL-17A and IL-17F in coordinating local tissue inflammation via the induction of proinflammatory chemokines and neutrophil-mobilizing cytokines. Substantial numbers of reports suggest a critical role for IL-17 family members in host defense and neutrophil recruitment. This is at least in part due to release of CXCL1, a potent attractant of neutrophils, in direct response to IL-17A signaling (Kolls et al, 2003). With respect to host defense against extracellular pathogens, IL-17A was shown to be induced in a time- and dose-dependent fashion during an immune response to Klebsiella pneumoniae (Happel et al., 2003; Ye et al., 2001a). Conversely, mice genetically deficient for the IL-17R succumb to a pulmonary challenge with the same bacteria (Ye et al., 2001b). This report documented a dramatic decrease in neutrophil recruitment in the infected lung, reduced granulopoietic output from the bone marrow and significantly reduced production of local G-CSF. In support of this data, antibody-mediated neutralization of IL-17A was able to reduce accumulation of neutrophils into the bronchoalveolar space after administration of lipopolysaccharide (LPS) (Ferretti et al., 2003; Miyamoto et al., 2003).

Recent evidence has shown clearly that the cellular source of IL-17A is largely restricted to T lymphocytes. Data obtained from SCID mice (lacking T cells) or mice depleted of T cells using antibodies have a 90% reduction of IL-17A concentrations in lung tissue after pulmonary administration of LPS (Ferretti et al., 2003; Happel et al., 2003). The production of IL-17A and IL-17F by T cells is regulated proximally by IL-23 produced by dendritic cells after TLR activation, and as such places IL-17A and IL-17F at a unique interface between adaptive and innate immune responses.

1.10 IL-17A and autoimmunity

Th1 responses that have escaped normal regulatory mechanisms have long been linked to organ-specific autoimmunity. Collectively, much evidence exists for the association of Th1 cells with autoimune pathology. For example, IFN-γ expression in the CNS and synovial fluid linked Th1 cells to EAE and collagen-induced arthritis (CIA), respectively. MOG-specific TCR transgenic Th1 cells are able to adoptively transfer

EAE. T-bet-deficient mice are also fully resistant to EAE. In addition to this, neutralizing IL-12p40 with monoclonal antibodies reduced severity of EAE and CIA. Taken together, these data strongly imply that autoantigen-specific Th1 cells can be autopathogenic.

Some evidence exists linking IL-17A to sites of autoimmune inflammation. For example, patients with inflammatory bowel disease (IBD) show elevated levels of IL-17A mRNA and protein in the intestinal mucosa (Fujino et al., 2003). With respect to arthritis, IL-17A is responsible for the release of potentially destructive proteases. IL-17A is responsible for the expression of MMP-1 in the joint synovium of rheumatoid arthritis patients (Chabaud et al., 2000). Finally, IL-17A was shown to be upregulated in CNS lesions of multiple sclerosis patients (Lock et al., 2002). One should note, however, that these are correlative relationships and the pathogenicity of IL-17A has been called into question (Haak et al., 2009), and in some cases IL-17A was even shown to play a protective role in autoimmune inflammation (O'Connor et al., 2009).

1.11 G-Protein signalling and autoimmunity

Lymphocyte mobility and homing is modulated by the chemoattractant receptor subfamily of G protein-coupled receptors (GPCRs). GPCR-dependent chemokine signaling plays an important role in animal models of disease that are dependent on T lymphocyte migration into sites of inflammation, such as experimental autoimmune encephalomyelitis (EAE), dextran sodium-sulphate (DSS)-induced colitis and acute colitis associated with graft-versus host disease (GVHD) (Dutt et al., 2005; Eijkelkamp et al., 2007a; Eijkelkamp et al., 2007b; Vroon et al., 2005). T cells deficient in classical homing molecules such as CD62L are known to inefficiently migrate to inguinal, axilliary and cervical lymph nodes (Wagner et al., 1998). However, artificial inhibition of G-protein signaling in pertussis toxin (Ptx)-treated T cells also results in a clear reduction of T cell motility within the lymph node (Okada and Cyster, 2007). Thus, enough evidence exists to demonstrate an overlap between G-protein signaling and migration of potentially pathogenic T cells to and from the lymph nodes, and subsequently into sites of inflammation.

In general, GPCR are regulators of various specialized cell functions including chemotactic cell migration of phagocytic cells and lymphocytes (Lombardi et al., 2002). A signaling event induced by an agonist binding its GPCR is quickly inhibited

by phosphorylation of the GPCR by a GPCR kinase (GRK) (Ferguson, 2001), resulting in rapid decoupling of the GPCR and bound G-protein heterotrimers. A much-accelerated onset in EAE was demonstrated in mice with genetic disruption of GRK2 (Vroon et al., 2005), a GRK highly expressed in activated T cells (De Blasi et al., 1995), which fits with the notion that mice with heightened migration sensitivities will develop stronger pathogenesis in disease models dependent on T cell migration. Proinflammatory cytokines in patients with RA are also known to induce a down-regulation of GRK2 expression in PBMC, which supports a model of inflammation-induced GPCR-signaling attenuation (Lombardi et al., 1999).

1.12 Aim of this thesis

Th17 cells have emerged as a proinflamatory cell type with strong links to autoimmunity and immunopathology. The aims of this thesis are two-fold; Firstly, generation of a novel mouse model that allows *in vivo* and/or *ex vivo* observation and manipulation of Th17 cells. Secondly, to generate a mouse model capable of conditionally overexpressing the hallmark Th17 cytokine, IL-17A. Given the expertise and experience in our lab with respect to conditional gene targeting, Cre-LoxP-mediated approaches were chosen and utilized to achieve this goal in both mouse models. The resulting strains and the knowledge generated from their useage are discussed in this work. Furthermore, the recently generated IL-6Rα conditional allele allows for ablation of IL-6 signaling in a cell type-specific manner. We wanted to analyze the role of IL-6 signaling with respect to EAE pathogenesis and development of pathogenic Th17 cells, and the results generated are published in this work.

2 MATERIALS AND METHODS

2.1 Chemicals and Biological Material

Chemicals were purchased from Sigma-Aldrich (Steinheim), Fluka Chemie (Deisenhofen), Merck (Darmstadt) or AppliChem (Darmstadt) unless stated otherwise. Solutions were prepared with double distilled water (ddH_2O). Bacterial media were autoclaved prior to use. Sterility of solutions and chemicals used in cell culture was maintained by working under a sterile hood (Heraeus, Germany).

Name of chemical	**Supplier**
β-Mercaptoethanol (β-ME)	Fluka Chemie GmbH, Switzerland
Acetone	Merck, Darmstadt
Agar	Gibco Life Technologies GmbH, Karlsruhe
Agarose, electrophoresis grade	AppliChem, Darmstadt
Ampicillin	Sigma-Aldrich, Steinheim
L-Arabinose	Sigma-Aldrich, Steinheim
Bovine serum albumin (BSA)	Sigma-Aldrich, Steinheim
Calcium chloride	Sigma-Aldrich, Steinheim
Chloroform	Merck, Darmstadt
2'-Deoxyguanosine Monohydrate	AppliChem, Darmstadt
Diethylpyrocarbonate (DEPC)	AppliChem, Darmstadt
Dextran sulfate	AppliChem, Darmstadt
Dithiothreitol (DTT)	Boehringer Mannheim GmbH, Mannheim
Dimethylsulfoxide (DMSO)	Merck, Darmstadt
dNTPs	Pharmacia Biotech, USA
Ethylendiamine tetraacetate (EDTA)	Fluka Chemie GmbH, Switzerland

Ethanol, abs.	AppliChem, Darmstadt
Ethidium bromide	Sigma-Aldrich, Steinheim
Fetal calf serum (FCS)	Boehringer Mannheim GmbH, Mannheim
Ficoll 400	Amersham Pharmacia, Freiburg
Glacial acetic acid	Fluka Chemie GmbH, Switzerland
Hydrochloric acid (37 %)	Merck, Darmstadt
Isopropanol	AppliChem, Darmstadt
Magnesium chloride	Sigma-Aldrich, Steinheim
Magnesium chloride (for PCR)	Gibco Life Technologies GmbH, Karlsruhe
Mineral oil	Sigma-Aldrich, Steinheim
Phenol	Sigma-Aldrich, Steinheim
Potassium acetate	Fluka Chemie GmbH, Switzerland
Potassium chloride	Merck, Darmstadt
Proteinase K	Roche, Switzerland
Salmon sperm DNA	Biomol, Hamburg
Sodium azide	Fluka Chemie GmbH, Switzerland
Sodium chloride	AppliChem, Darmstadt
Sodium citrate	Fluka Chemie GmbH, Switzerland
Sodium dodecyl sulfate	AppliChem, Darmstadt
Sodium hydrogencarbonate	Fluka Chemie GmbH, Switzerland
Sodium hydroxide	Fluka Chemie GmbH, Switzerland
Tris base	Fluka Chemie GmbH, Switzerland
Tris/ HCl	AppliChem, Darmstadt

Table 1: Chemicals

2.2 Molecular biology

2.2.1 Competent Cells and Isolation of Plasmid DNA

Competent *Escherichia coli* DH5α cells were prepared according to the protocol of Inoue *et al*. (Inoue et al., 1990) and used in heat shock transformations of plasmid DNA. DNA ligation was performed with the Takara DNA ligation Kit (Takara, Japan) according to the manufacturer's instructions. Plasmid DNA was isolated from transformed *Escherichia coli* DH5α bacteria with an alkaline lysis method (QIAGEN, Hilden, Germany). Plasmid DNA of higher purity was obtained with QIAGEN columns (QIAGEN, Hilden, Germany) following the supplier's instruction.

2.2.2 Isolation of Genomic DNA from ES Cells and Mouse Organs

Cells were lysed over night at 56°C in lysis buffer (10 mM Tris-HCl, pH 8; 10 mM EDTA; 150 mM NaCl; 0.2% (w/v) SDS; 400 mg/ml proteinase K). Subsequently, DNA was precipitated from the solution by the addition of an equal volume of isopropanol. DNA was pelleted by centrifugation, washed in 70% (v/v) EtOH and resuspended in TE-buffer (10 mM Tris-HCl, pH 8; 1 mM EDTA). From ES cell clones, grown in 96-well tissue culture dishes, DNA was extracted and prepared according to the protocol of Pasparakis and Kollias. Mouse tissue was incubated over night at 56°C in lysis buffer (0.1 M Tris-HCl, pH 8.5; 5 mM EDTA; 0.2% (w/v) SDS; 0.2 M NaCl; 600 mg/ml proteinase K). Undissolved debris was pelleted and the supernatant was mixed with an equal volume of isopropanol to precipitate the DNA. The DNA was washed in 70% (v/v) EtOH, dried at RT and resuspended in TE-buffer.

2.2.3 RT-PCR and Quantitative Real-Time PCR

RNA from isolated cellular subsets was prepared using the RNeasy mini kit (QIAGEN, Hilden, Germany) or Trizol (Invitrogen) according to the manufacturer's protocol. DNA was removed by DNAseI digestion (Promega, Mannheim, Germany). cDNA synthesis of 5 µg total RNA was performed as described in superscript II protocol

(GIBCO, Karlsruhe, Germany). cDNA was subsequently used for RT- and Real-Time PCR. Quantitative Real-Time PCR was performed using primers from QIAGEN as described on their homepage https://www1.qiagen.com/GeneGlobe/Default.aspx.

2.2.4 Agarose Gel Electrophoresis and DNA Gel Extraction

Separation of DNA fragments by size was achieved by electrophoresis in agarose gels (0.8% - 2% (w/v); 1x TAE (Sambrook, 1989); 0.5 mg/ml ethidium bromide). DNA fragments were recovered from agarose gel slices with either the QIAEX II or the QIAquick Gel Extraction Kit (QIAGEN, Hilden, Germany) following the manufacturer's instructions.

2.2.5 DNA Sequencing

DNA was sequenced using the 'Big Dye termination Cycle Sequencing Kit' (Applied Biosystems, Foster City, USA), which is a PCR-based modification of the original Sanger protocol (lexSanger et al., 1977). The fluorescently labeled DNA fragments were separated and analysed with the ABI373A and ABI377 systems (Applied Biosystems, Foster City, USA).

2.2.6 Quantification of DNA

The concentration of nucleic acids was determined by measuring the absorption of the sample at 260 nm and 280 nm, respectively, in a spectrophotometer. An OD_{260} of 1 corresponds to approximately 50 µg/ml for double stranded DNA or 40 µg/ml for RNA and single stranded DNA. Purity of nucleic acids was estimated by the ratio OD_{260}/OD_{280}, with 1.8 and 2.0 optimal for DNA and RNA, respectively. Alternatively, the DNA was electrophorated in an agarose gel, and the concentration was evaluated from the band intensity in comparison with a standard.

2.2.7 Polymerase Chain Reaction (PCR)

PCR (Mullis and Faloona, 1987) was used to screen mice and ES cells for the presence of targeted alleles or transgenes and to amplify fragments for sequencing (primers shown in Table 2 and 4). Reactions were performed in either Hybaid machines (MWG-Biotech, Ebersberg, Germany) or Triothermocyclers (Biometra, Göttingen, Germany). Genotyping of mice and ES cells was generally performed in a total volume of 50 µl in the following reaction mix: 50 pmol of each primer, 1.5 U of *Thermus aquaticus* (*Taq*) DNA polymerase (homemade), 250 mM dNTPs, 10 mM Tris-HCl pH 8.3, 50 mM KCl, 2.5 mM $MgCl_2$, 100 ng template DNA. Amplification started with denaturation for 4 min at 94 °C followed by 30-35 cycles of 94 °C for 30 sec, 52-60 °C for 30 sec, 72 °C for 30 sec and a final extension step at 72 °C for 10 min.

Name of primer	**Sequence (5´-3´)**	**T_{Ann}. °C**
Cre3	TCC AAT TTA CTG ACC GTA CAC	58
Cre7	TCA GCT ACA CCA GAG ACG G	58
CD4cre (AG-CD4L6)	CCC AAC CAA CAA GAG CTC	59
CD4cre (AG-CD4L6)	CCC AGA AAT GCC AGA TTA CG	59
EBI2Δ F	AGT CTA ACG CCT GTC TAG AAT GT	57
EBI2Δ R	CTC CTG GAC GTA GCC TTC GG	57
RosaFA	AAA GTC GCT CTG AGT TGT TAT	58
RosaRA	GGA GCG GGA GAA ATG GAT ATG	58
SpliAcB	CAT CAA GGA AAC CCT GGA CTA CTG	58
IL-17F-Cre F	GCT GGC CCA AAT GTT GCT GG	58
IL-17F-Cre R	GGG TGG GCT TAG AAG AGA GG	58
gp9997 (gp130)	GGC TTT TCC TCT GGT TCT TG	58
gp9998 (gp130)	CAG GAA CAT TAG GCC AGA TG	58

To amplify cDNA fragments for cloning or sequencing, the High Fidelity Master Kit with proofreading activity was used (Roche, Mannheim, Germany) with the primers shown in Table 2. PCR of transgenic Cre lines was performed as published.

2.2.8 Southern Blot Analysis

Digestion of 5-15 µg DNA was performed overnight with 50-100 U of the appropriate restriction enzyme. Subsequently, the DNA fragments were separated by agarose gel electrophoresis and transferred onto Hybond™-N+ (Amersham, Illinois, USA) or GeneScreenPlus (Dupont, Wilmington, USA) nylon membranes by an alkaline capillary transfer according to the method of Chomczynski and Qasba (1984). Membranes were baked at 80°C for 20 min to fix the DNA, equilibrated in 2x SSC and then prehybridised at 65 °C for 4 h in hybridisation solution (1 M NaCl, 1% (w/v) SDS, 10% (w/v) dextran sulfate, 50 mM Tris-HCl pH 7.5, 250 µg/ml sonicated salmon sperm DNA). The radioactively labeled probe was added to the hybridization solution and allowed to hybridize at 65 °C for 10 h in a rotating cylinder.

Aliquots of 50 ng DNA of the above probes were radioactively labeled with 2.5 µCi [α^{32}P]dATP (Amersham, Braunschweig, Germany) using the Ladderman™ Labeling Kit (Takara, Japan), based on the principle of random primed oligolabeling (Feinberg and Vogelstein, 1984). Unincorporated radiolabeled nucleotides were removed with MicroSpin™ S-200HR columns to reduce background during hybridisation (Pharmacia, Freiburg, Germany). The probe was denatured at 100°C for 5 min, cooled on ice, and then added to the hybridization solution. After hybridisation, stringent washes were initially performed twice in 2x SSC / 0.1 % (w/v) SDS and then followed by washes in 1x SSC / 0.1 % (w/v) SDS and 0.5x SSC / 0.1 % (w/v) SDS, if necessary. All washes were performed at 65 °C under gentle shaking for 30 min. After each wash, the filter was monitored with a Geiger counter and the washes were stopped when specific signals reached 50 to 200 cps. Then, the filter was sealed in a plastic bag and exposed to X-ray film (Kodak XAR-5 or BioMAX MS; Eastman Kodak) at -80°C. Films were developed in an automatic developer or alternatively, filters were exposed to a phosphoimager screen (Fuji, Fuji, Japan) and analysed on a Bio-Imaging Analyser (Fuji Bias 1000; Fuji, Japan).

2.2.9 Purification of linearized BAC DNA

50μg of BAC Maxiprep DNA was digested overnight using the appropriate linearizing restriction enzyme, PI-SceI, in a total volume of 500μl. During the digestion period, columns were prepared to purify the linearized BAC. Air was forced into 5ml plastic pipettes to move the cotton bung to the opposite end of the pipette and create the column. CL-4B Sepharose beads (Pharmacia) were shaken well and gradually added to the column. Sepharose was slowly added until the 5ml marker on the column was reached. Injection buffer (10mM Tris.HCl, pH 7.5, 0.1mM EDTA and 100mM NaCl) was added to the column. 30ml of injection buffer was passed through the column to remove excess ethanol present in the Sepharose bead suspension, keeping the column saturated with injection buffer at all times. 5μl of loading buffer was added to the digested BAC DNA. The BAC DNA mixed with loading buffer was added to the column exactly as the injection buffer drains to reach the upper level of the sepharose beads. It is possible to visualize the loading buffer moving through the sepharose. 1ml fractions were collected at the bottom of the column until the loading buffer reached the end of the column. Each fraction was run on a gel to determine the fractions containing BAC DNA, and these samples were further analysed for exact DNA concentrations using a photometer (Eppendorf). DNA for pronuclear injection was further diluted to a final concentration of 1.6-2 ng/ml in injection buffer.

2.3 Cell Biology

2.3.1 Embryonic Stem Cell Culture

All gene targeting experiments were performed in C57BL/6 (Bruce-4) ES cells. Culturing and transfection of ES cells was performed according to standard laboratory protocols. To maintain the pluripotency of the ES cells, the latter were cultured in ES cell medium in the presence of leukaemia inhibiting factor (LIF) on a layer of embryonic feeder (EF) cells. The ES cell medium (DMEM, 15% (v/v) FCS, 1 mM sodium pyruvate, 2 mM L-glutamine, 1 x non essential amino acids, 1:1000 diluted LIF supernatant, 0.1 mM 2-β-mercaptoethanol) contained FCS that had been tested to promote ES cell growth and to prevent *in vitro* differentiation (Gibco, Karlsruhe, Germany). ES and EF cells were grown in tissue culture dishes (Falcon, Bedford, USA) and kept at 37°C under humid atmosphere with 10% CO_2. EF cells in DMEM supplemented with 10% (v/v) FCS, 1 mM sodium pyruvate, 2 mM L-glutamine, were never passaged more than three times and then mitotically inactivated by mitomycin C treatment (10 μg/ml for 2 h), before seeding with ES cells. ES cell colony growth was stopped before they became confluent. Colonies were washed twice with PBS and then treated shortly with trypsin (0.05 % (w/v), 0.02 % (v/v) EDTA in PBS; Gibco, Karlsruhe, Germany) at 37°C, until the cells detached from the dish. The cell suspension was then used for passaging, transfection or freezing. ES cells were frozen in 90% (v/v) FCS, 10% (v/v) DMSO at -80°C and later transferred into liquid nitrogen for long term storage. For transfection, 1 x 10^7 ES cells were mixed with 30 to 40 μg DNA in 800 μl transfection buffer (RPMI w/o phenol red, Gibco, Karlsruhe, Germany) and electroporated at 23°C (500 mF, 240 V). After 5 minutes of incubation, ES cells were transferred onto an embryonic feeder layer and 48 h later placed under G418 (300 μg/ml, 71% active) selection. On approximately day 10 after transfection, resistant colonies were picked and split into EF-containing 96-well tissue culture dishes for expansion.

2.3.2 HTNC Treatment

$2x10^5$ ES cells were plated in a well of a 6-well culture dish with MEFs, 5 h prior to HTNC treatment. The medium was removed and replaced with DMEM without FCS/PBS, 1:1, 4-0.25 µM HTNC from a 50% (v/v) glycerol stock solution of 180 µM HTNC for 20 h (Peitz et al., 2002; M. Peitz, unpublished). Thereafter, the cells were cultured as described above. The deletion efficiency at 2 µM HTNC was around 50%.

2.3.3 Preparation of Mouse Embryonic Fibroblasts (MEFs)

Females of the desired genotype were mated with males of the desired genotype. Mating was detected by a daily plug check. Thirteen and a half days to fourteen and a half days after mating, the pregnant mice were sacrificed by cervical dislocation. The embryos and uterine horns were separated from the abdomen, carefully detached from the animal and placed in a dish with PBS where the liver and as many red blood cells as possible were removed. The tissue was minced in a dish containing Trypsin/EDTA. The minced embryos were placed in an incubator for 10 min and then all the contents of the dish were transferred into a 50 ml conical tube. The tube was centrifuged at 3.500 rpm for 10 min. The pellet was resuspended in MEF medium supplemented with Pen/Strep and plated on 10 cm plates. After 24 h, the medium was changed to remove cellular debris. Confluent plates were either expanded or frozen.

2.3.4 Preparation of Cells from Lymphoid Organs

Thymus, spleen, and lymph nodes were squashed between two frosted sides of a microscope slide to obtain single cell suspensions. Bones were flushed with medium (DMEM, 10% (v/v) FCS, 2 mM L-glutamine) to extract bone marrow cells. Erythrocytes were lysed from spleen and thymus preparations in 140 mM NH_4Cl, 17 mM Tris-HCl pH 7.65 for 2 min. Blood from the tail vein was collected in a tube with heparin (Liquemin, Roche, Mannheim, Germany) and then layered on top of 7% (w/v) Ficoll 400 (Pharmacia, Freiburg, Germany). After 1400 g centrifugation at 23°C for 15 min, lymphocytes were recovered from the interphase of the gradients and resuspended in DMEM, 10% (v/v) FCS, 2 mM L-glutamine and kept on ice.

2.3.5 Culture of ex vivo lymphocytes

Spleen and LN were aseptically removed from mice and then passed through a sterile sieve. Erythrocytes were lysed for 2 min by NH_4Cl (140 mM NH_4Cl, 17 mM Tris-HCl pH 7.65). Lymphocytes were kept in RPMI 1640 (supplemented with 10% (v/v) FCS (decomplemented), 1 mM sodium pyruvate, 2 mM L-glutamine, 1x non-essential amino
acids, 0.1 mM 2-β-mercaptoethanol, and 10 mM HEPES (Gibco), supplemented with the indicated compounds, e.g. MOGp35-55, in the indicated concentration for 3-5 days at 37°C.

2.3.6 Cell counting

Viable cells were assessed using the trypan blue dye exclusion test and counted using a Neubauer chamber (Assistent, Sondheim, Germany). To this end, an aliquot of the cell suspension was diluted with physiological trypan blue solution (Gibco, Long Island, NY, USA). Dead cells are stained blue whereas live cells cannot take up the dye due to their intact membrane. After counting 16 single quadrants, the counted cell number (N) was multiplied by the dilution factor (V) and the 'chamber factor' (10_4) resulting in the number of live cells per ml ($N \times V \times 10_4$ = cell number /ml).

2.3.7 Adoptive transfer

After enrichment, cell suspensions were washed with PBS, counted, and diluted to the desired concentration. Cells were injected in PBS intravenously (i.v.) into the tail vein of recipient mice (200 µl/mouse).

2.3.8 Flow Cytometry

Single cell suspensions were prepared from all tested organs. Red blood cells from LN and spleen were lysed in cell suspension with Tris-ammoniumchloride, pH 7.2. Cells (10^6 per sample) were surface stained in 30 µl PBS, 0.1% (w/v) BSA, 0.01% (w/v) NaN_3 with combinations of fluoresceine isothiocyanate (FITC), phycoerythrine (PE) and Cy-Chrome™ (Cyc), APC or bio-conjugated mAbs for 20 min on ice. Stainings with biotinylated mAbs were followed by a secondary staining step with Streptavidin-Cychrome™ (Pharmingen). After staining, the samples were washed and resuspended in PBS-BSA-NaN_3. Stained cells were analysed on a FACSCalibur and data were evaluated using CellQuest software (Becton Dickinson, Mountain View, USA). Dead cells were labeled with Topro-3 and excluded from the analysis. Monoclonal antibodies, listed in Table 1, were either homemade (C. Uthoff-Hachenberg, B. Hampel, Institute for Genetics, Cologne, Germany) or purchased from Pharmingen (San Diego , USA).

Specificity	Clone	Supplier
CD4	GK.1.5/4	Pharmingen
CD4	RM4-5	Pharmingen
CD8	53-6.7	Pharmingen
CD8	53-6.7	eBioscience
CD62L (L-Selectin)	MEL-14	Pharmingen
CD69	H1.2F3	Pharmingen
CD90.2/Thy1.2	CFO-1	Pharmingen
CD44	KM114	Pharmingen
MHC II	M5/114	Pharmingen
CD25 (IL-2Rα)	7D4	Pharmingen
TCRβ	H57-597	Pharmingen
B220/CD45R	RA3-6B2	Pharmingen
CD19	1D3	Pharmingen
IFN-γR1	2E2	eBioscience
IL-6Rα (CD126)	D7715A7	eBioscience
GR1 (Ly6G)	RB6-8C5	Pharmingen
Foxp3	FJK-16s	eBioscience

IL-17A	eBio17B7	eBioscience
IL-17A	TC11-18H10	Pharmingen
IL-17F	12-7471-80	eBioscience
IFN-γ	R4-6A2	Pharmingen

Table 2: List of antibodies used for flow cytometry

2.3.9 Magnetic Cell Sorting and FACS Sorting

Specific cell populations were either sorted or depleted from a heterogenous cell suspension by magnetic cell sorting (MACS; Miltenyi Biotec, Bergisch Gladbach, Germany). Cell populations were labeled with antibody-coupled microbeads (10 µl beads, 90 µl PBS-BSA-N_3 per 10^7 cells) and separated on VS or CS MACS columns in a magnetic field (Miltenyi et al., 1990)). For cell sorting, B cells were purified by MACS and then stained with antibodies against various cell surface markers. B cells of individual B cell subsets were then sorted using a dual laser FACStar (Becton Dickinson, Franklin Lakes, USA). The purity of isolated populations was subsequently tested by FACS analysis: MACS-isolated B cells were normally >80% pure and sorted B cell subpopulations were 95% pure. FACS sorting was performed with the help of Christoph Göttlinger (Institute for Genetics, Cologne, Germany).

2.3.10 Culture of *ex vivo* Splenocytes and Lymphocytes

The spleens were aseptically removed from mice and then pressed through a sterile sieve. Erythrocytes were lysed for 2 min by NH_4Cl (140 mM NH_4Cl, 17 mM Tris-HCl pH 7.65). Splenocytes or isolated T cells were kept in RPMI supplemented with 10% (v/v) FCS, 1 mM sodium pyruvate, 2 mM L-glutamine, 1x non-essential amino acids, 0.1 mM 2-β-mercaptoethanol supplemented with various activation compounds (LPS; ConA; PMA; BAFF) for no longer than four days.

2.3.11 Induction of Cre recombinase activity and IL-17A expression in vivo

Cre activity of ROSA-CreERT2 mice was induced *in vivo* by a sequential i.p. injections with 200 µl containing 2 mg of tamoxifen (TAM; ICN Biomedicals Inc., Aurora, OH, USA). TAM was suspended in 96% EtOH, 9 volumes of olive oil (ICN Biomedicals Inc., Aurora, OH, USA) were added, and TAM was dissolved at 37°C.

2.4 *In vivo* depletion of CD25+ cells

Endogenous $CD25^+$ cells were depleted from mice two days before induction of EAE by i.p. injection with 1 mg of anti-CD25 (PC61; rat IgG1; lab-made). Control mice received an i.p. injection of 1 mg of HRPN (rat IgG1). Confirmation of $CD25^+$ cell depletion by PC61 was determined staining peripheral blood of all mice two or three days after treatment with an Ab that recognizes a different epitope of CD25 (7D4), and it resulted in upwards of 90% $CD25^+$ cell depletion.

2.5 Histological Analysis and Immunohistochemistry

Shock frozen tissues were sectioned in 5-8 µm slices, fixed in ice cold acetone for 10 min and air dried for 10 min. Using a Pap pen, the tissue was outlined on the glass slide, placed in a wet chamber, and TBS was added for 5 min at RT. Slides were then incubated with quenching buffer containing 0.3% (v/v) H_2O_2 for 30 min and washed once with TBS. The sections were incubated with avidin solution and biotin solution for 15 min each and subsequently washed three times with TBS. The sections were then incubated with primary antibodies for 60 min. Sections were washed three times with TBS.

2.6 Cytokine Determinations

2.6.1 FlowCytomix

Multiple cytokine and chemokine levels were detected using FloxCytomixTM technology (BenderMedsystems, Vienna) according to the manufacturers instructions.

2.6.2 ELISA

Detection of cytokines (IFN-y and IL-17A) was performed with ELISA (BDBiosciences, Heidelberg, Germany) according to the manufacturer's instructions. The IL-17F ELISA kit (R&D systems) was utilised according to the manufacturers instructions.

2.7 Mouse Experiments

2.7.1 Induction and assessment of EAE

MOG_{35-55} peptide (amino acid sequence: MEVGWYRSPFSRVVHLYRNGK) was obtained from Research Genetics (Huntsville, Alabama, USA). Active EAE was induced by immunization with 50 µg of $MOG_{35–55}$ peptide emulsified in CFA (Difco Laboratories, Detroit, Michigan, USA) supplemented with 8 mg/ml of heat-inactivated *Mycobacterium tuberculosis* H37RA (Difco Laboratories, Detroit, Michigan, USA). The emulsion was administered as a 100 µl subcutaneous (s.c.) injection into the tail base. Mice also received 200 ng of Pertussis toxin (Sigma Aldrich, Steinheim, Germany) i.p. on the day of immunization and two days later. Passive EAE was induced by i.p. injection of MOG-reactive lymphocytes (20-30 x 10_6/mouse, generated as described in 2.3.7). Mice also received 200 ng of Pertussis toxin i.p. on the day of immunization and two days later. Clinical assessment of EAE was performed daily according to the following criteria: 0, no disease; 1, decreased tail tone; 2, abnormal gait (ataxia) and/or impaired righting reflex (hind limb weakness or partial paralysis); 3, partial hind limb paralysis; 4, complete hind limb paralysis; 5, hind limb paralysis

with partial fore limb paralysis; 6, moribund or dead.

2.8 Statistics

Values are typically represented as mean ± SEM (standard error of mean). Statistical significance was assessed using 2-tailed Student's *t*-test. p-values < 0.05 were regarded significant, displayed by '*' in the figures (** = p-value < 0.05; *** = p-value < 0.005).

3 Results

3.1 IL-17A^{ind} Screening and Testing

The ROSA-CAGs-STOP-EGFP vector was a kind gift from F. Thomas Wunderlich at the Institute for Genetics, University of Köln. Using this vector, it was possible to clone a PCR-amplified IL-17A open reading frame (ORF) from activated T cells into a unique AscI restriction site located downstream of the CAG promoter and a LoxP-flanked transcriptional STOP cassette. The IL-17A ORF was amplified using primers tipped with a rare-cutting restriction site, AscI. An AscI site is located between the 3' LoxP site and the 5' frt site in the ROSA-CAGs-STOP-EGFP vector. Thus, the PCR product can be amplified using primers tipped with AscI restriction sites, and further digested using AscI. The digested product can then be cloned into the empty vector linearized with AscI. This vector can be further linearized using SgfI (AsisI), another rare-cutting enzyme (Fig.1).

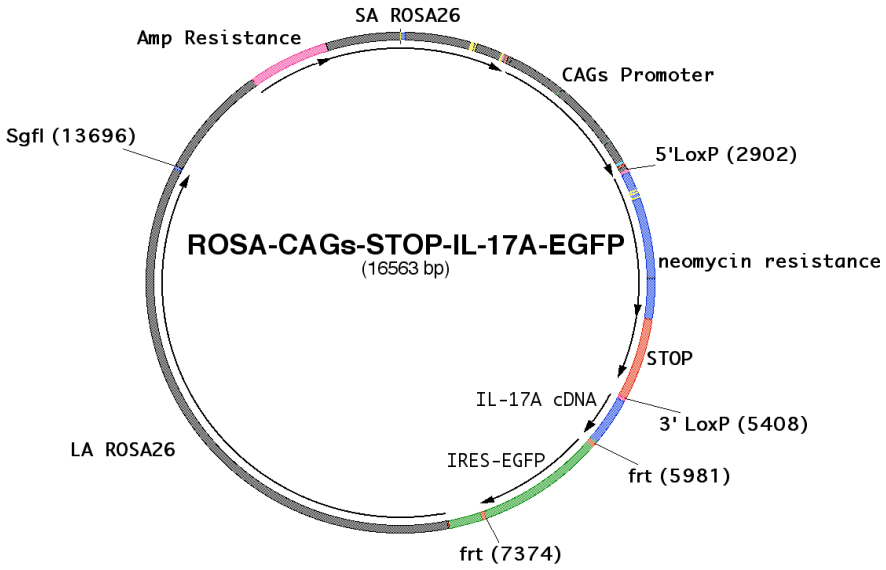

Fig. 1: ROSA-CAGs-STOP-IL-17A-EGFP schematic: Short and long arms of homology to direct homologous recombination to the ROSA26 locus flank the IL-17A^{ind} construct. A neomycin-resistance cassette and a transcriptional STOP cassette are situated between LoxP sites. Thus, the upstream CAGs promoter is held distal to the IL-17A cDNA. After Cre-mediated recombination, both the neomycin resistance and transcriptional STOP cassetttes are excised, permitting expression of IL-17A and EGFP under the control of the CAGs promoter.

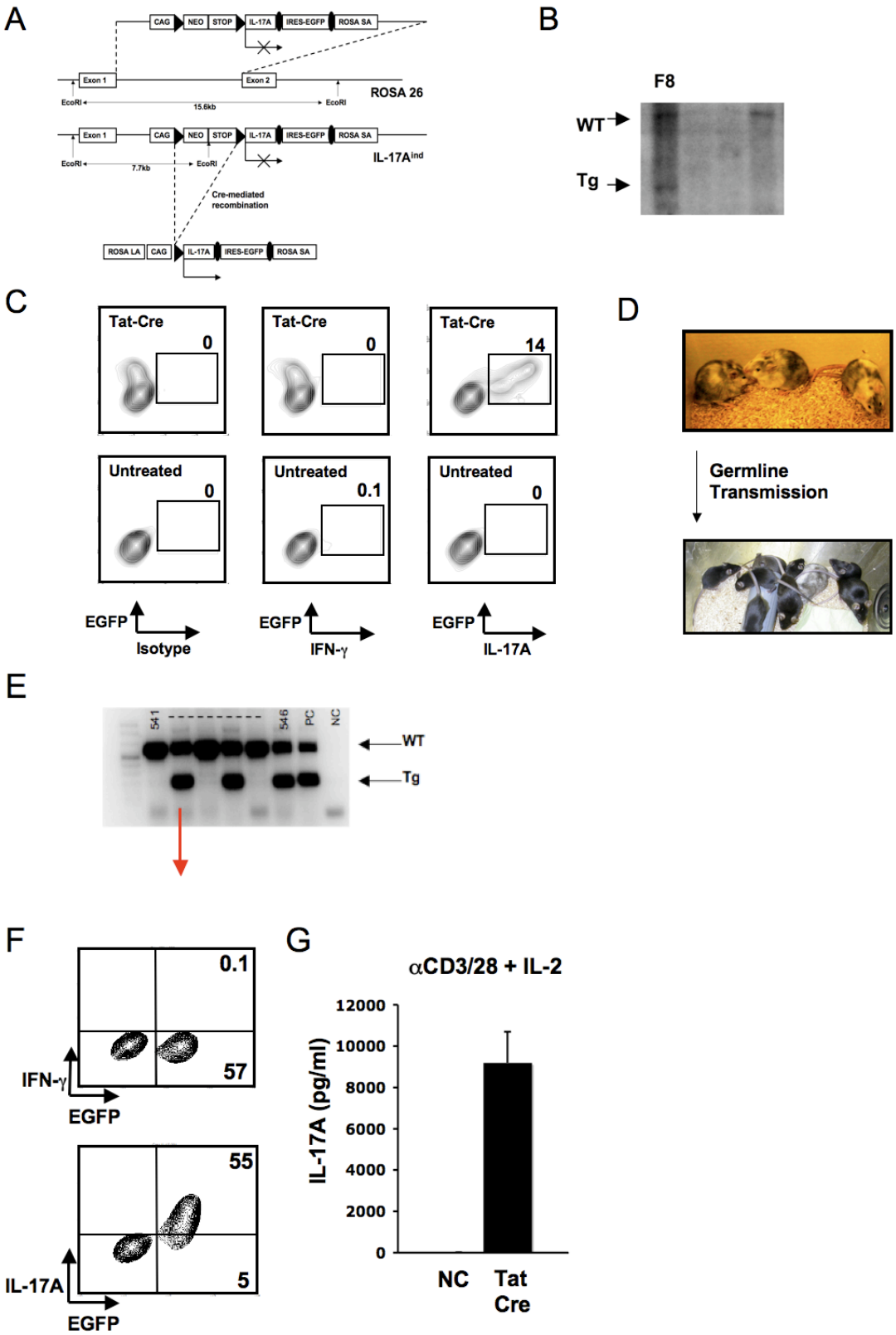

Fig 2. Schematic of IL-17A^{ind} targeting construct: (A) A Lox-P-flanked neomycin resistance (NEO) cassette and transcriptional STOP-cassette lie downstream of the chicken b-actin (CAG) promoter. After Cre mediated recombination, both the NEO and STOP cassettes would be excised and allow expression of an IL-17A cDNA. An IRES-EGFP element results in simultaneous EGFP and IL-17A expression. This construct was used to target the wild type ROSA26 locus. EcoRI digestion yields a wt band of 15.6kb. Successful targeting introduces another EcoRI site, and successful homologous recombination

between the IL-17A^{ind} targeting vector and the ROSA26 locus gives a band of 7.7kb. (B) Homologously recombined colonies were subjected to reconfirmation Southern blot analysis. Arrows indicate wild type (WT - 15.6kb) and IL-17A^{ind} (Tg – 7.7kb) band sizes. A single clone, F8, was identified and reconfirmed. (C) The F8 ES cell clone was treated with the transducible TAT-Cre protein. F8 cells were subsequently intracellularly stained for IL-17A, or control antibody directed against IFN-γ. (D) After injection into BALB/c blastocysts injection, chimeric mice were crossed to C57BL/6 mice and black offspring, which signal germline transmission, selected for genotyping for the IL-17A^{ind} allele. (E) PCR analysis showed successful transmission of the IL-17A^{ind} allele to F1 mice, of the genotype IL-17A$^{ind/+}$. (F) LN cells were isolated from IL-17A$^{ind/+}$ mice and treated with TAT-Cre for 4h to induce IL-17A and EGFP expression. Cells were subsequently activated with anti-CD3, anti-CD28 and IL-2 (10ng/ml) for 48h. After this time, cells were stained intracellularly for IL-17A. Percentages are given in the quadrants. (G) IL-17A-specific ELISA was performed on supernatants from (F). Error bars represent +/-SD.

Completion of the targeting vector (ROSA-CAGs-STOP-IL-17A-EGFP) created a construct from which IL-17A and EGFP would be strongly expressed in tissue or cell types with a transgenic expression of the Cre recombinase (Fig.2A). This completed vector was used to generate the IL-17A^{ind} allele.

Bruce4 embryonic stem cells were thawed and cultured on a mouse embryonic fibroblast (MEF) or ‚feeder' layer. After a single passage, 1x10^7 stem cells were elcctroporated with the linearized targeting vector. After electroporation and a period of recovery, stem cell medium was supplemented with G418. Stem cell colonies without integration of the targeting vector were sensitive to G418 treatment and only colonies bearing an integration of the targeting vector (containing a neomycin resistance cassette) would be conferred protection against the G418. Colonies surviving on the feeder cells longer than 10 days were picked and reintroduced into stem cell medium without the selection reagent.

Growth in G418-containing medium confirms an integation of the targeting vector into the genome of the electroporated stem cells. However, the neomycin cassette is active in cells in which a random integration has taken place. To confirm integration of the ROSA-CAGs-IL-17A-EGFP construct into the ROSA26 locus, southern blot analysis was performed on stem cells found to be resistant to G418. A 900bp, 5' external probe, termed the ‚Orkin' probe, was used to hybridize digested genomic DNA. Digestion of genomic DNA and successfully targeted genomic DNA will give bands of 15.6kb and 7.7kb, respectively (Fig. 2A). Of 100 colonies picked, one homologous recombinant was identified, termed F8. This single clone was selected, and a reconfirmation southern blot was performed to ensure that the correct clone was picked. Band sizes of 15.6kb (WT) and 7.7kb (Tg) were found for a second time in this single clone (Fig.2B). The positive identification of the F8 clone harbouring a homologous recombination between the targeting vector and the

ROSA26 locus pointed to a potential blastocyst injection. However, prior to the injection the construct was tested *in vitro* for functionality of the IL-17A and EGFP expression. Soluble Tat-Cre was added to trypsinized F8 cells and the treated cells assayed for expression of IL-17A and EGFP by intracellular staining. F8 cells stained positively for IL-17A, and a significant overlap was observed between EGFP expression and IL-17A expression (Fig.2C). This finding confirmed fidelity and functionality of the ROSA-IL-17A-EGFP construct in the homolgously recombined F8 clone. F8 was used for multiple injections into BALB/c blastocysts. The third injection yielded 7 chimeras, ranging in 60-100% chimerism. These chimeras were crossed to C57BL/6 mice and germline transmission of the F8 stem cells was achieved (Fig.2D). Subsequent to germline transmission, the ROSA-IL-17A-EGFP construct was reclassified as the IL-17A^{ind} allele, and will hereafter be named as such.

The transgenic allele was identified in ~50% of young mice (Fig.2E) and showed no preference for gender, as expected by mendelian autosomal inheritance ratios. Ample offspring were obtained from the initial germline transmission and as such not all positive mice were required for breeding. Having positively tested the F8 stem cells using Tat-Cre (Fig.2C), it was of interest to test the construct post-germline transmission. Whole lymph nodes (LN) from a single IL-17A$^{ind/+}$ mouse were cultured for in the presence or absence of Tat-Cre. As could be observed in the stem cells some months previously, CD4^{+} T cells were able to recombine and express both EGFP and IL-17A simultaneously (Fig.2F). No signal was detected in the control staining. To confirm highly elevated expression levels of IL-17A, LN cells were re-cultured with T cell medium containing a cocktail of anti-CD3, anti-CD28 and IL-2 to induce a proliferative response from the T cells. After a period of 48h in culture, supernatants were collected from both treated and untreated IL-17A$^{ind/+}$ T cell cultures and assayed for presence of IL-17A by ELISA. Highly elevated levels of IL-17A were detected in supernatants of transgenic T cells treated with Tat-Cre, but not in the absence of recombination (Fig.2G). Collectively, these data confirmed successful transmission of the IL-17A^{ind} allele and solid functionality and fidelity of the construct in the resulting offspring.

Cre-expression is necessary to induce both IL-17A and EGFP expression in this strain. Prior to crossing to well estabilised Cre lines available in our laboratory, IL-17A$^{ind/+}$ mice were intercrossed to achieve homozygosity of the IL-17A^{ind} allele. IL-17A$^{ind/ind}$ mice were identified and it was agreed to keep the strain homozygous in the

SPF facility in Mainz. IL-17A$^{ind/ind}$ mice were then used for subsequent breedings to Cre-expressing strains and shipments for collaborations.

3.1.1 IL-17A overexpression induces granulocytosis and anaemia.

We reasoned that a cross to the Deleter Cre strain, in which Cre activity takes place shortly after gamete fusion (Schwenk et al., 1995), would allow us to observe the IL-17A expression from our construct and its biological effects *in vivo*. To this end, an IL-17A$^{ind/+}$ male was crossed to homozygous Deleter Cre females. This is the optimal arrangement for this breeding, as the Deleter Cre allele is located on the X-chromosome. Resulting offspring from this cross showed an extremely striking phenotype. Mice were visibly impaired in growth from as early as 1 week of age, and mice reaching maturity suffered obvious and highly significant growth retardation (Fig.3A). Single cell suspensions taken from secondary lymphoid organs including spleen, bone marrow, lymph nodes and thymus showed a highly upregulated expression of IL-17A being secreted in these organs from Deleter-IL-17A$^{ind/+}$ mice (Fig.3B). Given this expression of IL-17A throughout the major immune compartments, and the well documented link between IL-17A expression and granulopoiesis (Kolls et al., 2003), samples of bone marrow single cell suspensions from Deleter-IL-17A^{ind} mice were stained for neutrophil and monocyte-defining markers GR1 and CD11b. In mice with a systemic overexpression of IL-17A, a highly significant and consistently reproducible increase in CD11b^{+}GR1^{+} cells was observed in the BM (Fig.3C). This phenotype, although already highly significant at three weeks of age, progressed and worsened with age and already at 8 weeks, greater than 80% of cells in the BM were of granulocyte phenotype (GR1^{+}CD11b^{+}), compared to less than 40% of WT control mice (Fig.3D). The observed granulocytosis correlated inversely with the survival of Deleter-IL-17A$^{ind/+}$ mice. Deleter-IL-17A$^{ind/+}$ mice rarely live longer than three months of age (Fig.3E). Blood samples taken from the heart of Deleter IL-17A$^{ind/+}$ mice were also analyzed in a routine complete blood count (CBC). Deleter-IL-17A$^{ind/+}$ showed highly significant reductions in hemoglobin (HGB) and hematocrit (HCT), and also mean corpuscular hemoglobin (MCH) and mean corpuscular volume (MCV) when compared to littermate controls (Fig.3F). Decreased hemoglobin and hematocrit levels are the hallmarks of a diagnosis of anaemia in human patients (Nau and Lewis, 2008). Taken together, overexpression of IL-17A in

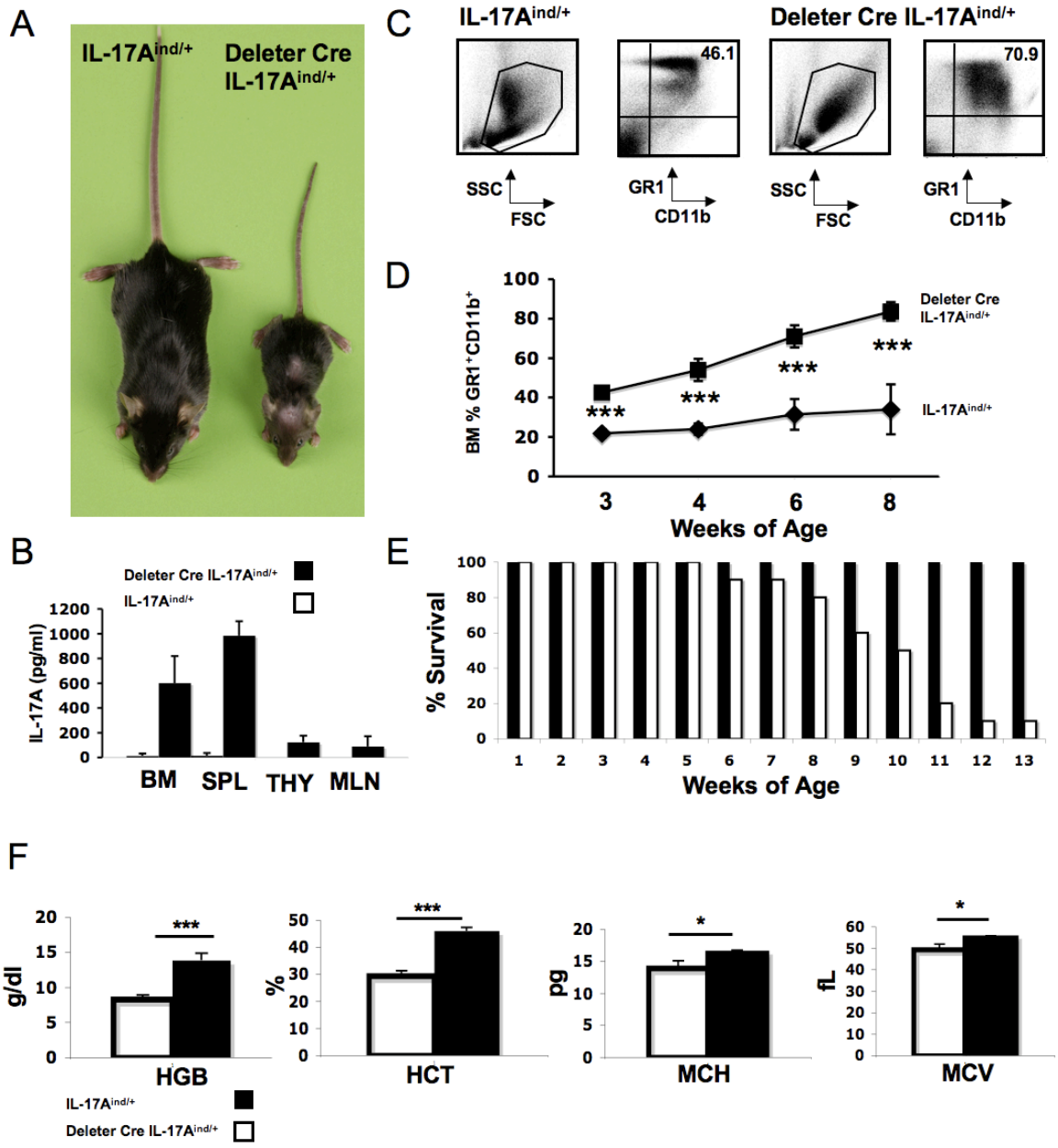

Fig. 3: Systemic overexpression of IL-17A results in lethal granulocytosis: (A) Deleter Cre IL-17A$^{ind/+}$ mice are dramatically reduced in size. The image shown is consistent with all mice analyzed. (B) Single cell suspensions from BM, SPL, Thy and MLN of Deleter Cre IL-17Aind show significant upregulations of IL-17A expression compared to IL-17A$^{ind/+}$ controls. (C) BM single cell suspensions form the indicated genotypes were stained for GR-1 and CD11b. Percentages of GR1^{+}CD11b^{+} cells are given in the quadrants. Data shown are representative of more than 10 independent experiments. (D) Cohorts of mice sacrificed at the indicated timepointd were antibody-stained as in (C). Percentages of GR1^{+}CD11b^{+} cells are shown for the indicated genotypes (n=3 in all cases). Error bars represent +/-SD. (E) Deleter Cre IL-17A$^{ind/+}$ mice dying of natural causes were recorded and compared to wt survival curves. (F) Blood samples from Deleter Cre IL-17A$^{ind/+}$ and littermate controls were subjected to routine CBC analysis. Levels of hemoglobin and hematocrit, as well as mean corpuscular hemaglobin and mean corpuscular volume are shown for the indicated genotypes.

the whole body results in growth retardation, granulocytosis, anaemia and premature death.

3.1.2 Neutrophils accumulate in the lungs of Deleter-IL-17A^{ind} mice.

IL-17R expression is expressed very widely in the body. Much work has already been done studying the role of IL-17A signaling in the lung tissue, and the importance of this cascade in mobilizing neutrophils into an infected lung (Ivanov et al., 2007b; Kolls and Linden, 2004). We reasoned that a proportion of the neutrophils generated in the BM of Deleter-IL-17A$^{ind/+}$ mice would migrate to the lung tissue in response to target genes induced by IL-17A signaling. To ensure that IL-17A expression was taking place in the lung tissue of Deleter-IL-17A $^{ind/+}$ mice, broncheo-alveolar lavage (BAL) fluid was extracted from the lungs of Deleter-IL-17A$^{ind/+}$ mice and control mice. Highly elevated levels of IL-17A were readily detectable in the BAL of Deleter-IL-17A$^{ind/+}$ mice compared to the WT control group (Fig.4A). Cytospin analysis was performed on the BAL samples and a clear increase in cellularity of lung infiltrates was observable (Fig.4B). Morphology-based counting revealed a highly increased total number of neutrophils in the BAL fluid (Fig.4C). Thus, using the lung as an example, IL-17A overexpression leads to infiltration of neutrophils in response to IL-17A signaling in lung tissue.

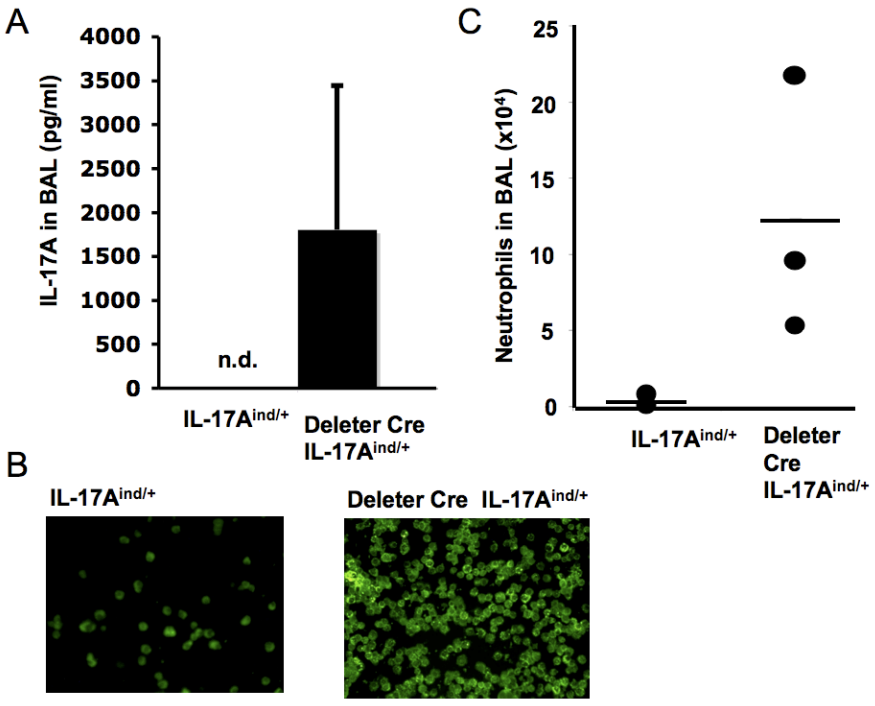

Fig. 4. Neutrophils accumulate in the lungs of Deleter Cre IL-17Aind mice: (A) BAL fluid was extracted from Deleter Cre IL-17A^{ind} mice and littermate controls. IL-17A-specific ELISA was performed on BAL fluid on cohorts of mice (n=3). Error bars represent +/-SD. (B) Cytopsin analysis in BAL fluid reveals a massive increase in cellular infiltrate in the BAL fluid. (C) Morphological

identification of neutrophils was performed on BAL fluid from Deleter-Cre IL-17A$^{ind/+}$ and IL-17A$^{ind/+}$ mice. Cell numbers and mean averages are shown (n=3).

3.1.3 Skin-specific IL-17A expression results in Psoriasis-like Dermatitis.

A well established link has been shown between IL-23, IL-17A and psoriasis (Di Cesare et al., 2009). Psoriasis is a chronic inflammatory disease causing red scaly patches on a patients skin. It is characterized by excessive skin tissue hyperproliferation, formation of new blood vessels and presence of proinflammatory cellular infiltrates. The study of psoriasis in humans has, however, been limited somewhat by the absence of a useful animal model.

The K14 keratin is an intermediate filament produced by squamous epithelial cells. We reasoned that by crossing the IL-17A^{ind} allele to the K14 Cre strain (Vasioukhin et al., 1999), a skin-specific IL-17A expression in skin would be achievable. We took advantage of the EGFP expression from the IL-17A^{ind} allele and analyzed K14-IL-17A$^{ind/+}$ mice using an in vivo imager. A clearly detectable EGFP signal was detectable in K14-IL-17A$^{ind/+}$ mice. Predictably, no signal was detectable in IL-17A$^{ind/+}$ mice (Fig.5A). However, to be sure that the Cre expression was restricted to the skin of K14-IL-17A$^{ind/+}$ mice, organs from a Deleter IL-17A$^{ind/+}$ mouse were used as a positive control. Ear, lung, liver, heart, kidney and gut were isolated from either IL-17A$^{ind/+}$, K14-IL-17A$^{ind/+}$ or Deleter IL-17A$^{ind/+}$ and exposed to the *in vivo* imager. As can be clearly seen in the Deleter IL-17A$^{ind/+}$ mouse, a strong EGFP signal is detectable in all organs assayed. However, in K14-IL-17A$^{ind/+}$ mice the EGFP signal is limited to the ear, indicating a skin-specific expression in K14-IL-17A$^{ind/+}$ mice (Fig.5B). Thus, the combination of the IL-17A^{ind} allele and the K14-Cre results in skin-specific recombination and expression of EGFP in the skin.

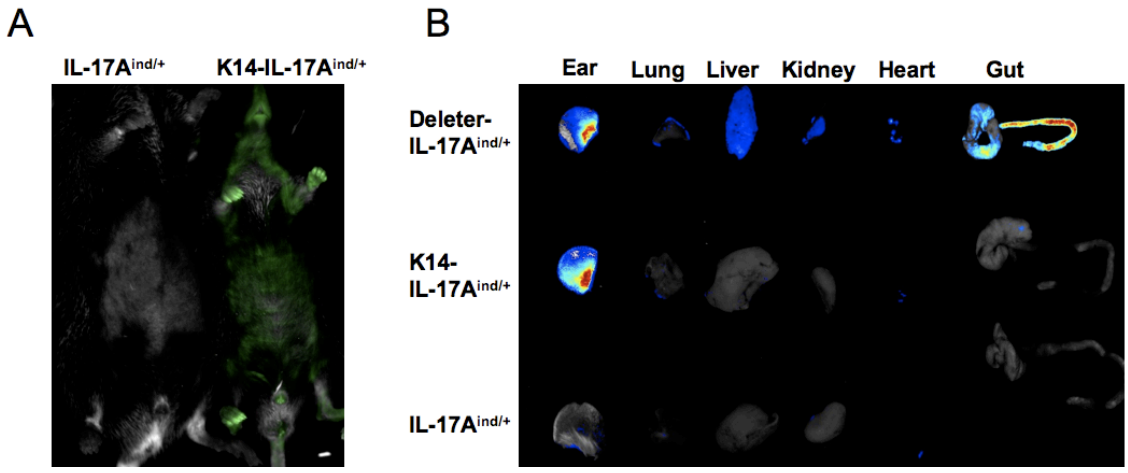

Fig. 5. K14-IL-17A^{ind} mice give a skin-specific expression of EGFP and IL-17A: (A) The IL-17A^{ind} allele was crossed to the K14-Cre to achieve a keratinocyte-specific expression of IL-17A. Anaesthetized K14-IL-17A^{ind} mice were placed in an in vivo imager and assayed for expression of EGFP. EGFP expression was detectable under the indicated genotypes. (B) Organs isolated from K14-IL-17A$^{ind/+}$ mice were subjected to in vivo imaging. EGFP signal is shown as a thermal gradient in the indicated organs of K14-IL-17A$^{ind/+}$, Deleter-IL-17A$^{ind/+}$ or IL-17A$^{ind/+}$ mice.

Skin sections from 6-week-old K14-IL-17A$^{ind/+}$ were prepared and cryosections stained for hematoxylin and eosin. Clearly observable phenotypes included an acanthotically-thickened epidermis with a lost stratum granulosum and multiple granulocyte-filled absesses in the horny layer of K14-IL-17A$^{ind/+}$ skin. Morphological analysis showed the infiltrate to consist mainly of neutrophils and T cells. The papillary dermis also appeared elongated. The hyper- and parakeratosis of the skin wih a lost stratum granulosum is typical for psoriasis (Fig.6A). To confirm indeed that the observed inflammation in K14-IL-17A$^{ind/+}$ skin was in part immune-mediated, single cell suspensions were prepared from back skin of K14-IL-17A$^{ind/+}$ and IL-17A$^{ind/+}$ mice. FACS analysis revealed a highly increased presence of both CD4 and CD8 T cells (Fig.6B). In addition to T cells, a highly significant increase of CD11b^{+}GR1^{+} granulocytes was present in the inflamed skin of K14-IL-17A$^{ind/+}$ mice when compared to littermate controls (Fig.6C). Taken together, IL-17A expression in the skin results in a phenotype resembling psoriasis, and introduces the K14-IL-17A$^{ind/+}$ strain as a potential new animal model for studying human psoriasis.

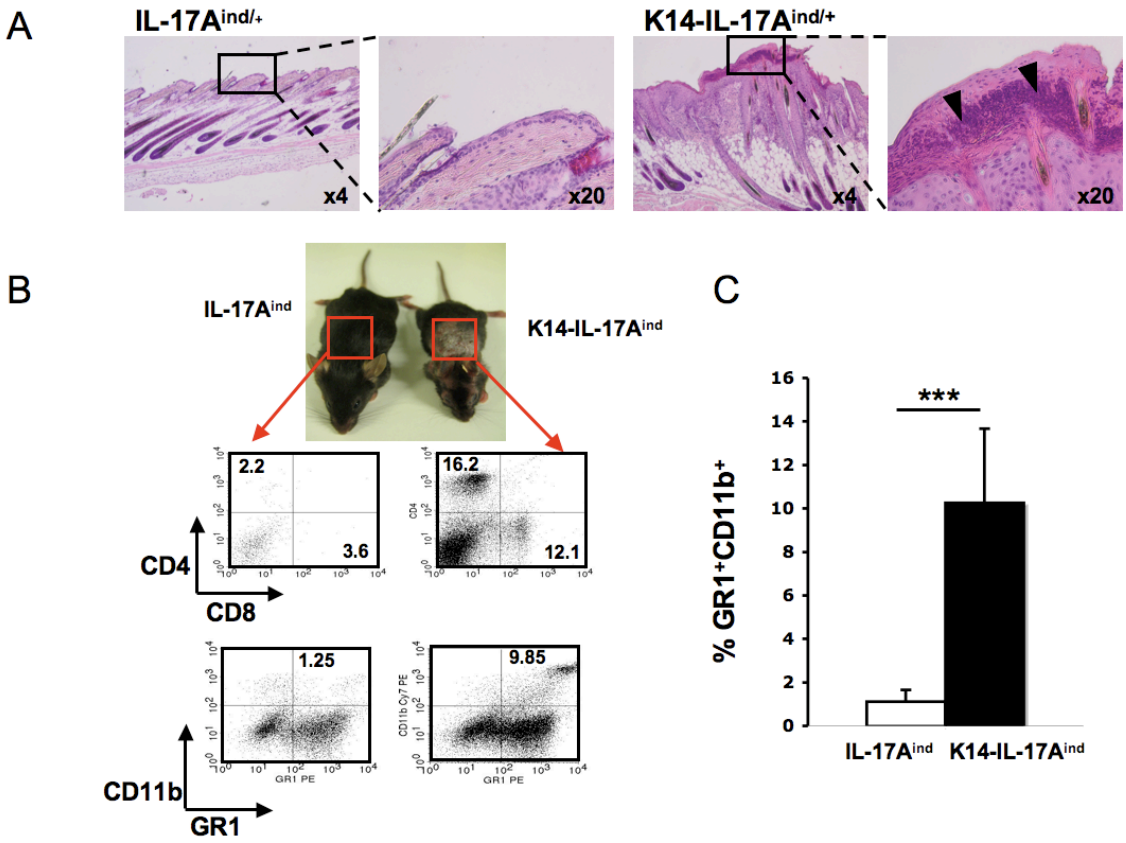

Fig. 6: K14-IL-17A^{ind} mice present with psoriasis-like dermatitis and lymphocyte infiltration: (A) Cryosections prepared from back skin of K14-IL-17A^{ind} and IL-17A^{ind} mice were stained using hematoxylin and eosin. Magnification is given on individual images. Multiple granulocyte abcesses are shown using black arrows. Data shown respresent two independent stainings. (B) Single cell suspensions were prepared from back skin of K14-IL-17A^{ind} and IL-17A^{ind} mice. Cellular yields were stained for CD4 and CD8 coreceptors, and also GR-1 and CD11b. Percentages of cells in quadrants are given on the dot plots. (C) Statistical quantification of data collected in (B) shown as a bar chart. Statistical significance was calculated using the student's t-test.

3.1.4 IL-17A signaling in skin induces synthesis of innate chemotactic proteins.

The increase in numbers of neutrophils in the skin of K14-IL-17A^{ind} mice implies that IL-17A signaling is inducing downstream molecules necessary for initiating migration of neutrophils into inflammatory foci. Macrophage chemotactic proteins (MCP) are potent attractors of macrophages into sites of inflammation. Chemotactic cytokines induced by IL-17A include the macrophage inflammatory proteins (MIP). MIP-1α, MIP-1β (also called CCL3 and CCL4, respectively) and RANTES (CCL5) mediate neutrophil recruitment via CCR1. It was demonstrated that genetic disruption of CCR1 expression abrogated neutrophil recruitment in response to MIP-1α treatment (Ramos et al., 2005). IL-6 is also induced by IL-17A signaling and was shown to protect

neutrophils from apoptosis (Asensi et al., 2004) and to increase expression of the effector molecule elastase (Johnson et al., 1998). With this in mind, we wanted to test whether expression of IL-17A in skin resulted in a cytokine environment well suited to attract neutrophils into the skin, which potentially induced the apparent inflammation in the skin of K14-IL-17A$^{ind/+}$ mice.

Single cell suspensions from back skin of K14-IL-17A$^{ind/+}$ and IL-17A$^{ind/+}$ mice were prepared and cultured for 48h. After this culture period, supernatants were taken and assayed for expression of IL-17A, IL-6, GM-CSF, MCP-1, MCP-3, MIP-1α, MIP-1β and RANTES. Highly significant upregulations in expression of IL-17A and the neutrophil-mobilizing chemokines and cytokines were found in K14-IL-17A$^{ind/+}$ skin

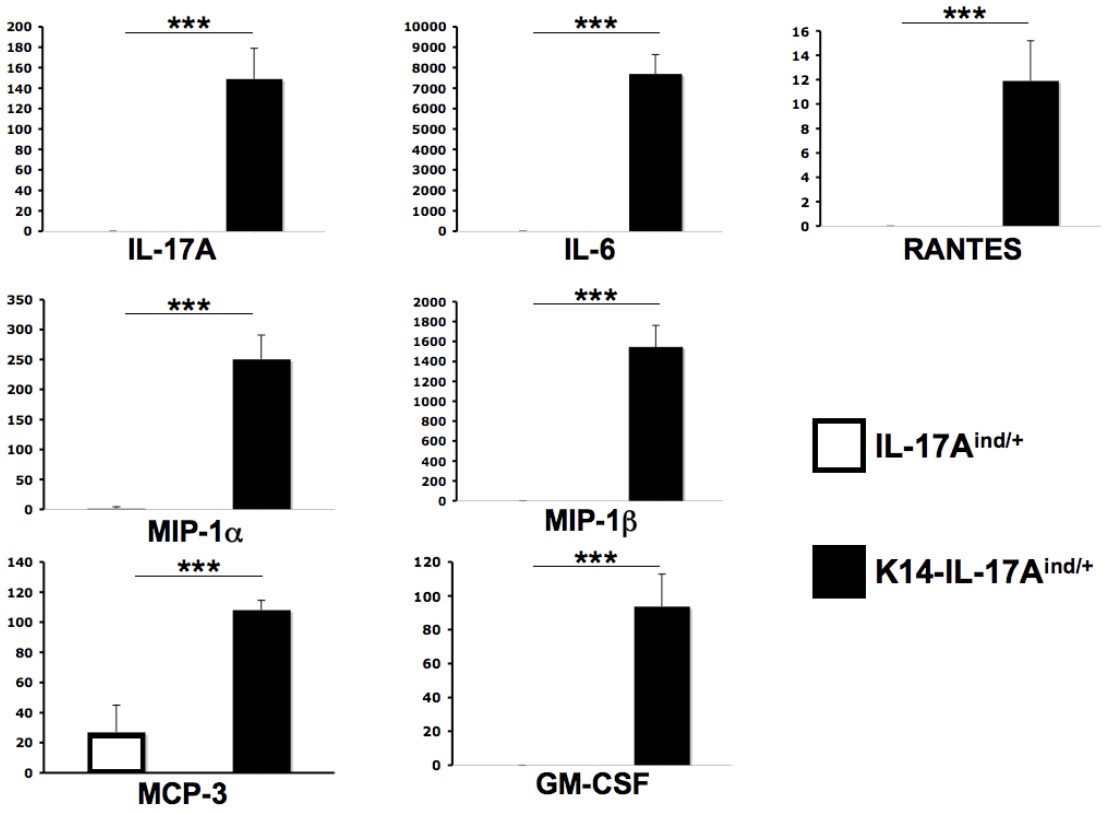

Fig. 7: Skin specific IL-17A overexpression induces neutrophil-mobilizing chemokine expression: (A) Single cell suspensions were prepared from back skin of K14-IL-17A^{ind} and IL-17A^{ind} mice. Cell suspensions were left unstimulated in culture for 72h and supernatants assayed for upregulation of the indicated proteins by flow cytomix. n=4 in both groups. Error bars represent +/-SD, represent and statistical significance was calculated using the student's t-test.

cultures (Fig.7). In particular, IL-6 was massively upregulated. MCP-1 expression was also highly upregulated, but levels detected were high above the reliable limit offered by the assay, and as such were excluded from the analysis. These data show that IL-17A expression in the skin results in chemokine expression, which attracts neutrophils into the skin and provides a potential first step for the observed pathogenesis in K14-IL-17A$^{ind/+}$ skin.

3.1.5 K14-IL-17A$^{ind/+}$ mice have systemic granulocytosis

Deleter-IL-17A^{ind} mice showed a highly significant and pathogenic increase in granulopoiesis. We wanted to check whether the skin-specific expression of IL-17A would result in an overt granulocytosis, as observed during systemic overexpression. Blood serum samples isolated from K14-IL-17A$^{ind/+}$ and IL-17A$^{ind/+}$ mice were assayed for IL-17A expression by ELISA. Highly significant levels of IL-17A were found in the serum of these mice, showing that IL-17A expression from K14-expressing cells resulted in ‚leakage' of IL-17A from the skin and into the circulation (Fig.8A). Already at 4 weeks of age, of K14-IL-17A$^{ind/+}$ mice show discernably elevated levels of GR1^{+}CD11b^{+} in the BM (Fig.8B). By 10 weeks of age, this phenotype is highly apparent, with upwards of 80% of cells in the BM being of a Ly6G^{+}CD11b^{+} phenotype (Fig.8C). These data imply that local overexpression of IL-17A in skin of the K14-IL-17A^{ind} mice will ultimately result in a phenotype similar to that observed in Deleter IL-17A$^{ind/+}$ mice.

To further explore the extent of the granulocytosis, Deleter-IL-17A$^{ind/+}$, K14-IL-17A$^{ind/+}$ and IL-17A$^{ind/+}$ peripheral blood samples were, in parallel, subjected to a routine complete blood count (CBC). Significant reductions in whole blood lymphocytes were apparent for both Cre-expressing strains (Fig.8D). On the other hand, significant upregulations of neutrophils and monocytes were observed in both experimental groups (Fig.8D). No significant alterations in the levels of eosinophils was recorded. Therefore, the increased granulopoiesis was indeed resulting in an overt granulocytosis.

K14-IL-17A^{ind} and IL-17A^{ind} mice were also checked for abnormalities in the secondary lymphoid organs. No significant alterations were observed in mesenteric or peripheral lymph nodes, but splenic cell counts revealed a discernable and significant splenomegaly in 8-week-old K14-IL-17A^{ind} mice compared to littermate controls

(Fig.8E). FACS analysis on spleens of K14-IL-17A^{ind} and IL-17A^{ind} mice gave highly contrasting results. IL-17A^{ind} mice presented with 55% B220^{+} cells and 21% CD90.2^{+} cells, and as such are indiscernable from WT mice. K14-IL-17A$^{ind/+}$ mice, on the other hand, were almost totally devoid of lymphocytes in the spleen (Fig.8F). Instead, over 80% of all cells in the spleen were of the myeloid lineage, and stained positively for Ly6G and CD11b (Fig.8F). Only 6% of splenic cells were of granulocyte phenotype in IL-17A$^{ind/+}$ mice. These findings showed to potency of IL-17A signaling in induction of granuolopoiesis, but also highlight a flaw in the K14-IL-17A$^{ind/+}$ model. It was deemed necessary to create a model of IL-17A expression, which can be controlled in a time-dependent manner. This would allow the timely induction of IL-17A expression in the skin without added complications of systemic granulocytosis throughout development.

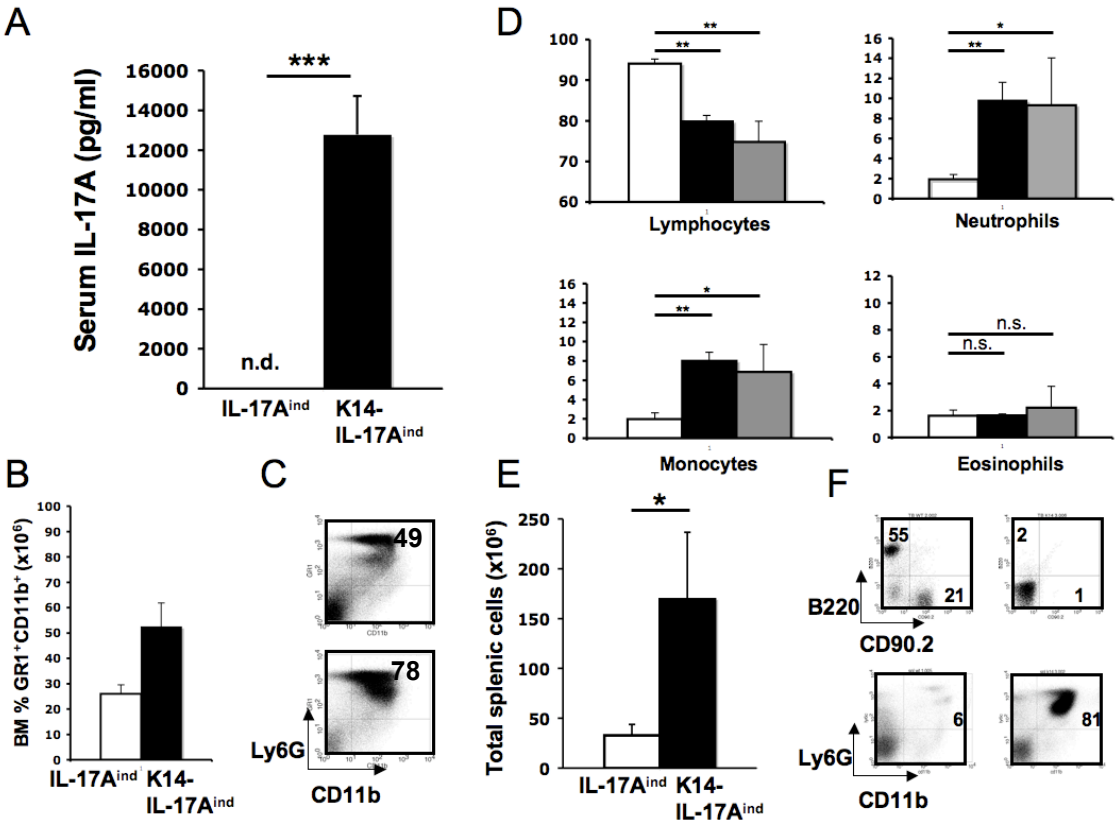

Fig. 8: K14-IL-17A^{ind} mice have systemic granulocytosis: (A) Serum was extracted from peripheral blood of K14-IL-17A^{ind} and IL-17A^{ind} mice. IL-17A-specific ELISA was performed on serum extracts. (B) BM from cohorts of 4 week old K14-IL-17A^{ind} and IL-17A^{ind} mice were stained for GR1 and CD11b. (C) BM isolated from 10 week old K14-IL-17A^{ind} and IL-17A^{ind} mice were stained for GR1 and CD11b. (D) Blood samples from Deleter- IL-17A^{ind}, K14-IL-17A^{ind} and IL-17A^{ind} mice were subjected to routine WBC analysis. Percentages of the indicated cell types from total PBMCs are given shown for the following genotypes (white bars = IL-17A^{ind}, black bars = K14-IL-17A^{ind}, grey bars = Deleter-IL-17A^{ind}) (n=4-10). (E) Total cell numbers from spleens of K14-IL-17A^{ind} and IL-17A^{ind} mice (n=3). (F) Splenic single cell suspensions from K14-IL-17A^{ind} and IL-17A^{ind} mice were stained with

anti-B220 and anti-CD90.2, or in parallel for Ly6G and CD11b. Percnetages of T cells, B cells and granulocytes are given in the indicated quadrants. In all panels, error bars represent +/-SD, represent at least two independent experiments and statistical significance was calculated using the student's t-test.

3.2 The ROSA-Cre^{ERT2}-IL-17A^{ind} system

Inducible function of Cre recombinase is an elegant method to control expression of Cre recombinase in a time- and perhaps dose-dependent manner. The Cre^{ERT} consists of a Cre recombinase and the estrogen receptor in the form of a fusion protein. In the steady state, the fusion protein remains in the cytoplasm, courtesy of heat shock protein 90 (HSP90) sequestration. Upon addition of tamoxifen, the bond between the estrogen receptor and the Hsp90 is disrupted, exposing the nuclear-localization sequence of the Cre recombinase and allowing translocation from the cytoplasm into the nucleus, where Cre can then catalyze recombination between LoxP sites in the genome.

The ROSA-Cre^{ERT2} strain was made available to our group by Prof. Dr. Ernesto Bockamp. We crossed the ROSA-Cre^{ERT2} allele to IL-17A$^{ind/ind}$ mice. In the resulting ROSA-Cre^{ERT2}-IL-17A$^{ind/+}$ mice, administration of tamoxifen, either systemically or locally, would allow recombination within the IL-17A^{ind} allele and result in EGFP and IL-17A expression. Mice from this cross were initially injected intraperitoneally with tamoxifen for four days. After a period of 1 week, mice were sacrificed and assayed for production of EGFP in LN-derived CD4^{+} T cells, which confirmed a successful recombination upon administration of tamoxifen (Fig.9A). High levels of recombination (66%) can be achieved in CD4^{+} T lymphocytes by systemic administration of tamoxifen (Fig.9B). Significantly elevated levels of IL-17A were also detectable in the serum of double-transgenic mice treated with tamoxifen (Fig.9C). Control mice in this group were also injected with tamoxifen, but lacked the ROSA-Cre^{ERT2} allele. No EGFP signal was detectable in these mice. In addition to the EGFP expression, IL-17A ELISA on serum from peripheral blood yielded a highly significant increase in IL-17A concentrations. Taken together, the ROSA-Cre^{ERT2} IL-17A$^{ind/+}$ mice can be utilised for the timely induction of IL-17A expression.

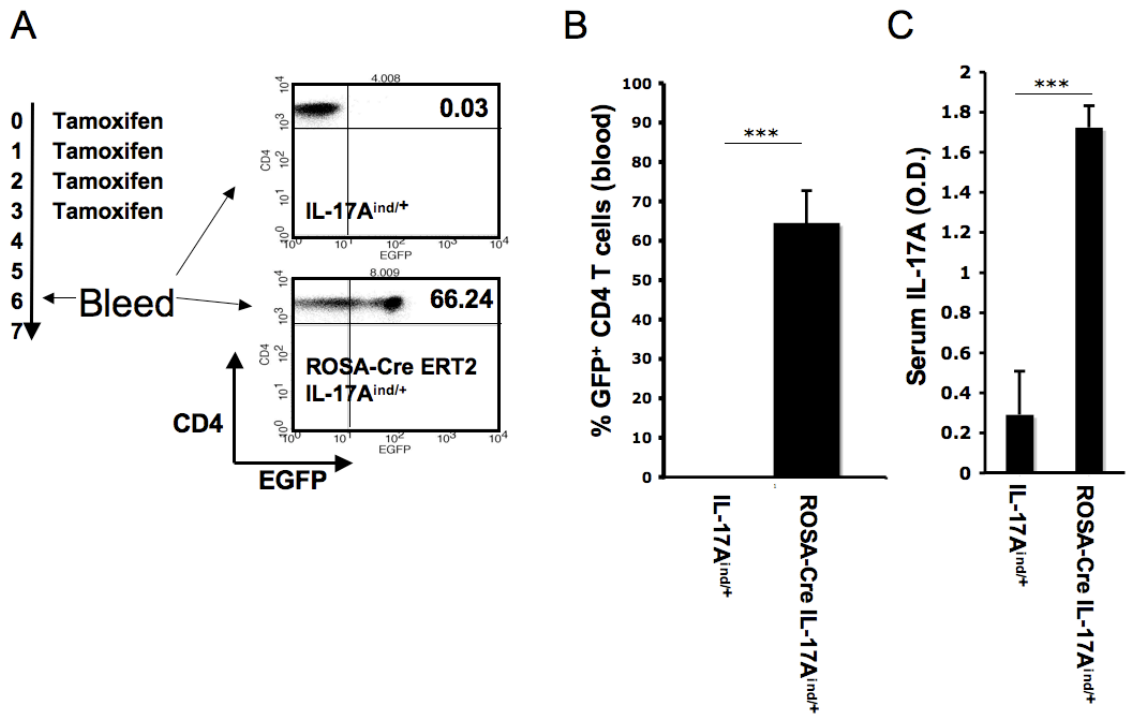

Fig. 9: Tamoxifen administration induces IL-17A expression in ROSA-Cre^{ERT2}-IL-17A$^{ind/+}$ mice: (A) ROSA-Cre^{ERT2}-IL-17A$^{ind/+}$ and control were injected i.p. with 4mg tamoxifen in olive oil for 4 days. After 1 week, ROSA-Cre^{ERT2}-IL-17A$^{ind/+}$ mice and Cre- control mice were bled and CD4+ T cells assayed for expression of EGFP. (B) Significant upregulations of EGFP+ T cells can be found after tamoxifen administration in ROSA-Cre^{ERT2}-IL-17A$^{ind/+}$ mice. (C) Serum from tamoxifen treated ROSA-Cre^{ERT2}-IL-17A$^{ind/+}$ and IL-17A$^{ind/+}$ mice were assayed for induction of IL-17A expression. Error bars represent +/-SD and statistical significance was calculated using the student's t-test.

3.2.1 Tamoxifen administration to ROSA-Cre^{ERT2}-IL-17A$^{ind/+}$ mice induces granulopoiesis.

To test whether a phenotype similar to that observed in both the Deleter-IL-17A^{ind} and K14-IL-17A$^{ind/+}$ strains could be induced using this system, cohorts of ROSA-Cre^{ERT2} IL-17A$^{ind/+}$ and IL-17A$^{ind/+}$ mice were again injected with tamoxifen as in Fig.9. After a period of two weeks, mice were sacrificed to analyze the effects of late onset IL-17A overexpression on granulopoiesis. Once again, a successful recombination could be seen in splenic T cells derived from tamoxifen-treated ROSA-Cre^{ERT2}-IL-17A$^{ind/+}$ mice (Fig.10A). Bone marrow and spleen samples taken from these mice were again stained for GR1 and CD11b. As in the Deleter-IL-17A$^{ind/+}$ and K14-IL-17A$^{ind/+}$ mice, ROSA-Cre^{ERT2}-IL-17A$^{ind/+}$ BM and SPL showed highly significant upregulations of granulocytes (Fig.10B and C). Cryosections prepared from spleens of tamoxifen-treated IL-17A$^{ind/+}$ and K14-IL-17A$^{ind/+}$ mice were further subjected to immunostaining. Antibodies specific to EGFP and GR1 were used to stain tissue

sections. EGFP^{+} cells can clearly be seen in ROSA-Cre-IL-17A$^{ind/+}$ mice, and this correlates highly with increased amounts of GR1^{+} cells in the SPL (Fig.10D). In conclusion, the ROSA-Cre-IL-17A$^{ind/+}$ system offers timely induction of IL-17A expression upon administration of tamoxifen.

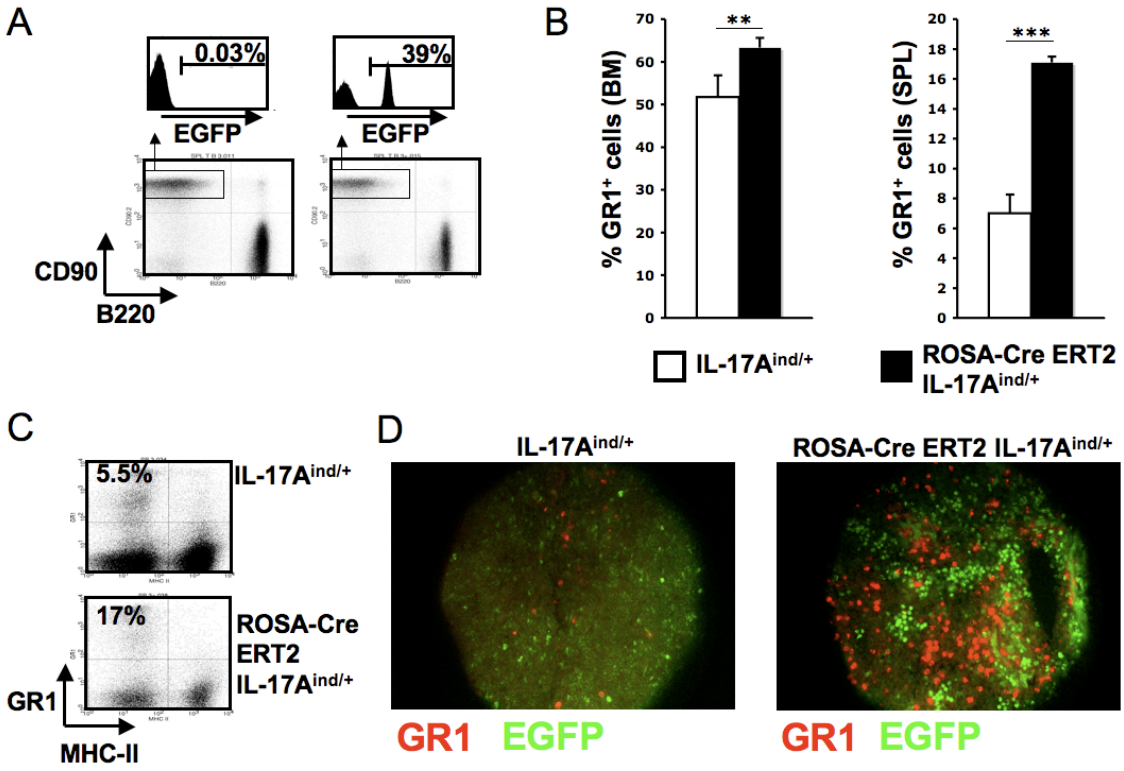

Fig. 10: Tamoxifen administration induces increased granulopoiesis in ROSA-Cre^{ERT2}-IL-17A$^{ind/+}$ mice: (A) Cohorts of ROSA-Cre^{ERT2}-IL-17A$^{ind/+}$ mice and Cre- control mice were treated with tamoxifen for 4d. Induction of IL-17A expression was confirmed from SPL-derived single cell suspensions after 10d. (B) BM and SPL single cell suspensions were stained for GR1. Percentages and significant differences between indicated groups are illustrated using bar charts. (C) SPL cells as in (B) were stained for MHC-class II and GR1. Percentages of cells are given in the FACS-plots. (D) Cryosections from spleens of tamoxifen-treated ROSA-Cre^{ERT2}-IL-17A$^{ind/+}$ and IL-17A$^{ind/+}$ mice were stained with anti-EGFP (FITC) and anti-GR1 (PE) antibodies.

3.3 CD4-Cre IL-17A^{ind} creates an IL-17A overexpressing T cell repertoire.

Cre recombinase can induce recombination in either a tissue or cell-type specific manner. As shown in the Deleter IL-17A$^{ind/+}$ and K14-IL-17A$^{ind/+}$ strains, systemic or skin-specific IL-17A overexpression results in an overt granulocytosis, which is ultimately pathogenic and potentially fatal. However, given the well-researched field

of Th17 cells, whose hallmark cytokine is IL-17A, it was a logical step to use the IL-17A^{ind} allele to create a T cell repertoire in which all T cells would express IL-17A. To this end, the IL-17A$^{ind/ind}$ mice were crossed to the CD4-Cre transgene, yielding the CD4-Cre-IL-17A$^{ind/+}$ strain. In this model, all T cells should overexpress IL-17A. We

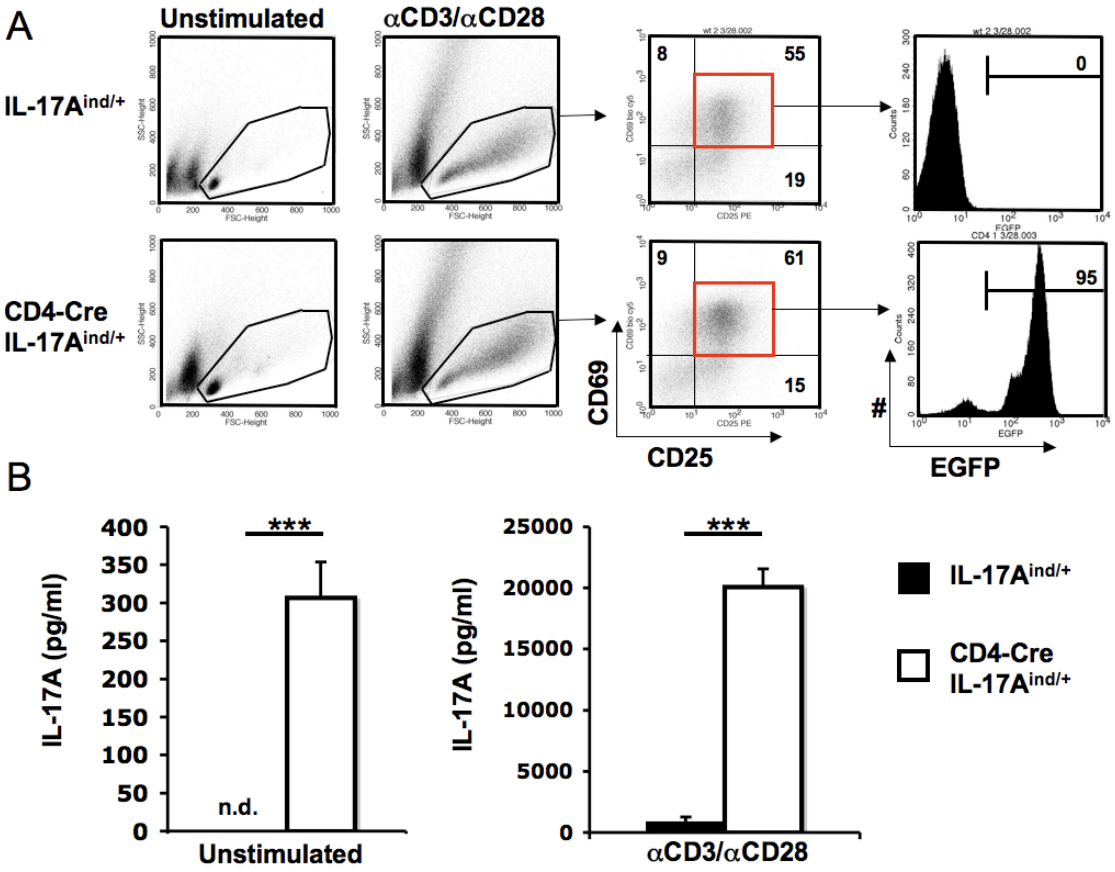

Fig. 11: CD4-Cre IL-17A$^{ind/+}$ T cells overexpress IL-17A: (A) MACS-purified CD4+ T cells from CD4-Cre- IL-17A$^{ind/+}$ and IL-17A$^{ind/+}$ mice were cultured in the presence of anti-CD3 and anti-CD28. 36h after activation, cells were stained for expression of CD25 and CD69. Histograms represent EGFP expression in CD25^{+}CD69^{+} T cells. (B) FACS-sorted CD4+ T cells from CD4-Cre- IL-17A$^{ind/+}$ or IL-17A$^{ind/+}$ mice were cultured in the presence or absence of anti-CD3 and CD28 for 24h. Supernatants from these cultures were taken and IL-17A-specific ELISA was performed. Error bars represent +/-SD and statistical significance was calculated using the student's t-test. Each panel respresents at least two similar experiments.

reasoned that the importance of IL-17A signaling in EAE would be obvious in mice where T cells were endowed with an overexpression of IL-17A. If current thinking on the pathogenic role of IL-17A was indeed correct, mice with an increase of IL-17A delivery into the CNS during autoimmune neuroinflmmation would increase the severity of the pathogenesis observed in WT mice. We sought to confirm IL-17A overexpression and functionality of T cells, and to address the role of IL-17A signaling in EAE in the context of the CD4-Cre IL-17A^{ind} model.

Lymph nodes were isolated from CD4-Cre IL-17A$^{ind/+}$ and littermate controls. CD4^{+} T cells were magnetically sorted and cultured for 3d in the presence of anti-CD3 and anti-CD28 to achieve a polyclonal activation of the lymphocytes. Both CD4-Cre IL-17A$^{ind/+}$ and IL-17A$^{ind/+}$ CD4^{+} T cells showed no differences in ability to blast in response to stimulation, or in upregulation of classical T cell activation markers CD25 and CD69 (Fig.11A). EGFP expression was also clearly detectable in activated CD4-Cre IL-17A$^{ind/+}$ T cells, but not detectable in control cultures (Fig.11A).

To verify the increased IL-17A secretion in CD4-Cre IL-17A$^{ind/+}$ T cells, we performed IL-17A–specific ELISA assays with FACS-sorted CD4-IL-17A$^{ind/+}$ and IL-17A$^{ind/+}$ CD4^{+} T cells after 24 hours in the presence or absence of CD3 and CD28 cross-linking. As expected, CD4-Cre IL-17A$^{ind/+}$ CD4^{+} T cells constitutively secreted elevated levels of IL-17A compared with control IL-17A$^{ind/+}$ T cells. This secretion was greatly enhanced after polyclonal stimulation with anti-CD3/anti-CD28 (Fig.11B).

3.3.1 CD4-IL17A$^{ind/+}$ T cells do not overtly affect lymphocyte development, homeostasis or peripheral tolerance.

Crossing the IL-17A^{ind} with CD4-Cre–expressing mice generated a T cell repertoire, in which both CD4^{+} and CD8^{+} T cells excise the STOP cassette and express the EGFP reporter. Given the early activity of the CD4-Cre transgene, we sought to determine whether early IL-17A expression in the thymus would effect thymocyte differentiation. Thymi from CD4-Cre IL17A$^{ind/+}$ and IL-17A$^{ind/+}$ mice were taken and assayed for EGFP^{+} thymocytes. As early as the double-negative (DN) stage of thymocyte development, a significant proportion of thymocytes express EGFP (Fig.12A). As thymocytes upregulate CD4 and CD8 coreceptors at the double positive (DP) stage, already 68% of thymocytes express EGFP. Single positive T lymphocytes were all EGFP^{+}, showing a full deletion of the STOP cassette before CD4-Cre-IL-17A$^{ind/+}$ leave the thymus. As expected, T cells also express EGFP in the periphery of CD4-Cre IL-17A$^{ind/+}$ mice. We also observed normal numbers of Tregs in the peripheral immune compartments of these mice.

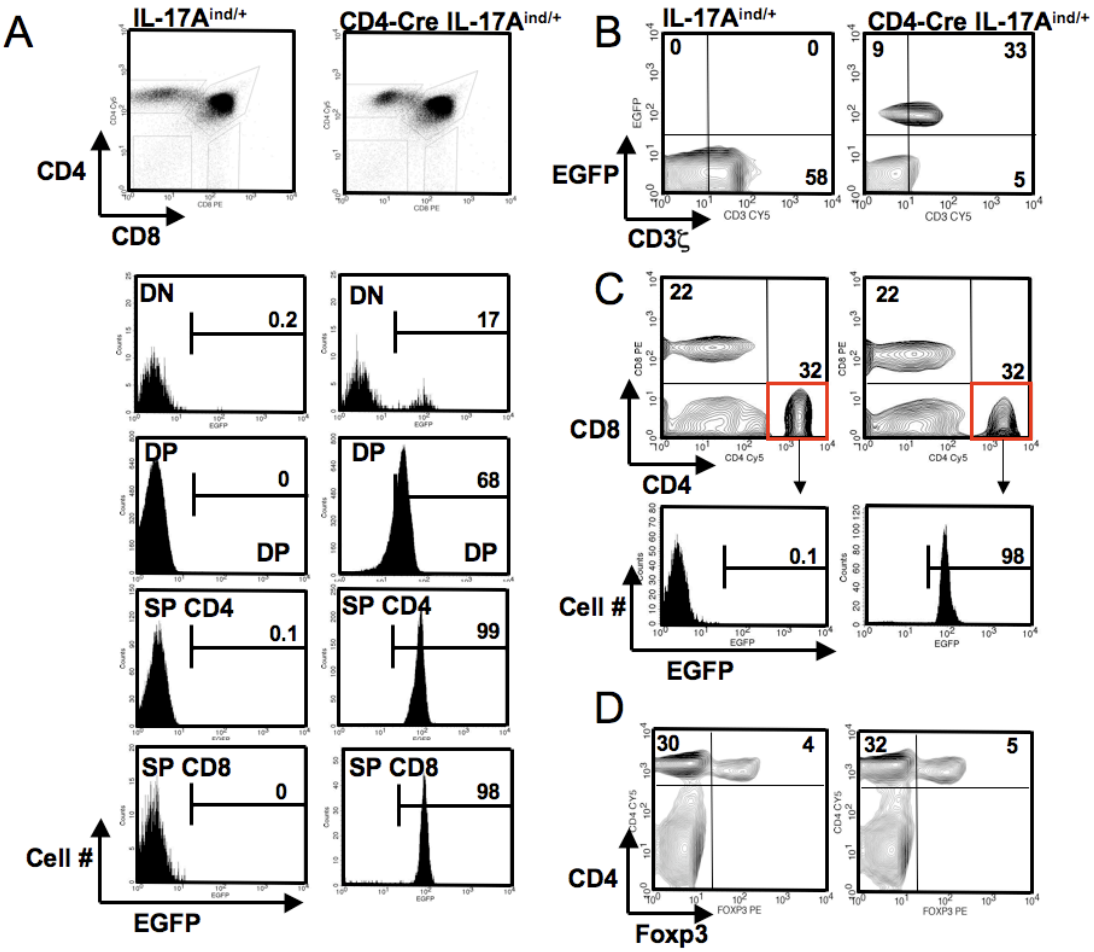

Fig. 12: T cell development is unaffected in CD4-Cre IL-17A$^{ind/+}$ mice. (A) Thymi from CD4-Cre-IL-17A$^{ind/+}$ and IL-17A$^{ind/+}$ mice were isolated and single cell suspensions prepared. Thymocytes were stained for CD4 and CD8 coreceptors, and EGFP expression asayed in double negative (DN), double positive (DP) and CD4 or CD8 single positive (SP CD4 and SP CD8, respectively) stages of thymocyte development. (B and C) Peripheral T cells were assayed for expression of EGFP. (D) LN-derived cells from CD4-Cre- IL-17A$^{ind/+}$ and IL-17A$^{ind/+}$ mice were stained for CD4 and Foxp3. Percentages are given in the quadrants.

3.3.2 CD4-Cre IL-17A$^{ind/+}$ mice show increased granulopoiesis.

Considering that no effects on T cell homoestasis were observed despite a successful recombination using the CD4-Cre transgene, but that CD4-Cre IL17A$^{ind/+}$ T cells constitutively express IL-17A in vitro (Fig.11A), we sought to examine if *ex vivo* T cells form this strain do indeed constitutively express IL-17A. It was found that CD4-Cre IL17A$^{ind/+}$ T cells constitutively produce IL-17A in the steady state, and this is shown to directly correlate with expression of EGFP (Fig.13A). Considering that IL-17A has been shown to affect granulopoiesis in our previous models, we examined granulocyte homeostasis in the CD4-Cre IL17A$^{ind/+}$ strain. CD4-Cre IL17A$^{ind/+}$ T cells

are readily detectable in the BM of naïve CD4-Cre IL17A$^{ind/+}$ mice, however no significant increase in CD11b^{+}GR1^{+} cells in the BM was detectable. We observed a minor but significant increase in the number of granulocytes in peripheral blood. Also, a reduction in the mean percentage of peripheral blood lymphocytes accompanied this increase.

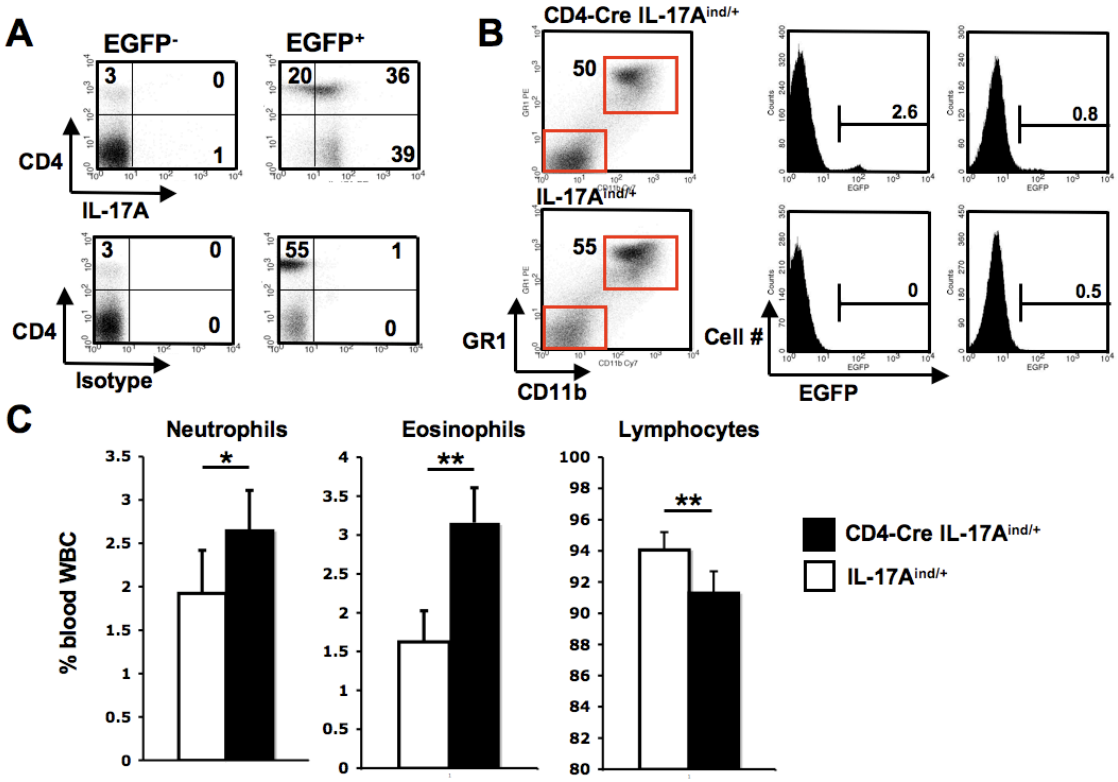

Fig. 13: CD4-Cre- IL-17A$^{ind/+}$ show increased granulopoiesis: (A) LN-derived CD4-Cre-IL-17A$^{ind/+}$ cells were restimulated in PMA, Ionomycin and Berfeldin A. Restimulated cells were stained intracellularly with anti-IL-17A or an isotype control antibody. (B) BM isolated cells from CD4-Cre- IL-17A^{ind} mice were stained for CD11b and GR1. Histograms show GFP expression in CD11b^{+}GR1^{+} and CD11b^{-}GR1^{-} gates of the indicated genotypes. (C) Blood samples from CD4-Cre- IL-17A$^{ind/+}$ and IL-17A$^{ind/+}$ mice were subjected to routine WBC analysis. Changes in percentages of the indicated cell types are shown. Error bars represent +/-SD and statistical significance was calculated using the student's t-test. Each panel respresents at least two similar experiments.

After subcutaneous immunization of CD4-Cre IL17A$^{ind/+}$ and littermate controls with myelin oligodendrocyte glycoprotein 33–55/CFA ($MOG_{35–55}$/CFA), we observed a highly significant increase in serum IL-17A, which correlated to enhanced neutrophil recruitment into the spleen, thus confirming *in vivo* the ectopic activity of IL-17A produced by CD4-Cre IL17A$^{ind/+}$ T cells.

3.3.3 IL-17A–overexpressing T cells do not enhance the pathogenesis and clinical development of myelin oligodendrocyte glycoprotein–induced EAE.

We immunized CD4-Cre IL-17A$^{ind/+}$ mice with MOG35–55/CFA and pertussis toxin to induce and follow progression of EAE. Surprisingly, no significant clinical differences were observed between CD4-Cre IL-17A$^{ind/+}$ and IL-17A$^{ind/+}$ littermates in a series of experiments (Fig.14A). Consistent with the clinical disease, cellular CNS invasion was virtually identical in both groups as measured by flow cytometry. However, a clearly identifiable population of IL-17A-overexpressing T cells was observed in the lymphocytes isolated from the inflamed spinal cord and brains of CD4-Cre IL-17A$^{ind/+}$ mice (Fig.14B). Despite similar clinical scores, flow cytometric cytokine analysis revealed a significant increase in IL-17A secretion from CNS-isolated CD4-Cre IL-17A$^{ind/+}$ T cells, while other proinflammatory cytokines associated with EAE, including IFN-γ, IL-6, IL-22 or GM-CSF, remained unaltered (Fig.14C). Taken together, exacerbated T cell–mediated delivery of IL-17A into the inflamed CNS during MOG-induced EAE does not result in an appreciable alteration of the disease course.

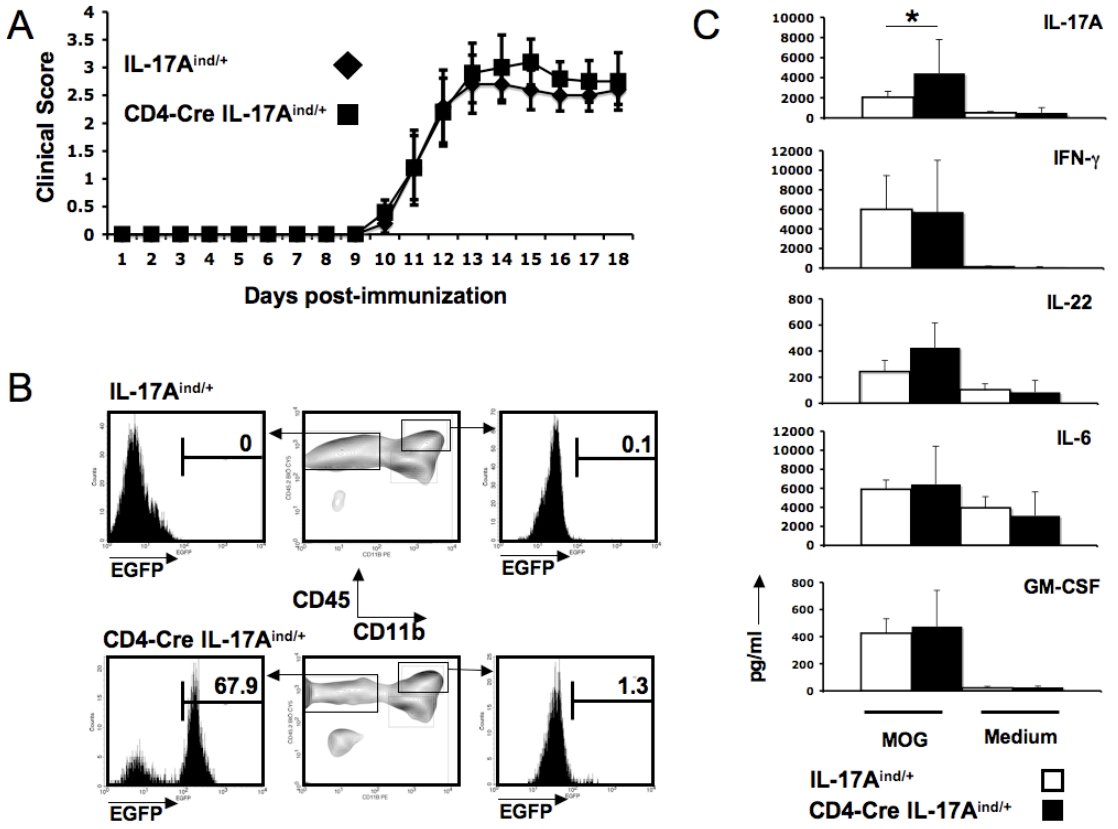

Fig. 14: T cell overexpression of IL-17A does not exacerbate EAE: (A) CD4-Cre- IL-17A$^{ind/+}$ and IL-17A$^{ind/+}$ mice were immunized with MOG peptide emulsified in CFA and pertussis toxin. Signs of paralysis were scored daily after disease induction. Data shown represent three independent experiments. (B) CNS-invading lymphocytes were isolated from brain and spinal cord homogenates at d14 after immunization. Cells were stained for CD45.2 and CD11b. Histograms show % EGFP expression in the indicated gates. (C) Cell suspensions as prepared in (B) were placed in culture with 10ug/ml MOG-peptide. After 48h, indicated cytokines were measured using flow cytomix. Significance was calculated using the student's t-test.

3.3.4 IL-17A overexpression does not exacerbate hapten-induced CHS-responses

Contact hypersensitivity (CHS) is a DC-dependent T cell-mediated immune response induced after epicutaneous sensitization with haptens, which become immunogenic after binding amino acid residues of proteins or peptides. CHS reactions in mice and humans are mediated by Th1/T cytotoxic 1 (Tc1) effector cells, and downregulated by Th2/T regulatory (Treg) CD4+ T cells (Bour et al., 1995; Kehren et al., 1999).

The CHS response develops in two distinct phases. In the sensitization phase (i.e., afferent or induction phase of CHS), haptens penetrating the skin are captured by resident DC, which migrate to regional lymph nodes and induce activation of specific T cell precursors. The elicitation phase (i.e., efferent phase) of CHS is induced by re-

exposure to the same hapten at a different skin site. This leads to the rapid recruitment and activation of specific T cells, and to the constitution of a local inflammatory response, which peaks at 24–48 h after challenge, and progressively decreases via active down-regulating mechanisms.

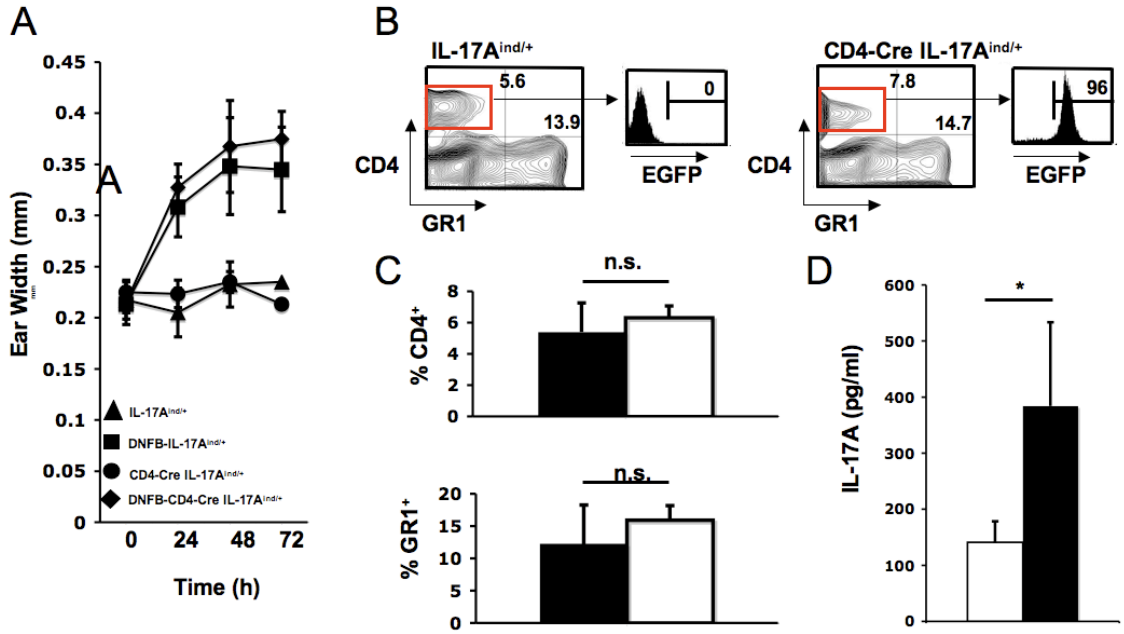

Fig. 15: T cell overexpression of IL-17A does not exacerbate hapten-induced ear swelling: (A) CD4-Cre- IL-17A$^{ind/+}$ and IL-17A$^{ind/+}$ mice were sensitized on the shaved belly with 2% DNFB in ethanol. 5 days later, 0.5% DNFB or vehicle was reapplied to the ears of sensitized mice. DNFB-induced ear swelling was measured daily. Data shown represents two independent experiments. (B) Single cell suspensions were prepared from DNFB-treated ears from indicated mice and stained for GR1 and CD4. EGFP signal is depicted in the histograms from indicated gates. (C) Percentages of either GR1+ or CD4+ cells are shown. (D) 2x10^5 cells from DNFB-treated ears of CD4-Cre- IL-17A$^{ind/+}$ mice were cultured for 48h. IL-17A-specific ELISA was performed on supernatants.

A mouse model of CHS, based on exposure to the hapten 2,4-dinitrofluorobenzene (DNFB) shows that CHS is exclusively mediated by CD8$^+$ Tc1 CTLs, which develop in secondary lymphoid organs upon hapten presentation by MHC class I-expressing DC. These CD8$^+$ effector T cells migrate to the challenged site (Desvignes et al., 1998) and initiate the skin inflammation via Fas and/or perforin-mediated cytolytic function (Kehren et al., 1999). These reports suggested that the development of CHS was secondary to the presentation of haptenated peptides by MHC class I-expressing skin cells to specific CD8 CTLs. It was shown that the development of the skin inflammation during the efferent phase of CHS is initiated by rapid recruitment of CD8$^+$ T cells in the epidermis of challenged skin, associated with

the induction of KC apoptosis (Akiba et al., 2002). $CD4^+$ T cell infiltration occurs hours later at a time where the CHS response starts to subside. Thus, the CHS reaction is secondary to differential recruitment in the skin of effector Tc1 $CD8^+$ T cells and down-regulatory Th2/Treg $CD4^+$ T cells. A role for IL-17A has been proposed in CHS using IL-17A deficient mice (Nakae et al., 2002). In addition, it was shown that depletion of neutrophils was sufficient to significantly inhibit the CHS response (Dilulio et al., 1999). We therefore tested the role of IL-17A overexpression in development of DNFB-mediated inflammation.

Cohorts of CD4-Cre IL-$17A^{ind/+}$ and IL-$17A^{ind/+}$ mice were shaved on the belly, and DNFB was applied. After 5 days, mice were rechallenged on one ear with DNFB to induce recruitment of specific T cells and the immune response to the reapplied hapten. The other ear remained treated only with ETOH, the vehicle used to apply the DNFB. The swelling induced by the reapplication of the hapten was measured for the next three days. No significant differences were observed in ear thickness between CD4-Cre IL-$17A^{ind/+}$ and IL-$17A^{ind/+}$ mice (Fig.15A). T cells stainings revealed that the $EGFP^+$ CD4-Cre IL-$17A^{ind/+}$ T cells successfully migrate to the site of inflammation (Fig.15B). Slight increases were noted in both $CD4^+$ T cell and $GR1^+$ populations, however this trend was statistically insignificant (Fig.15C). Samples of cellular infiltrates isolated from the ears of CD4-Cre IL-$17A^{ind/+}$ and IL-$17A^{ind/+}$ mice after 72h were placed into culture and assayed for local IL-17A production. Despite the lack of augmented inflammation, significant upregulations of IL-17A were detectable in ears taken from CD4-Cre IL-$17A^{ind/+}$ mice compared to controls (Fig.15D). Collectively these data show that increased IL-17A expression does not dramatically augment hapten-induced CHS responses in this system.

4 IL-17F-Cre^{EYFP}

An ever-increasing list of publications has resulted in the establishment of pathogenic T helper 17 (Th17) cells, a T cell subset definable by expression of CD4, interleukin (IL)-17A, IL-17F and to varying extents IL-6, IL-21, IL-22, TNF-α and CCR6 (Awasthi et al., 2007; Korn et al., 2007b; Park et al., 2005). The required signaling molecules for murine Th17 differentiation have already been characterized, with IL-6 or IL-21 in combination with TGF-β1 being the basic *in vitro* requirement (Bettelli et al., 2006; Korn et al., 2007a). Further signaling through the IL-23 receptor is required to expand and render the new Th17 cells effective and pathogenic, such that experimental autoimmune encephalomyelitis (EAE) can be passively transferred (McGeachy et al., 2007) (McGeachy et al., 2009).

With the interest in Th17 cells escalating so vehemently, new questions have appeared concerning the location of *in vivo* generation, migration, expression profiles, proliferation and fate of these potentially pathogenic cells. Reporter mice for T helper cell subsets including Th1 (Mayer et al., 2005), Th2 (Mohrs et al., 2005), and Tregs (Fontenot et al., 2005) have been generated. Until very recently, Th17 cells have lacked reporter strains able to account for their activity (Yang et al., 2008b). Here we introduce a new transgenic strain, in which Cre-recombinase is expressed exclusively from the IL-17F promoter.

4.1 Generation of IL-17A-Cre and IL-17F-Cre alleles

Recombineering with Red/ET allows unlimited cloning, subcloning, and modification of DNA at any given position. Engineering DNA molecules of varying size, including very large ones such as bacterial artificial chromosomes (BACs) or the E.coli chromosome is possible. In Red/ET Recombineering, target DNA molecules are precisely altered by homologous recombination in strains of E.coli, which express the phage-derived protein pair RecE and RecT from the Rac prophage. RecE is a 5´->3´ exonuclease, and RecT is a DNA annealing protein. A functional interaction between RecE and RecT is required to catalyse the homologous recombination reaction. Homologous recombination allows the exchange of genetic information between two DNA molecules in a precise, specific and faithful manner. RedET cloning simplifies the process of achieving homologous recombinaiton at any chosen site of a target DNA molecule (http://www.recombineering.net/gb/red_et_principles.php).

Given the proximity of both the IL-17A and IL-17F locus in the genome, it was possible to select a 165kb BAC containing both the IL-17A and IL-17F loci (Fig.16A). BAC-containing E. Coli was purchased commercially from the ‚BACPAC' resources centre. (http://bacpac.chori.org). After arrival of the BAC, we used Red/ET recombineering protocols to carry out a homologous recombination into both IL-17A and IL-17F loci.

The same targeting construct was used to generate both IL-17A-Cre and IL-17F-Cre alleles. From the initial targeting vector, a kind gift from Dr. Thorsten Buch in Zürich, we used primers to amplify the Cre-recombinase ORF, a bovine Poly-A tail (BPA) and an frt-flanked double resistance cassette for kanamycin and neomycin. The double resistance cassette allows selection in both prokaryotic and eukaryotic cells, respectively. The primers were tipped with 60bp homology arms. The 5' arm was homologous to the promoter region of the IL-17F-locus, and the 3' arm homologous to a 60bp region located in intron 2 of the IL-17F locus (Fig.16A). In this configuration, a successful recombination will ablate expression of IL-17F, but simultaneously place expression of the Cre-recombinase under the control of the endogenous IL-17F promoter.

Subsequent to electroporation in E. Coli and selection of Kanamycin-resistant colonies, we needed to confirm that the entire construct had been successfully recombined into the endogenous IL-17A and IL-17-F loci. To this end, primers placed

at the most 5' and 3' ends of the modified BACs were used to amplify the targeting cassette. The correct product was detectable in both IL-17A-Cre and IL-17F-Cre BACs, but remained undetectable in unmodified BAC template DNA (Fig.16B). To confirm a homologous recombination, a 5' primer was placed upstream of the 5' arm of homology. The 3' primer was located in the ORF of the Cre recombinase. Control PCRs for the unmanipulated exon 3 in both IL-17F and IL-17A loci were performed in parallel. Correctly sized PCR products for both the IL-17A-Cre (1.35kb) and IL-17F-Cre (1.5kb) modified BACs were identified (Fig.16C). Modified BAC DNA from both constructs was then linearized with restriction enzyme (PI-SceI) and cleaned using Sepharose beads. Linearized DNA was used for pronuclear injection at a final concentration of 1.6ng/ml. Offspring obtained from the pronuclear injection were genotyped from a tail biopsy (Fig.16D).

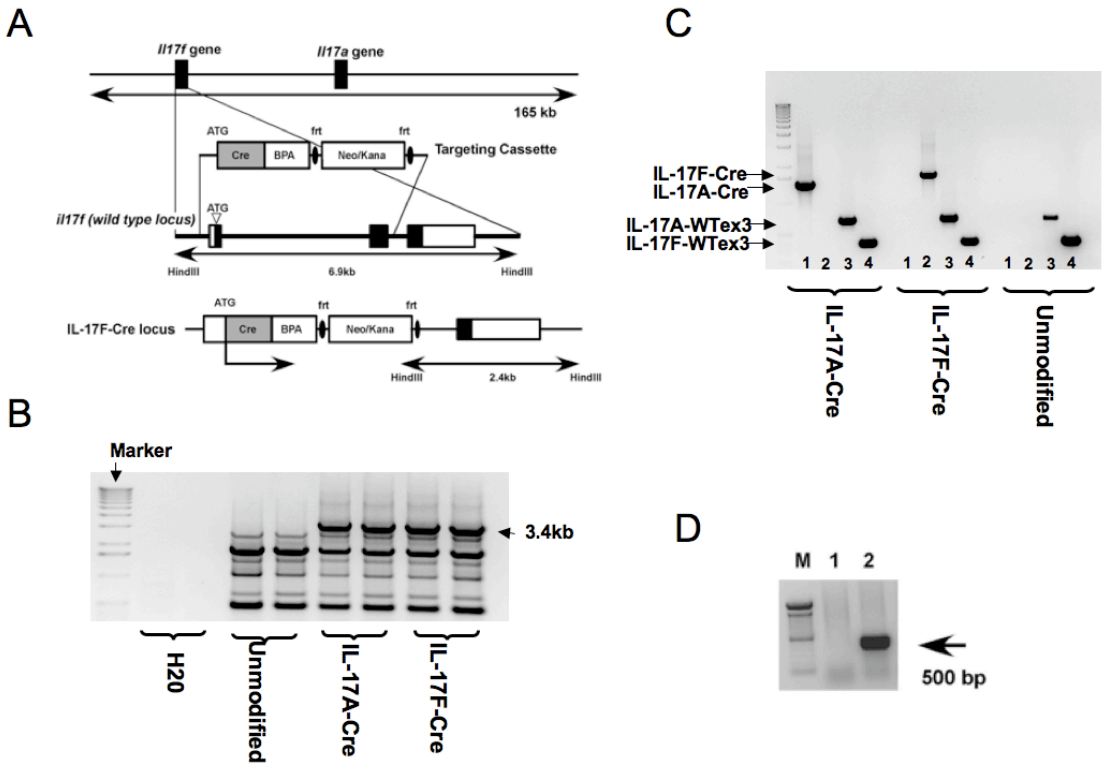

Fig. 16: Generation of IL-17A-Cre and IL-17F-Cre alleles BAC: (A) Schematic representing the generation of the IL-17F-Cre allele. (B) PCR to amplify the targeting vector was performed in BAC DNA isolated from modified IL-17A-Cre and IL-17F-Cre modifed BACs. The 3.4kb band represent the integration of the entire targeting cassette. (C) PCR to confirm homologous recombination of IL-17A-Cre and IL-17F-Cre modified BACs (D) PCR for the IL-17F-Cre allele in a tail biopsy of a founder IL-17F-Cre transgenic mouse (lane 2) and a wt control (lane 1).

Crossing the newly generated IL-17F-Cre mice to inducible ROSA26-EYFP reporter mice (Srinivas et al., 2001) allowed us to analyze the generation and location of Th17

cells. Cre-mediated highlighting of Th17 cells also induces a non-reversible fluorescence in IL-17F-expressing T cells, allowing us to map the fate of IL-17F-expressing cells *in vivo*. From this point onwards, the IL-17F-Cre x ROSA26 EYFP strain will be referrred to as IL-17F-Cre^{EYFP}.

It is also worth noting that the work for generation of IL-17A-Cre and IL-17F-Cre alleles was performed in parallel. Both pronuclear injections were performed, and founder animals were obtained for both IL-17A-Cre and IL-17F-Cre alleles. Unfortunately, no functionality from any of the 6 IL-17A-Cre founder animals was identified after crossing to the ROSA26 EYFP strain. As a result of this, all work hereafter presented in this section is based on the functional IL-17F-Cre allele.

4.1.1 Th17 conditions induce IL-17F expression in both CD4 and CD8 IL-17F-Cre^{EYFP} T cells

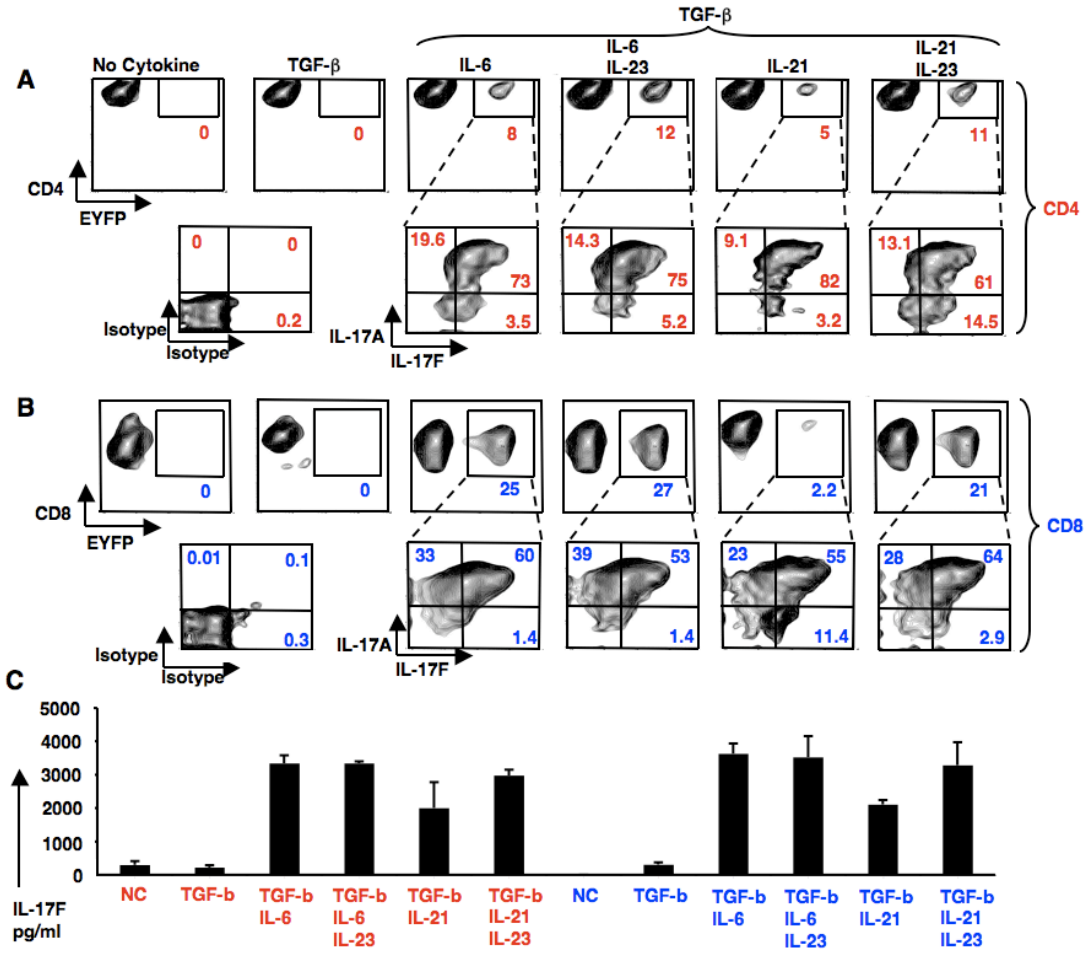

Fig. 17: IL-17F-Cre^{EYFP} T cells express EYFP in response to Th17-polarizing cytokines: Purified naïve CD4 (A) or CD8 (B) T cells were activated in the presence of the indicated cytokine combinations. EYFP induction is shown in the gates. The same cells were stained for expression of IL-17A and IL-17F (A and B). (C) Supernatants from these cultures were assayed for IL-17F secretion.

Most published Th17 differentiations show expression of IL-17A. We wanted to observe the expression of IL-17F under conditions shown to promote Th17 differentiation and to examine how this expression relates to that of its relative, IL-17A. In addition to TGF-β, both IL-21 and IL-6 have been shown to promote Th17 differentiation (Korn et al., 2007a), with IL-23 being thought to drive expansion of newly formed Th17 cells (McGeachy et al., 2009). To this end, we purified CD4^{+}CD25^{-} or naïve CD8 T cells and activated them in the presence of Th17-

promoting cytokine cocktails for five days. We observed IL-17F expression from both CD4 and CD8 T cells from IL-17FCre^{EYFP} mice under all Th17-polarizing conditions. The majority of IL-17F expressing Th17 cells also expressed IL-17A (Fig.17A). CD8 T cells also robustly expressed IL-17F in response to the same cytokine cocktails. As observed in Th17 cells, the majority of Tc17 coexpress IL-17A and IL-17F. However, a greater proportion of Tc17 cells downregulate IL-17F, and express IL-17A alone (Fig.17B). In addition to the intracellular staining for IL-17F, we measured cytokine secretion to confirm that EYFP expression correlated with IL-17F protein secreted from IL-17FCre^{EYFP} T cells. A strong correlation was observed between EYFP^{+} cells and IL-17F secretion (Fig.17C). Thus, EYFP^{+} T cells generated from IL-17FCre^{EYFP} mice are bona fide Th17 cells.

In addition to cytokine staining, expression signatures of Th17-related molecules including *il23r* and *irf4* were assayed by real time PCR. Both Th17 and Tc17 cells from IL-17FCre^{EYFP} mice were generated after 5 days of Th17 cultures (Fig.18). Highly elevated levels of both both *il17a* and *il17f* were noted in both Th17 and Tc17 cells. A strong increase in *il23r* expression and a slight increase in *irf4* were also observed. Taken together, this evidence shows that IL-17FCre^{EYFP} T cells both express and secrete Th17-associated molecules.

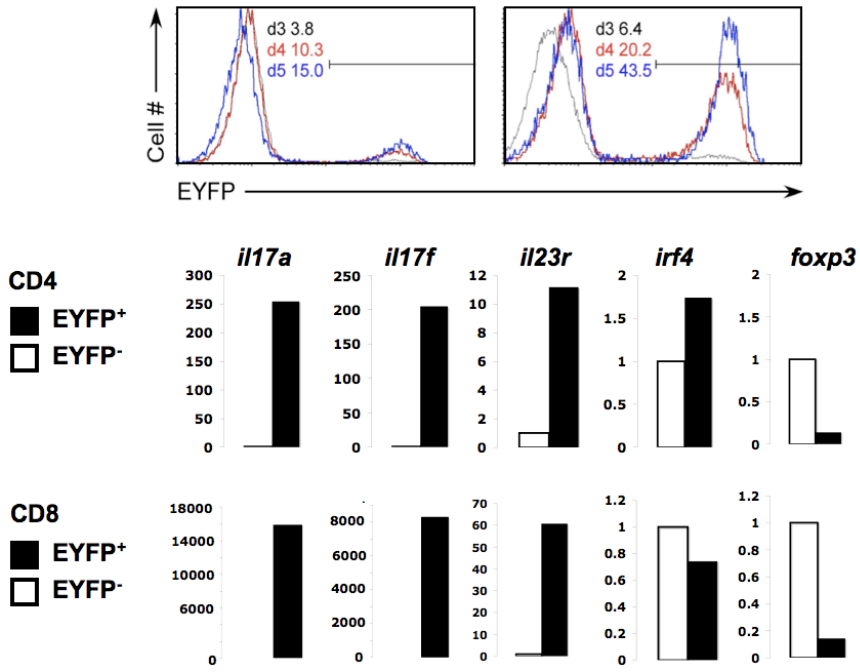

Fig. 18 IL-17F-CreEYFP cells have a Th17 expression signature: Whole splenocytes from IL-17FCre^{EYFP} mice were activated with anti-CD3 and anti-CD28, TGF-β, IL-6 and IL-23 for 5d. Culture wells were sampled at the indicated times and gated for CD4 or CD8 expression by flow cytometry.

Histograms represent the induction EYFP expression at d3 (black line), d4 (red line) and d5 (blue line) of culture. Real time PCR analysis was performed on total RNA isolated from FACS-sorted $EYFP^+$ CD4 or CD8 T lymphocytes (closed) after 5d in Th17 culture conditions for the indicated genes. Control bars (open) represent RNA isolated from FACS-sorted anti-CD3 and anti-CD28-activated CD4 or CD8 T cells. Each panel is representative of at least two independent experiments, with triplicate sorted samples.

4.1.2 IL-17F expression is restricted to $CD4^+$ T cells during MOG-induced EAE

IL-17A is thought to be a major contributor to a number of inflammatory disease models. Following clarification of the IL-17F-expression fidelity in the IL-17FCre^{EYFP} strain and the finding that CD8 T cells robustly express IL-17F and IL-17A, we investigated the localization of IL-17F-expressing T cells during myelin oligodendrocyte glycoprotein (MOG)-induced experimental autoimmune encephalomyelitis. A completely CD4 T cell-restricted (Fig.19A), and more specifically $CD90.2^+CD4^+CD62L^-$ T cell-restricted IL-17F expression was observed in spleen and blood (Fig.19B). Thus, peripheral CD8 T cells readily express IL-17F *in vitro* in response to culture conditions designed to induce Th17 cells, but not during EAE, a predominantly Th1 and Th17-mediated disease.

At d14 after EAE induction, IL-17FCre^{EYFP} mice were sacrificed at a mean clinical score of 3.5 (hind limb paralysis) and brain and spinal cord were analyzed. CNS infiltrates were surface-stained for CD45.2, CD11b, CD4 and intracellular IL-17A. IL-17A and IL-17F expression was restricted to $CD45.2^+CD11b^-$ lymphocytes (Fig.19C). Of these the vast majority were CD4 positive (Fig. 19D). This confirmed a peripherally derived and CD4 T-lymphocyte-restricted expression of IL-17F in the inflamed CNS during EAE. Infiltrating cells were stained in addition for intracellular IL-17A. Of CNS-isolated T cells from EAE-afflicted mice, the majority of Th17 cells present, as defined by either expression of IL-17A, IL-17F, or both, expressed only IL-17A. A proportion of CD4 T cells were co-expressers of both IL-17A and IL-17F, while another population expressed IL-17F exclusively (Fig.19D).

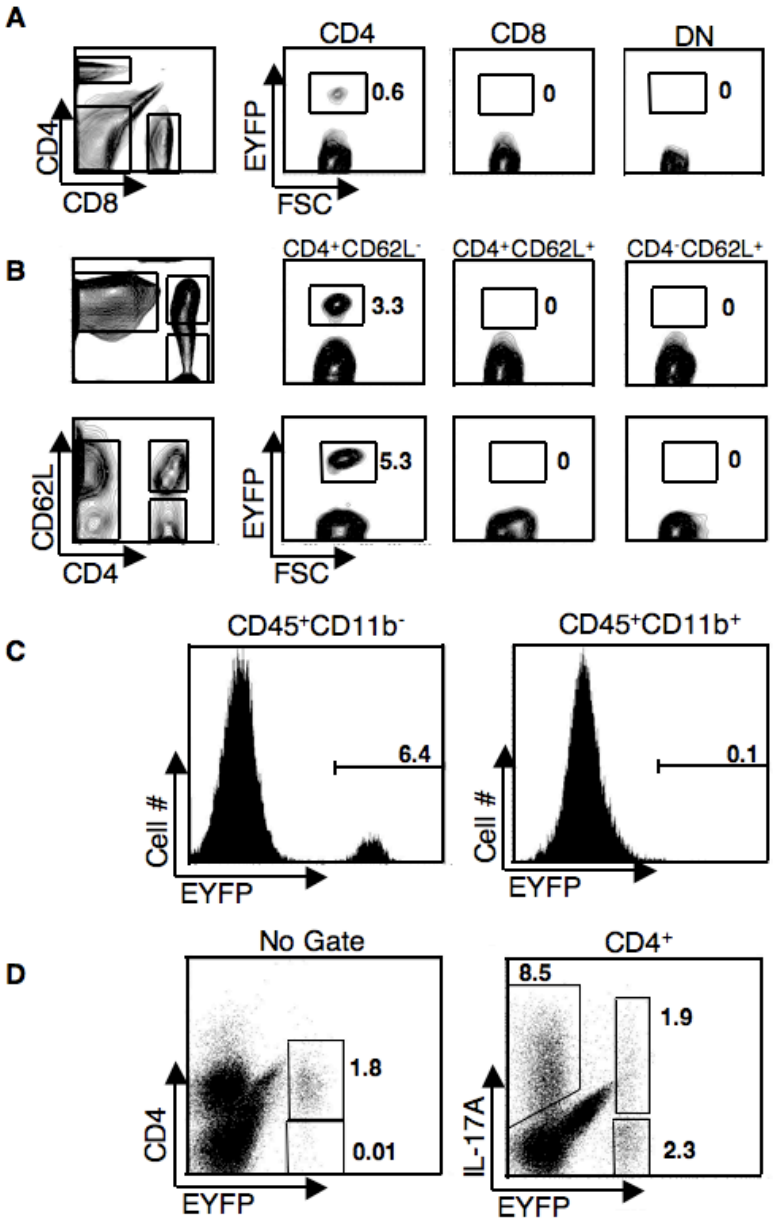

Fig. 19: IL-17F expression is restricted to CD4 T cells during EAE: (A) Splenocytes from EAE-sick mice (d14) were stained for CD4 and CD8 coreceptors. Percentages of gated cells expressing EYFP are given in the gates. (B) Splenocytes (upper row) and PBMC (lower row) were stained for CD62L and CD4. The percentages of gated cells are shown in the regions. (C) CNS-infiltrating cells were isolated and stained for CD45.2 and CD11b. EYFP expression in the indicated populations is shown in the histograms. (D) Total CNS-isolated cells were stained for CD4 and IL-17A. EYFP expression is shown in the indicated cell types.

4.1.3 Th17 cells are resistant to expression of Foxp3 in vivo

The recently described relationship between the developmental pathways of both Th17 and Foxp3-expressing induced regulatory T cells (iTregs) demonstrates TGF-β-signaling as necessary for Foxp3 induction, but TGF-β in combination with IL-6 as a requirement for Th17 differentiation (Bettelli et al., 2006). It has also recently been demonstrated that naturally occurring regulatory T cells can be driven to IL-17A expression in the presence of IL-6 (Yang et al., 2008b). From IL-17FCre^{EYFP} mice, no EYFP expression was detectable in *ex vivo* isolated regulatory T cells or *in vivo* differentiated iTregs (data not shown). We wanted to use the IL-17FCre^{EYFP} system to address whether or not fully differentiated Th17 cells could redifferentiate to Foxp3-expressing T cells whilst in culture, or *in vivo*. IL-17FCre^{EYFP} splenocytes were incubated for five days in culture conditions favoring Th17 differentiation or TCR-stimulated in the absence of the necessary cytokine milieu. After induction of IL-17F expression (Fig.20A), both Th17 and Tc17 cells were sorted and injected i.v. into RAG1$^{-/-}$ hosts. After a period of two weeks, EYFP^{+} cells from both CD4 and CD8 were assayed for expression of IL-17A and IL-17F expression. Both Th17 and Tc17 cells significantly downregulate expression of IL-17A and IL-17F.

We wanted to test if this downregulation in Th17 cytokines was twinned with an upregulation of Foxp3. Th17 cells were differentiated (as in Fig.18), and CD4^{+}EYFP^{+} or CD4^{+}EYFP^{-} cells were sorted and re-cultured in the presence of TGF-β for a further three days (Fig. 20C). Th17 cells were unable to upregulate Foxp3 under these circumstances despite an upregulation in CD4^{+}EYFP^{-} cells derived from non-Th17-stimulated cultures (Fig.20C). We wanted to test whether Th17 cells would differentiate into Tregs *in vivo*. After 5 days in Th17 polarizing conditions, cells were sorted from the cultures according to CD4^{+}EYFP^{+} or CD4^{+}EYFP^{-}. Cells were again transferred i.v. into RAG1$^{-/-}$ host mice. Prior to transfer, cells were stained for Foxp3 to ensure no contaminating Tregs in the transferred cell population (Fig.20D). After two weeks, EYFP^{+} Th17 cells were not able to upregulate Foxp3 expression, but EYFP^{-} cells showed an increase in Foxp3 expression (Fig.20E).

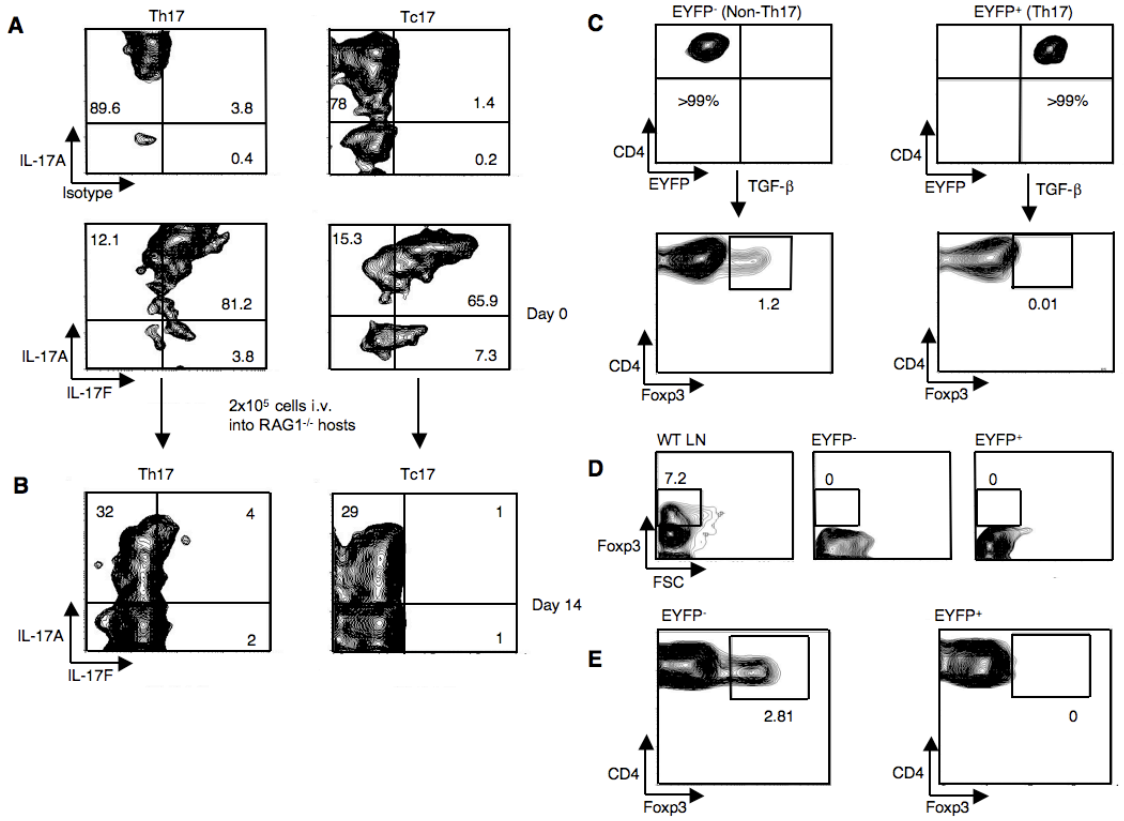

Figure 20: Th17 cells are resistant to Foxp3 upregulation: Th17 and Tc17 cells were raised in a culture from pooled splenocytes isolated from MOG-CFA-immunized IL-17FCre^{EYFP} mice. (A) Whole splenocytes were restimulated using MOG peptide (50 µg/ml) TGF-β, IL-6 and anti-IFN-γ for 4d, then for a further 3d with IL-23 and IL-2. After this culture period, extracted cell samples were stained intracellularly for IL-17A, IL-17F and a fluorochrome-matched isotype control antibody after restimulation with PMA, Ionomycin and Brefeldin A. Dot plots are gated on Th17 (CD4$^+$EYFP$^+$) or Tc17 (CD8$^+$EYFP$^+$) cells. (B) CD90.2$^+$EYFP$^+$ cells were cell sorted from these cultures (>99%), after which 2x10^5 cells were injected into the tail vein of RAG1$^{-/-}$ mice. Dot plots represent IL-17F and IL-17A expression of the transferred Th17 or Tc17 cells after a 14d period of expansion. Percentages of EYFP$^+$ gated cells are shown in the representative quadrants. (C) Magnetically-enriched IL-17F-Cre^{EYFP} CD4$^+$ cells from spleen and lymph nodes were cultured for 5d with anti-CD3, anti-CD28, TGF-β, IL-6 and neutralizing anti-IFN-γ, or TCR-stimulated in the absence of Th17 cytokines. After 5 days, cells were sorted from the cultures according to CD4$^+$EYFP$^+$ or CD4$^+$EYFP$^-$. The sorted cells were switched into 2ng/ml TGF-β-containing medium. After a further 3d, Th17 and control cells were analyzed for upregulation of Foxp3. Numbers in the quadrants represent percentages of CD4+ gated cells. (D) 1x10^5 CD90.2$^+$EYFP$^-$CD25$^-$ or CD90.2$^+$EYFP$^+$ cells from Th17 cultures were FACS sorted (99%) and stained for Foxp3. Percentages of Foxp3$^+$ T cells are given in the gates. (E) 1x10^5 sorted cells (as in (E)) were injected i.v. into RAG-deficient hosts. After 14d, recovered cells were stained for Foxp3. Quadrant numbers represent the percentage of Foxp3-expressing CD4 T cells.

4.1.4 Th17 cells downregulate IL-17 cytokines and express IFN-γ

We further crossed IL-17F-Cre^{EYFP} mice to the 2D2 transgenic strain (Bettelli et al., 2003). The resulting strain was named 2D2-IL-17F-Cre^{EYFP}. From this strain, pure MOG-specific Th17 cells can be generated. Having found in the previous series of

experiments that Th17 cells are resistant to expression of Foxp3 during a period of homeostatic expansion, we wanted to further address the issue of Th17 plasticity with respect to IFN-γ expression. Since Cre-mediated excision of the floxed-STOP-cassette results in EYFP expression from the ROSA26 promoter, cells expressing Cre are irreversibly highlighted, independent of their later expression pattern. We sorted *in vitro*-generated $CD4^+EYFP^+$ T cells and injected them into $RAG1^{-/-}$ hosts. As expected, CD4 T cells were able to expand and repopulate the secondary lymphoid organs (Fig. 21A). We found a large proportion of

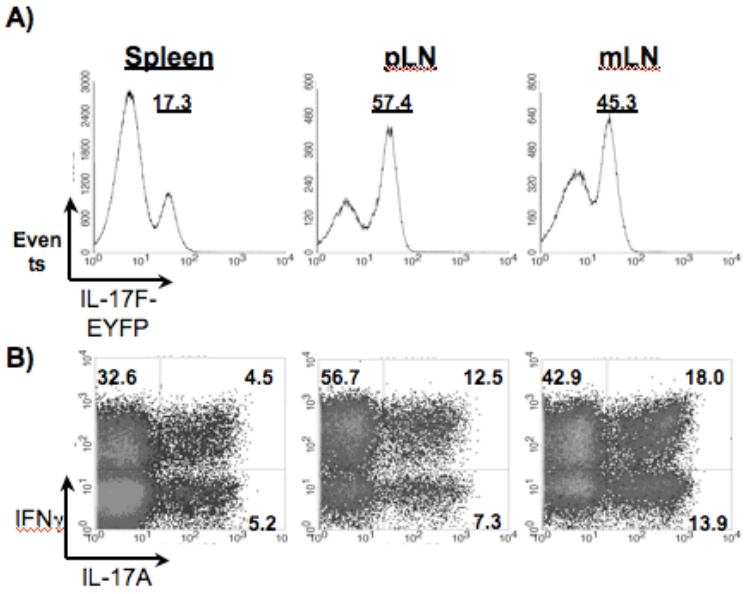

Fig. 21: Th17 cells express IFN-γ after homeostatic expansion : (A) Th17 cells from 2D2-$IL17FCre^{EYFP}$ mice were raised *in vitro* with MOG peptide, TGF-β, IL-6 and anti-IFN-γ in the presence of BMDCs for 5d. CD4 T cells were isolated from pooled splenic and lymph node-derived $CD4^+$ T cells. The resulting $EYFP^+$ cells were sorted through a $CD4^+EYFP^+$ gate. To a purity of 99%. $2x10^5$ cells were immediately injected intravenously into $RAG1^{-/-}$ host mice. After a period of two weeks, SPL, MLN and PLN from $RAG1^{-/-}$ host mice were isolated. $EYFP^+$ cells present in these organs are shown in histograms. Percentages of $EYFP^+$ cells in the gates are shown. (B) Cells from (A) were intracellularly stained for IFN-γ and IL-17A. Dot plots represent $CD4^+EYFP^+$ gated cells after 14d in $RAG1^{-/-}$ hosts.

the transferred Th17 cells were able to redirect their expression from IL-17A expression to IFN-γ (Fig.21B). Peripheral LNs (pLN) were analyzed separately from mesenteric LNs (mLN). Most prominently in mLNs a double positive population (12.5% and 18%) was observed. Interestingly, a large proportion of these cells ceased to express IL-17A, and expressed only IFN-γ. These data suggest that IL-17 cytokine expression is a temporary phenomenon, and clearly show that Th17 lineage

‚commitment' does not exclude a subsequent Th1-like phenotype. Therefore, no irreversible epigenetic changes take place in in vitro generated Th17 cells that later inhibit upregulation of IFN-γ, the hallmark cytokine of Th1 cells. These data collectively illustrate that the plasticity of the transferred Th17 population when in a lymphopenic environment and undergoing homeostatic expansion.

To clarify whether Th17 cells can shift to become IFN-γ expressors during the course of EAE, we polarized 2D2-IL-17F-Cre^{EYFP} CD4^{+} T cells to a Th17 phenotype for 5 days, and sorted these cells based on expression of EYFP. 2x10^{5} EYFP^{+} CD4 cells (95% purity) were intraveinously tranferred into RAG1-deficient host mice. We reasoned that these numbers would be insufficient to induce fulminant passive EAE, and therefore co-transferred 1x10^{7} polarized 2D2-Th1 cells, which expressed IFN-γ and negligible amounts of IL-17A.

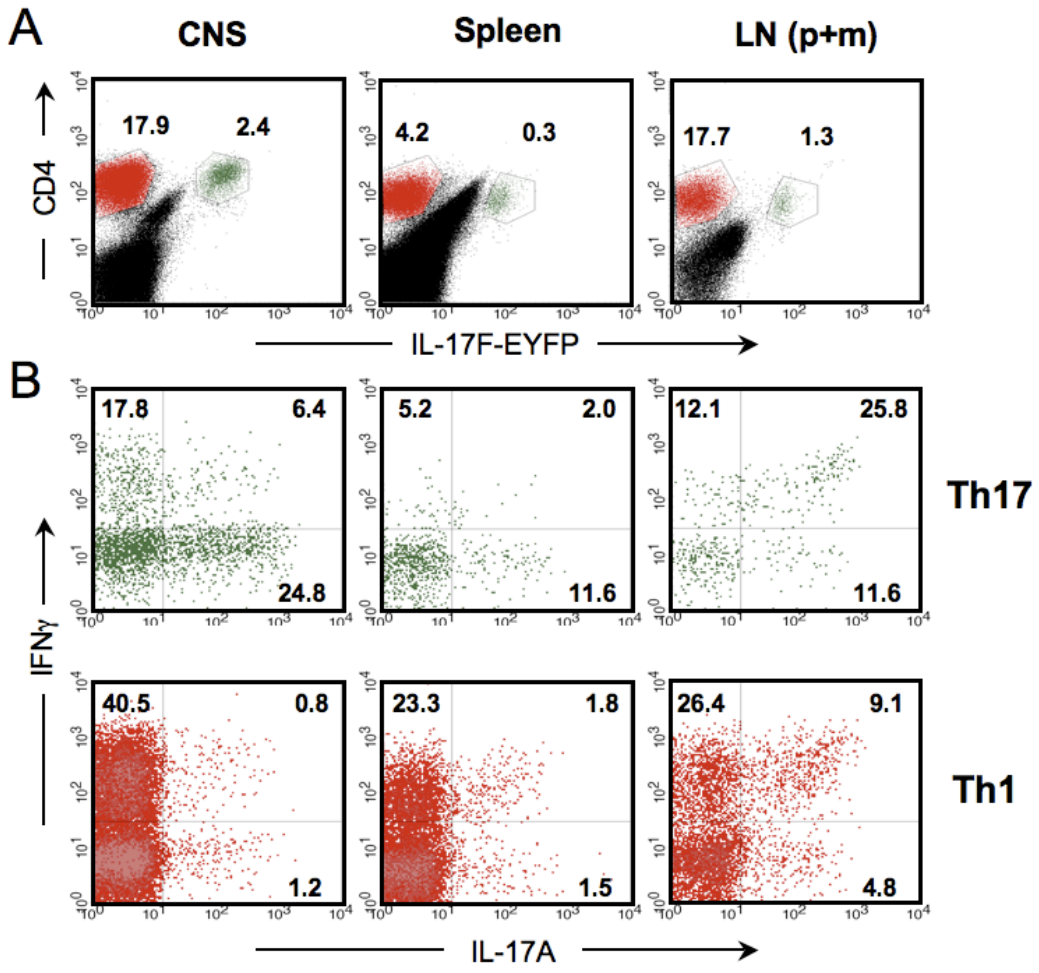

Fig. 22: In vitro-generated Th17 cells express IFN-γ during passive EAE transfer : (A and B) 14d after cotransfer of Th1 and Th17 cells, lymphocytes were isolated from the indicated organs and stained for CD4, IL-17A and IFN-γ. Red cells indicate 2D2 Th1 transferred cells, and green cells represent

Th17 cells, based on expression of CD4 and presence of absence of EYFP. Percentages of gated cells are shown in the quadrants.

The combination of Th17 cells and Th1 cells successfully induced a passive EAE. At the peak of disease, we reanalyzed the transferred cells in the CNS, spleen and lymph nodes (Fig. 22A and B). According to EYFP expression, transferred Th1 could easily be differentiated from transferred Th17 cells (Fig. 22A). Th17 cells recovered from the CNS lost their expression of IL-17A to a large extent and a proportion of these cells expressed only IFNγ (17.8%) or both cytokines (6.4 %) (Fig.F). Of all organs analyzed, the loss of IL-17A expression was most striking in the spleen. Interestingly Th17 cells harvested from the LNs tended to express both IL-17A and IFNγ (25.8%). Compared to Th17 cells, the transferred 2D2-Th1 cells recovered from CNS and spleen retained largely their pre-transfer Th1 expression phenotype. Interestingly, CNS infiltrating Th1 cells kept the largest IFNγ positive population. Surprisingly, Th1 cells recovered from the pLNs showed a consistent population of IL-17A/IFN-γ double positive cells (9.1%) (Fig. 22B). These data prove that Th17 cell populations are able to change their programming with respect to cytokine secretion.

4.1.5 IFN-γ does not act on mature Th17 cells to inhibit Th17 differentiation.

Since the finding that IL-23 instead of IL-12 is necessary for active EAE induction (Cua et al., 2003), the previously common dogma of pathogenesis in EAE and MS has changed. Th1 cells induced by IL-12 are now either seen as secondary or even as Th17 inhibitory population, whereas Th17 cells, which were soon shown to depend on IL-23 (McGeachy et al., 2009; McGeachy and Cua, 2007), have been regarded by some as the major initiators for the orchestration of pathogenesis. Very well fitting to this model of Th17 cells as primary initiators is the fact that Th17 cells secrete chemokines and cytokines which by themselves induce chemokines and other cytokines important for the immigration of harmful leukocytes such as granulocytes and lymphocytes

Having clearly shown that Th17 cells are indeed able to switch their expression profiles from IL-17A and IL-17F expression to IFN-γ expression, we reasoned that IFN-γ expression may indeed act on fully mature Th17 cells to inhibit expression of Th17 cytokines. It has been previously shown that *in vivo* neutralization of IFN-γ exacerbates autoimmune pathogenesis (Alexander et al., 1999) (Wang et al., 2004)

(Fenner et al., 2006). It has also recently been described that addition of blocking antibodies directed against IFN-γ increase efficiency of Th17 polarizations *in vivo*. We were able to confirm this finding with LN-derived cells stimulated in the presence of

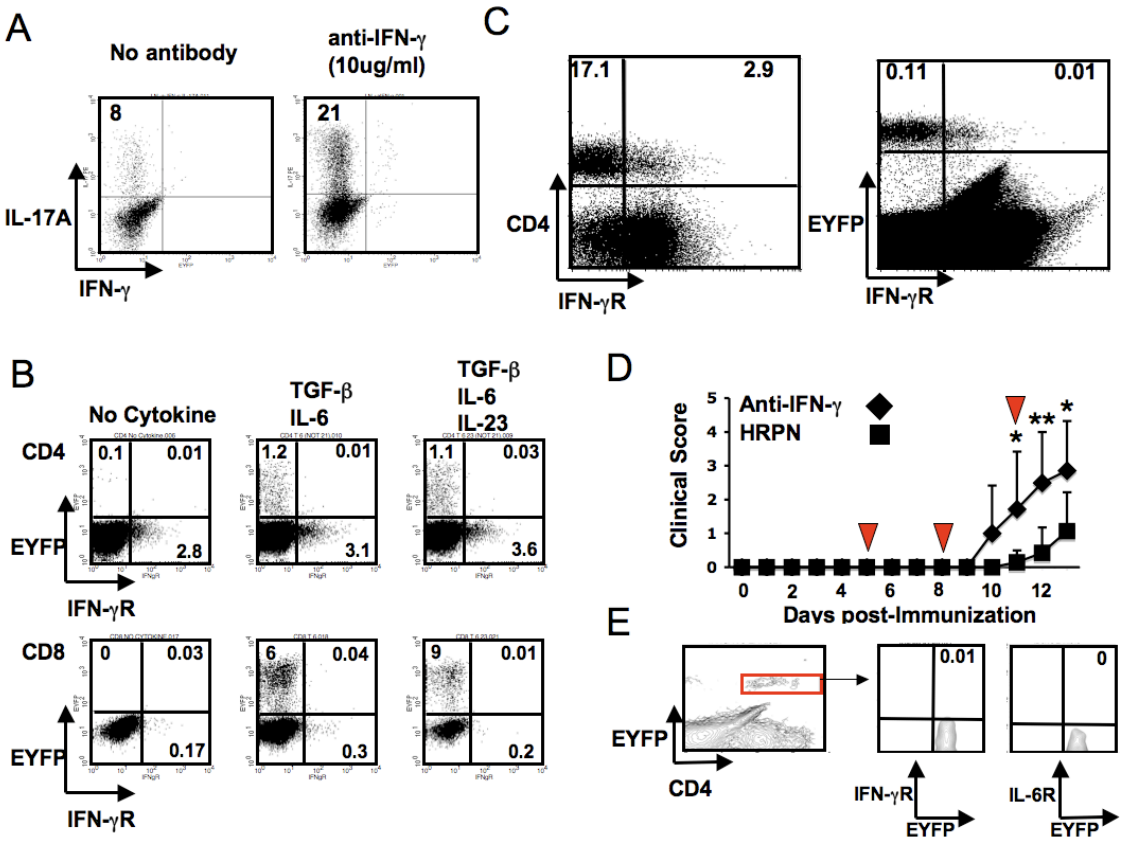

Fig. 23: IFN-γ does not act on mature Th17 cells to exacerbate EAE. (A) Whole LN from wt mice were activated in the presence of TGF-β and IL-6 and in the presence or absence of neutralizing anti-IFN-γ. Percentages of IL-17A+ cells are sown in the upper left quadrant. (B) IL-17F-Cre^{EYFP} CD4+ or CD8+ T cells were magneitcally enriched and activated in the presence of TGF-β and IL-6, or with additional IL-23. IFN-γR surface expression was assayed by FACS staining. Percentages cells expressing EYFP+ and IFN-γR in the indicated CD4 or CD8 gates are shown in the quadrants. (C) IL-17F-Cre^{EYFP} mice were immunized with MOG-CFA and pertussis toxin. 14d after immunization, splenic T cells were isolated and assayed for expression of CD4, EYFP and IFN-γR. Percentages of CD4+IFN-γR+ or EYFP+IFN-γR+ T cells are shown in the quadrants. (D) IL-17FCre^{EYFP} mice immunized with MOG-CFA nad pertussis toxin, with one group being given additional anti-IFN-γ at the indicated timepoints after immunization. The control group was treated with an isotype antibody (HRPN). Clinical EAE score was measured daily for the next 14d. Bars represent +/-SD and signifiance was calculated using the student's t-test. (E) CNS-isolated T cells from untreated IL-17FCre^{EYFP} mice at the peak of disease were stained for CD4 and either IFN-γR or IL-6Rα. Percentages are given in the quadrants.

TGF-β and IL-6. Addition of neutralizing anti-IFN-γ did indeed augment differentiation of Th17 cells (Fig. 23A). Interestingly, these findings open two possibilities. Either IFN-γ acts on naive T cells to inhibit their initial differentiation into Th17 cells, or IFN-γ acts on fully differentiated Th17 cells via its receptor, and causes them to downregulate signature cytokine expression. Using the IL-17F-Cre^{EYFP} strain, we were

able to see if *in vivo* and *in vitro*-generated fully mature Th17 cells express the receptor for IFN-γ. Magnetically enriched $CD4^+$ or $CD8^+$ T cells were activated in culture in the presence of TGF-β and IL-6, or these cytokines and additionally IL-23. After 36h in culture, the newly generated $EYFP^+$ Th17 cells or Tc17 cells do not co-express IFN-γ receptor (Fig. 23B). Thus, *in vitro* generated Th17 or Tc17 cells do not upregulate IFN-γ receptor in this setting.

Given the ability to control cytokine exposure *in vitro*, we also wanted to check if *in vivo* generated Th17 cells were able to express IFN-γR. In a MOG-CFA immunized mouse, T lymphocytes will be exposed to a wide range of proinflmmatory stimuli, which may induce IFN-γR expression on Th17 cells not detectable in vitro. To this end, IL-17F-Cre^{EYFP} mice were immunized with MOG-peptide emulsified in CFA, with additional pertussis toxin administration. On d14, spleens were isolated from IL-17F-Cre^{EYFP} mice and assayed for the expression of IFN-γR. A proportion (~15%) of splenic CD4 T cells in these mice expressed IFN-γR (Fig. 23C). However, $EYFP^+$ Th17 cells in these mice do not express IFN-γR, despite a strong expression of IFN-γR by other SPL-resident cells (Fig. 23C).

We were indeed able to confirm previous findings that treatment of EAE-immunized mice with neutralizing anti-IFN-γ antibodies exacerbated clinical disease course (Fig. 23D). Thus, IFN-γ has a protective role in EAE pathogenesis. However, $EYFP^+$ Th17 cells isolated from the central nervous system of EAE-stricken IL-17F-Cre^{EYFP} mice do not express the receptor for IFN-γ. IL-6R expression is also absent from CNS-derived Th17 cells (Fig. 23E). These data suggest that the protective role of IFN-γ is not carried out via an inhibition of IL-17A production of encephalitogenic T cells, but rather acts independently of Th17 cells or via a secondary and as yet unidentified mediator to reduce pathogenictiy of Th17 cells in the inflamed CNS.

4.2 The IL-17F-Cre^{RFP}-DEREG dual reporter system.

Another advantage of using a Cre strain to achieve a reporter mouse is that the Cre can be crossed to any number of conditional reporter mice or floxed alleles. In previous experiments, the IL-17F-Cre allele was crossed to a conditional EYFP reporter. Recently, a similar mouse was generated in the lab of Hansjörg Fehling (Luche et al., 2007). This mouse allows ubiquitous expression of the red fluorescent protein (RFP)

from the ROSA26 promoter following excision of a transcriptional STOP cassette. Thus, in the same manner as the IL-17F-Cre^{EYFP} mice were generated, we also generated the IL-17F-Cre^{RFP} strain.

Recently another strain was generated using BAC-transgenesis in the lab of Tim Sparwasser in Munich. This strain, called the DEREG strain, bears a transgene from which the diptheria toxin receptor is expressed as a fusion protein in tandem with GFP under the control of the Foxp3 promoter (Lahl et al., 2007). In this strain, injection of diptheria toxin (DT) will delete all Foxp3-expressing cells. These mice were crossed to the IL-17F-Cre^{RFP}-strain, yielding the IL-17F-Cre^{RFP}-DEREG strain. In these mice, Th17 cells and Treg cells can both be traced based on expression of RFP or GFP, respectively.

Once the IL-17F-Cre^{RFP}-DEREG mice were available, the functionality of the dual reporter was tested using T cell polarizing cytokines TGF-β and IL-6. TGF-β alone will induce Foxp3 expression (GFP), and TGF-β and IL-6 will induce IL-17A and IL-17F, and thus result in Cre expression and RFP signal. As expected. TGF-β alone induced a strong Foxp3-GFP expression (77%). Additional IL-6 inhibited this Foxp3 expression, and RFP+ Th17 cells were strongly induced (Fig. 24A). To test the system *in vivo*, the IL-17F-Cre^{RFP}-DEREG mice were immunized with MOG-CFA and pertussis toxin. 14 days after immunization, lymph nodes, spleens, brains and spinal cords from EAE-sick IL-17F-Cre^{RFP}-DEREG were isolated and assayed for expression of GFP and RFP (Fig. 24B). In spleens and lymph nodes of these mice, more Tregs than Th17 cells were present. However, in the inflamed brains and spinal cords (CNS) the balance between regulatory and proinflammatory cells was shifted in the direction of Th17 cells, with fewer GFP^{+} Tregs present in the site of inflammation (Fig. 24C).

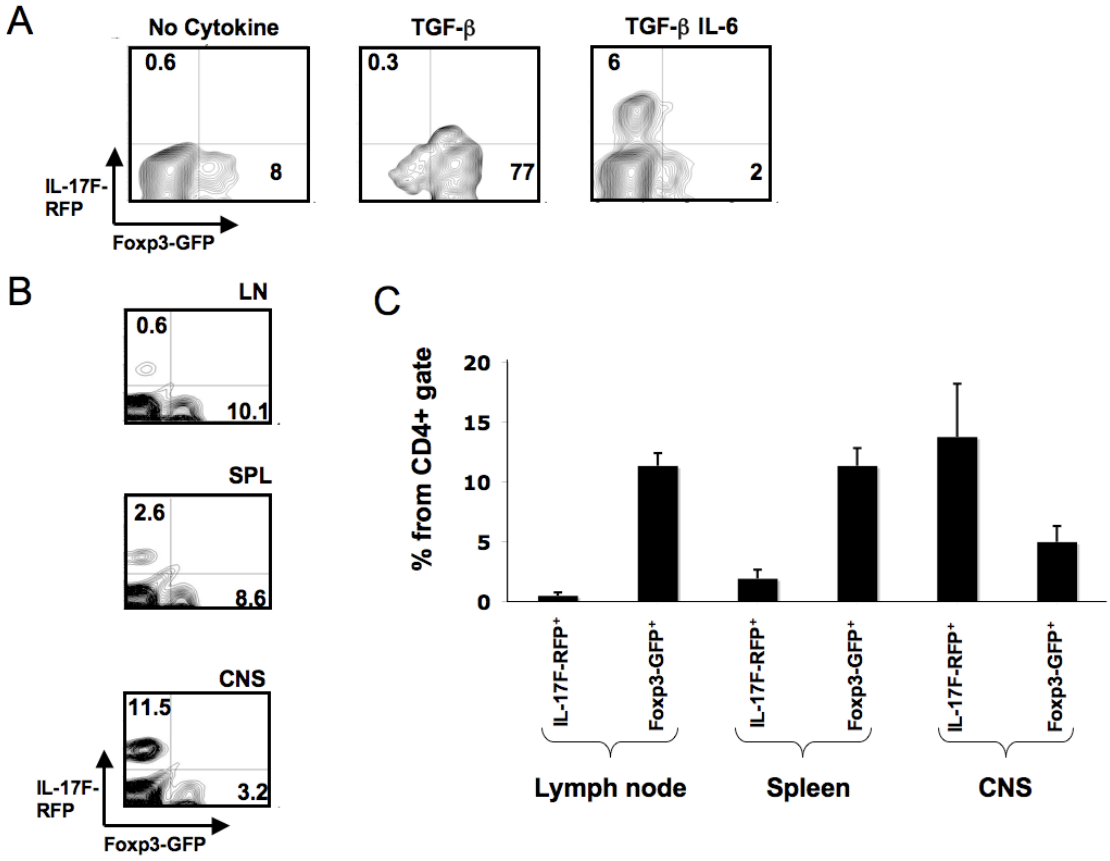

Fig. 24: IL-17FCre^{RFP}DEREG mice are a dual reporter system for Tregs and Th17 cells: (A) MACS-purified CD4 T cells from IL-17FCre^{RFP}-DEREG mice were cultured in the presence of the indicated cytokines and activating anti-CD3 and anti-CD28. Percentages of Foxp3-GFP+ or IL-17F-RFP+ cells are shown in the quadrants. (B) IL-17FCre^{RFP}-DEREG mice were immunized with MOG-CFA and pertussis toxin. 14d after immunization, lymphocytes were isolated from CNS, SPL and LN. Shown is a representative dotplot from 5 similar mice. (C) Statistical representation of data shown in B, gated on CD4+ cells (n=5). Error bars represent standard deviation.

4.2.1 Th17 cells are resistant to Foxp3 expression in the IL-17F-Cre^{RFP}-DEREG system.

The DEREG allele allows for the deletion of regulatory T cells after administration of diptheria toxin. This can be achieved either by injecting DT into a DEREG mouse to delete Treg cells *in vivo*, or by addition of DT to cells in culture to delete in vitro. We wanted to confirm our findings shown previously in this chapter illustrating that cells were resistant to upregulation of Foxp3 during a period of homeostatic expansion. To confirm these findings using the the IL-17F-Cre^{RFP}-DEREG system, CD4+ T cells were purified from these mice and cultured for 5d with TGF-β and IL-6 to induce RFP^{+} Th17 cells. DT was added to the cultures on d3 and d4 to delete remaining Tregs from the cultures. Deletion of Tregs was successful in this setting, with a 20-fold reduction of

GFP^{+}Foxp3^{+} regulatory T cells (Fig. 25A). The resulting DT-treated population consisted of RFP^{+}GFP^{-} Th17 cells and RFP^{-}GFP^{-} CD4 T cells. These cells were transferred intraveinously into RAG1-/- hosts. After a period of 14d, LN cells from RAG1-/- hosts were isolated and the resulting T cell populations analysed for expression of RFP and GFP. Transferred Th17 cells were clearly identifiable as CD4^{+}RFP^{+} (Fig. 25B). Gating on both CD4^{+}RFP^{-} and CD4^{+}RFP^{+} populations revealed a slight increase in Foxp3 expression in the CD4^{+}RFP^{-} fraction. However, no GFP was detectable in CD4^{+}RFP^{+} Th17 cells, indicating that Th17 cells are again resistant to Foxp3 upregulation when compared to undifferentiated T cells.

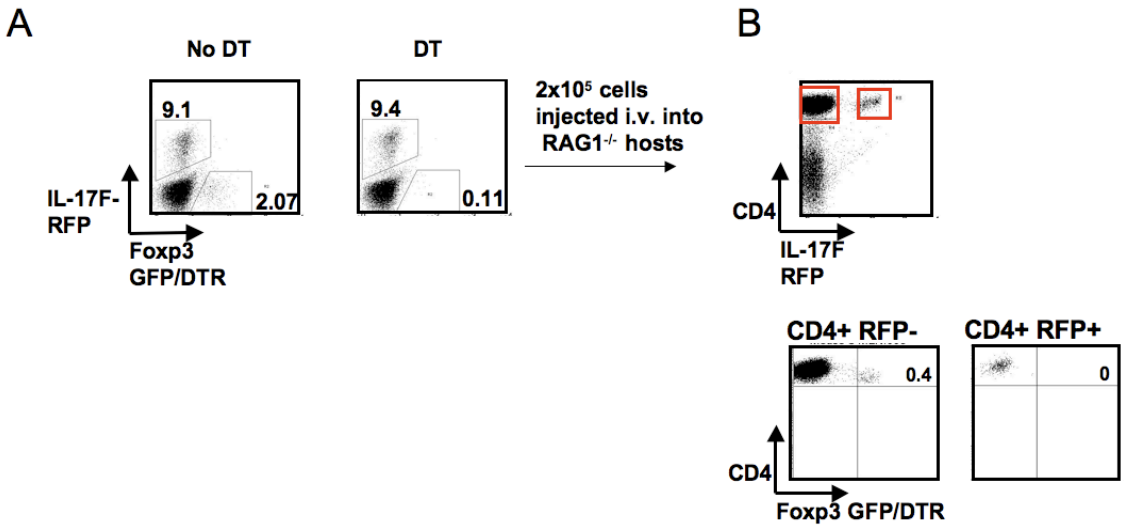

Fig. 25: IL-17FCre^{RFP}-Th17 cells are resistant to Foxp3 expression in vivo: (A) Th17 cells were raised in vitro from magnetically purified IL-17FCre^{RFP}DEREG CD4+ T cells using CD3/28 activation with TGF-β and IL-6, and in the presence or absence of DT. Prior to i.v. injection into RAG1-deficient hosts, DT-mediated ablation of Foxp3 GFP/DTR cells is shown in the gate. (B) After 3 weeks, T cells were isolated from LN of RAG1-/- hosts. Foxp3-GFP expression in either CD4+RFP- or CD4+RFP+ T cells is shown. Data shown represent 4 mice and two independent experiments.

5 CD4-Cre IL-6R$^{fl/fl}$

5.1 IL-6 Signaling regulates the Th17/Treg axis by inhibiting iTreg generation *in vivo*

IL-6 was initially described as B cell-stimulatory factor (Hirano et al., 1986) and as an important trigger of acute-phase responses. IL-6 signals through a receptor complex consisting of the ligand-binding subunit IL-6Rα (CD126) and the signaling subunit gp130 (Taga et al., 1989). Whereas gp130 is ubiquitously expressed, the expression of IL-6Rα is restricted to hepatocytes, intestinal epithelial cells, endocrine glands, and leukocytes with the exception of naïve B cells (Kamimura et al., 2003). Mice deficient in gp130 have been generated. However, in contrast to *Il6-/-* mice, homozygous loss of gp130 is perinatally lethal (Yoshida et al., 1996). In fact, gp130 is the receptor signaling subunit for at least 6 additional members of the IL-6 family of cytokines, including IL-11, oncostatin M, leukemia inhibitory factor, cardiotrophin-like cytokine, ciliary neurotrophic factor, and cardiotrophin-1.

We have previously investigated the role of IL-6 in the lineage decision of antigen-specific CD4 T cells during an autoimmune response *in vivo* (Korn et al., 2008). We found that T cell unresponsiveness to IL-6 is sufficient to mount an overwhelming T-reg response to immunization, which prevents the induction of Th1 and Th17 effector cells, resulting in full resistance to EAE. However, T-reg-depleted CD4-gp130$^{fl/fl}$ mice were able to mount a Th17 response upon immunization with MOG-peptide in CFA. Thus, alternative pathways exist to induce Th17 cells in the absence of IL-6 signaling. We reasoned that the IL-21-IL-21R pathway was still functioning in CD4-gp130$^{fl/fl}$ mice, and that the EAE pathogenesis observed after antibody-mediated depletion of Tregs in CD4-gp130$^{fl/fl}$ mice was due to a fully operational IL-21-mediated generation of Th17 cells. Absence of gp130 in T cells will, however, have the drawback of ablating signaling of a number of IL-6 family members, mentioned above. Recently, generation of a conditional allele for the second component of the IL-6R, IL-6Rα, was successfully completed by F. Thomas Wunderlich and Jens. C Brüning in the Institute for Genetics in Cologne, Germany. This strain was crossed to the CD4-Cre transgene in our lab. Through precise targeting of the IL-6 signaling pathway using this conditional allele, this strain would have a genetic deficiency resulting in ablation of IL-6 signaling in all Cre recombinase-

expressing cells without disrupting other potentially influential pathways during an immune response.

5.2 CD4-IL-6R$^{fl/fl}$ mice lack expression of the IL-6Rα protein and IL-6 signaling capability

Recently, a reciprocal developmental relationship between Foxp3$^+$ Tregs and Th17 cells was identified and published (Bettelli et al., 2006). TGF-β triggers the expression of Foxp3 in naïve T cells, whereas IL-6 inhibits the TGF-β driven expression of Foxp3. Simultaneous TGF-β and IL-6 signaling induces RORγt, initialising the developmental program of Th17 cells (Bettelli et al., 2006). In the absence of IL-6, IL-21, which is a member of the IL-2 family of cytokines, can substitute for IL-6, and activation with TGF-β and IL-21 might constitute an alternative pathway to induce Th17 cells (Korn et al., 2007a). Together, these findings suggested that IL-6 and possibly IL-21 are switch factors between the induction of T-regs and Th17 cells. Thus, the reciprocal relationship between Tregs and Th17 cells was investigated in the context of this new model of IL-6Rα deficiency. After successful breeding of the CD4-Cre IL-6R$^{fl/fl}$ strain, anti-IL-6Rα antibody staining was carried out on LN-derived T cells from these mice. It was clearly appreciable that CD4-Cre IL-6R$^{fl/fl}$ T cells lacked surface expression of IL-6Rα. As expected, both CD4 and CD8 had undetectable expression of the IL-6Rα protein in CD4-Cre IL-6R$^{fl/fl}$ mice (Fig. 26).

To ensure that not only the IL-6Rα protein was absent, but also that cells were not able to respond to IL-6 through another mechanism, CD4$^+$ T cells were purified and cultured in a variety of Th17 polarizing conditions. In the absence of polarizing cytokine, no expression of IL-17A was induced from either WT or IL-6R-deficient T cells. Th17 cells cultured with TGF-β and IL-21 were generated in both CD4-Cre IL-6R$^{fl/fl}$ and IL-6R$^{fl/fl}$ control cultures, indicating that the IL-21/IL-21R axis is also not disturbed in this strain, and that a secondary mechanism of Th17 differentiation distinct from IL-6 signaling remains intact in CD4-Cre IL-6R$^{fl/fl}$ mice. This differentiation was enhanced in the presence of IL-23, likely due to the role of IL-21 in inducing *il23r* expression in T cells. However, CD4-Cre IL-6R$^{fl/fl}$ showed a profound block in Th17 generation in response to TGF-β and IL-6, indicating that the IL-6 signaling cascade is severely impaired in CD4-Cre IL-6R$^{fl/fl}$ T cells (Fig. 27). The small amount of CD4$^+$IL-17A$^+$ T cells in CD4-Cre IL-6R$^{fl/fl}$ cultures may possibly have arisen from incomplete

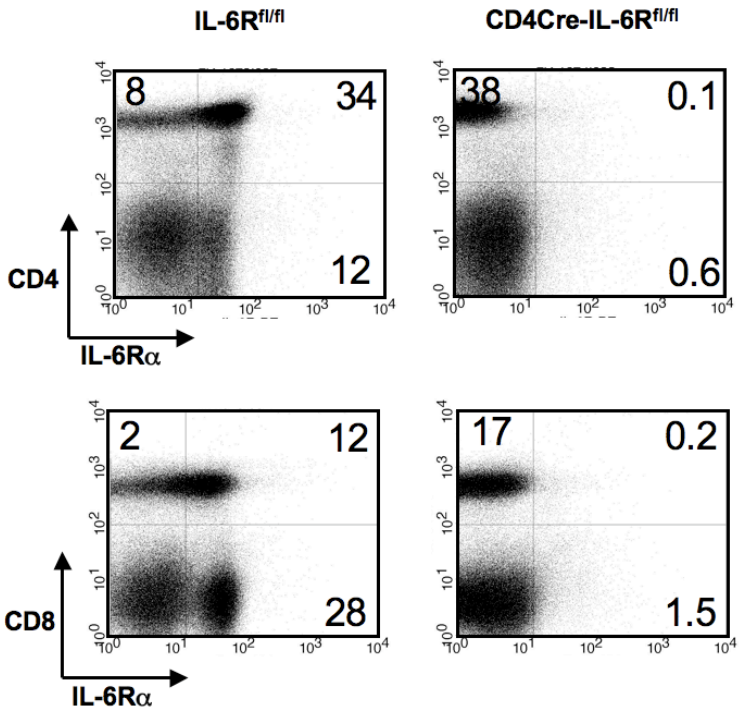

Fig. 26: CD4-Cre-IL-6Rα$^{fl/fl}$ mice do not express IL-6Rα protein. (A) Lymph node-derived lymphocytes from IL-6Rα$^{fl/fl}$ and CD4-Cre-IL-6Rα$^{fl/fl}$ mice were isolated and stained for CD4, CD8 and IL-6Rα. FACS analysis shows percentages of CD4+ and CD8+ T cells in the LN and their expression of IL-6Rα. Data shown represent three different stainings.

recombination in the CD4$^+$ T cells, or by IL-21 expression induced during T cell activation. Thus, CD4-Cre IL-6R$^{fl/fl}$ T cells have massively impaired IL-6 signaling capabilities, but IL-21 signaling is still intact and may provide a signaling mechanism resulting in generation of Th17 cells *in vivo*.

To explore the impact of IL-6 signaling on other cytokines *in vivo*, mice were immunized with MOG-CFA and pertussis toxin to induce a Th1 and Th17 response. CFA is a potent iducer of IL-6 production, and as such is a useful reagent for generation of proinflammatory T helper cell subsets. After 14d, spleens and lymph nodes from CD4-Cre IL-6R$^{fl/fl}$ and IL-6R$^{fl/fl}$ mice were harvested, and T cells, B cells and innate immune compartments enriched using magnetic labelling and sorting. Real time PCR analysis was performed on these cellular subsets, and expression levels of *il17a, ifng, il6* and *il21* were measured. Expression of *il17a* was dramatically reduced *in vivo*, indicating that the IL-21-mediated Th17 differentiation witnessed *in vitro* by CD4-Cre IL-6R$^{fl/fl}$ T cells represents only a minor differentiation pathway under these conditions (Fig. 27). However, significantly higher levels of *ifng* expression were

observed in T cells derived from both spleen and lymph nodes of CD4-Cre IL-6R$^{fl/fl}$ mice. IL-6 expression remained unaltered in T cells, however IL-21, a target gene of IL-6 signaling, was dramatically reduced in CD4-Cre IL-6R$^{fl/fl}$ mice. Thus, although IL-21 mediated generation of Th17 cells is fully functional *in vitro*, Th17 generation *in vivo* is largely dependent on IL-6 signaling. It is possible that the decrease in IL-21 expression levels may also contribute to this phenotype.

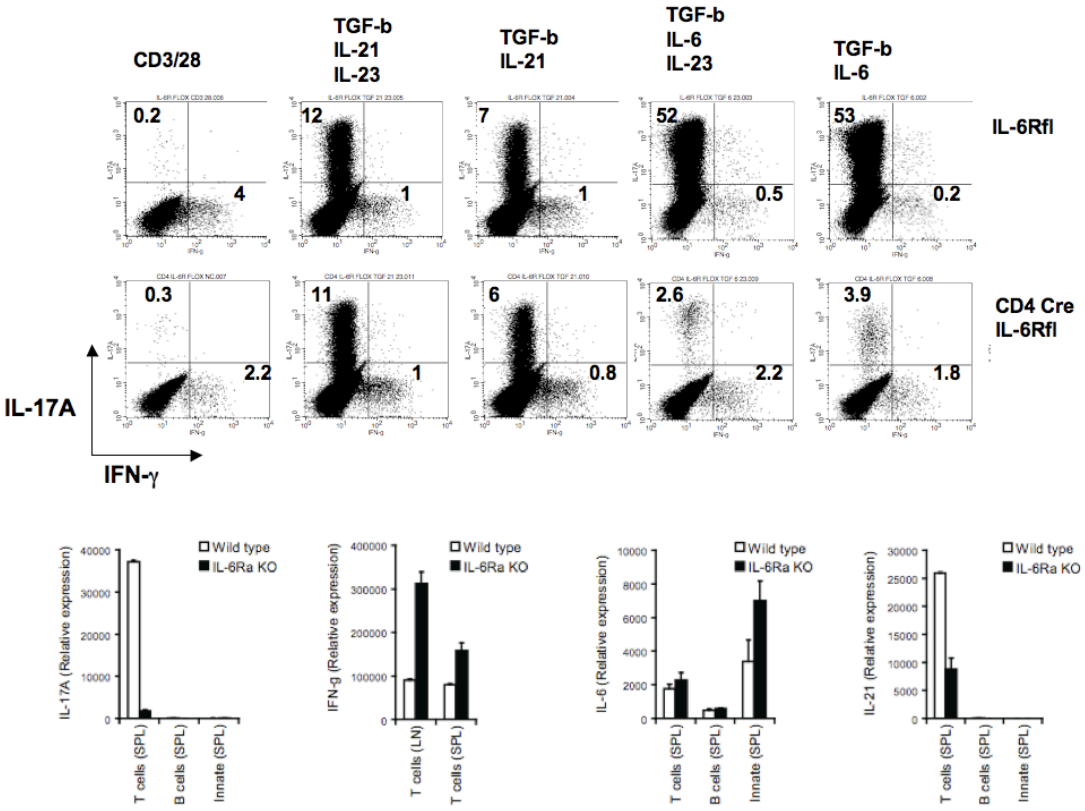

Fig. 27: IL-21-mediated Th17 differentiation is undisturbed in CD4-Cre-IL-6Rα$^{fl/fl}$ mice: (A) CD4+ T cells were MACS-purified from IL-6Rα$^{fl/fl}$ and CD4-Cre-IL-6Rα$^{fl/fl}$ mice. Cells were activated with anti-CD3, anti-CD28 and neutralizing anti-IFN-γ for 4d in the presence of the indicated cytokines. Percentages of IL-17A+ and IFN-γ+ T cells are shown after gating on CD4+ cells. (B) MACS-purified CD90.2+, CD19+ and flow through fractions from pooled spleens of IL-6Rα$^{fl/fl}$ and CD4-Cre-IL-6Rα$^{fl/fl}$ mice 14d after immunization with MOG-CFA and pertussis toxin were isolated (n=2 mice per group). RNA was prepared from these cellular isolates and assayed for expression of IL-17A, IFN-γ, IL-6 and IL-21 in both IL-6Rα$^{fl/fl}$ (open bars) and CD4-Cre-IL-6Rα$^{fl/fl}$ (closed bars) T cells, B cells and innate fractions by TaqMan RT-PCR analysis. Error bars represent +/-SD.

5.3 CD4-Cre-IL-6R$^{fl/fl}$ mice show enhanced Treg responses after MOG-CFA immunization

Given the relationship between IL-6 signaling and inhibition of Foxp3 signaling, we hypothesized that the absence of IL-6 signaling might lead to an imbalance in peripheral T-reg numbers, even in the steady state. We compared cohorts of naive CD4-Cre IL-6R$^{fl/fl}$ to both WT controls and CD4-Cre gp130$^{fl/fl}$ mice. No overt differences were detected in numbers of regulatory T cells in peripheral blood (Fig. 28A). Differences in CD4^{+}Foxp3^{+} T cells from CD4-Cre IL-6R$^{fl/fl}$ and CD4-Cre gp130$^{fl/fl}$ proved also to be statistically insignificant (Fig. 28B). Although no differences were detectable in numbers of all Foxp3+ Tregs, we considered that perhaps only induced Treg (iTreg) numbers would be affected by lack of IL-6 signaling. No true marker exists to this date for making the distinction between iTregs when compared to nTregs. However, it has been suggested that CD62L is potentially a marker for iTregs. No differences were observed in either CD62L^{+}Foxp3^{+} Tregs, or CD62L^{-}Foxp3^{+} ‚iTregs' (Fig. 28C). Taken together, these data suggest that ablating IL-6 signaling does not affect homeostasis of Tregs in the steady state.

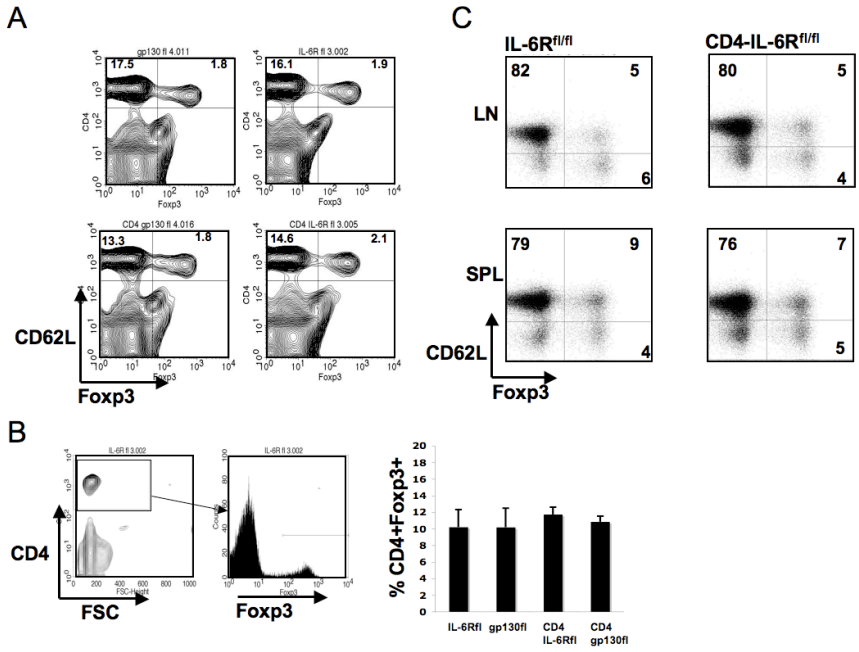

Fig. 28: Treg homeostasis is unaffected in naive CD4-Cre-IL-6Rα$^{fl/fl}$ mice: (A) Splenic cells from IL-6Rα$^{fl/fl}$, CD4-Cre-IL-6Rα$^{fl/fl}$, CD4-Cre-gp130 $^{fl/fl}$ and gp130 $^{fl/fl}$ mice were stained for CD4 and Foxp3. Percentages are given in the quadrants. (B) Total CD4 cells were stained for Foxp3. Statistics for Foxp3+CD4+ T cells from the indacted gating are shown in the bar chart (n = at least 3 mice per group). (C) Splenic and lymph node-derived T cells from IL-6Rα$^{fl/fl}$ and CD4-Cre-IL-6Rα$^{fl/fl}$ mice were isolated

and stained for CD4, CD62L and Foxp3. Percentages of cells in each quadrant are shown. Data represent three mice per group.

We have previously shown using gp130-deficient T cells that absence of IL-6 signaling results in the expansion of $Foxp3^+$ Tregs in response to MOG-CFA immunization {Korn, 2008 #31}. We wanted to confirm these findings using the CD4-Cre IL-$6R^{fl/fl}$ strain. To this end, cohorts of CD4-Cre IL-$6R^{fl/fl}$ and IL-$6R^{fl/fl}$ control mice were immunized subcutaneously with MOG-CFA. CFA is a potent inducer of IL-6 expression from the innate immune system largely due to bacteria-derived molecules, which activate Toll-like Receptor (TLR) signaling pathways on antigen presenting cells (APC). On d8, draining lymph nodes were isolated from immunized and non-immunized IL-6R-deficient and WT mice. Significant increases of $Foxp3^+$ T cells were detectable in immunized CD4-Cre IL-$6R^{fl/fl}$ mice (Fig. 29A and B). This difference was not statistically significant in unimmunized animals. These data suggest that CD4-Cre IL-$6R^{fl/fl}$ T cells are insensitive to the IL-6 secreted by TLR-activated innate cells, and as such activated T cells favour conversion to a regulatory phenotype due to a lack of inhibition of TGF-β-mediated upregulation of Foxp3.

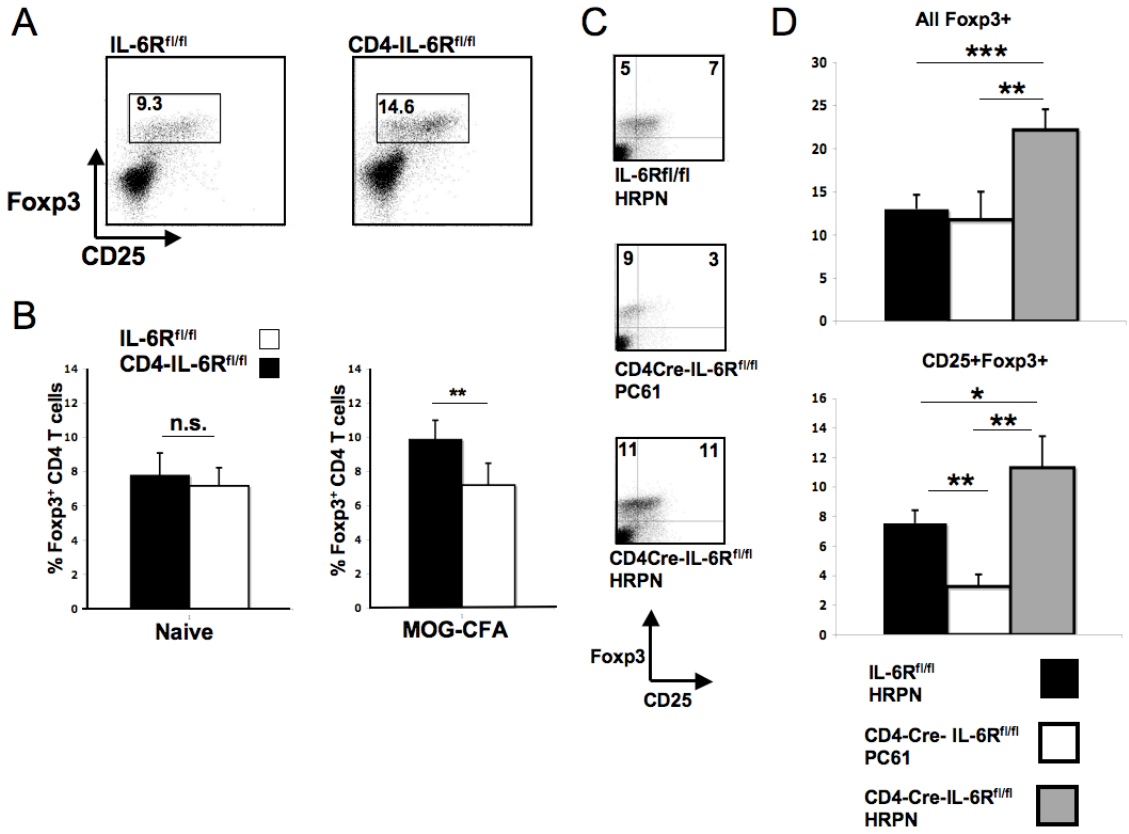

Fig. 29: Blockade of IL-6 signaling augments Treg responses in vivo: (A) 4 weeks old IL-6Rα$^{fl/fl}$ and CD4-Cre-IL-6Rα$^{fl/fl}$ mice (n=4-8) were immunized s.c. with MOG-CFA, or not immunized. After 10d, spleens were isolated and stained for CD4, CD25 and Foxp3. Percentages of CD4+ cells expressing CD25 and Foxp3 are shown in the dot plots for immunized mice of indicated genotype. (B) Statistical analysis of Foxp3 upregulation in the absence of IL-6 signaling (n = 8-10). Statistical significance was calculated using the student's t-test. (C) Mice of indicated genotypes were treated with PC61 (anti-CD25) or HRPN (isotype to PC61) antibodies at d-5 and -3 prior to immunization with MOG-CFA and pertussis toxin. On d14, spleens were analyzed for depletion of CD25+ cells. Percentages of cells in each quadrant are shown. (D) Mice treated as in C were analyzed for depletion of Foxp3+CD25+ T cells by PC61. Bar charts show statistics for each group (n=4) for all CD4+Foxp3+ cells, or CD4+Foxp3+CD25+ cells. Statistical significance was calculated using the student's t-test. Error bars represent +/-SD.

5.4 Treg depletion renders CD4-Cre IL-6R$^{fl/fl}$ mice susceptible to EAE.

Both IL-6 and IL-21 are, together with TGF-β, capable of inducing Th17 cells (Korn et al., 2007a). Therefore, we wanted to know whether the induction of Th17 cells would occur in the complete absence of IL-6R signaling in T cells from CD4-IL-6R$^{fl/fl}$ mice. Given our previous findings, we had expected an almost complete abrogation of Th17 development in response to IL-6 and TGF-β. However, given that TGF-β plus IL-21 induced Th17 cells as efficiently in CD4-Cre IL-6R$^{fl/fl}$ T cells as in wild-type T cells

(Fig.27A), suggesting that the combination of TGF-β plus IL-21 is operational independently of IL-6-mediated signal transduction. To test this hypothesis *in vivo*, we treated CD4-Cre IL-6R$^{fl/fl}$ mice with a control antibody or depleted them of CD4^{+}CD25^{+}Foxp3^{+} T-regs by means of a monoclonal antibody against CD25, named PC61. Treatment of CD4-Cre IL-6R$^{fl/fl}$ mice with PC61 resulted in a strong depletion Tregs expressing CD25 (Fig. 29C and D). This system allowed us to investigate the induction of pathogenic T cell populations *in vivo* in the absence of an exaggerated T-reg response that confounds the induction of effector T cell populations. Splenic T cells were analyzed for the expression of both IL-17A and IFN-γ at d10 after immunization with MOG-CFA and pertussis toxin. We successfully identified both Th17 and Th1 cells in WT mice at this timepoint (Fig. 30A). Th17 populations were significantly reduced in CD4-Cre IL-6R$^{fl/fl}$ mice. No significant impact was observed on generation of Th1 cells in PC61-treated CD4-Cre IL-6R $^{fl/fl}$ mice (Fig. 30B).

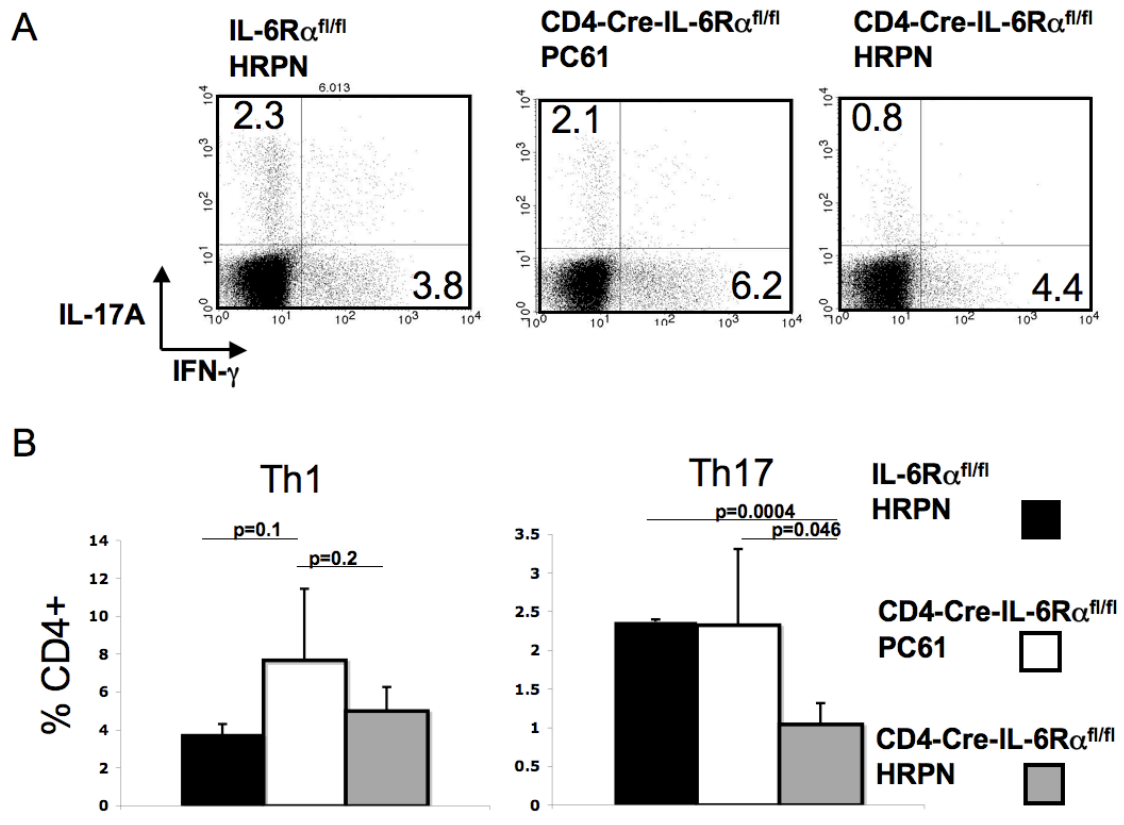

Fig. 30: Depletion of Tregs restores Th17 responses in vivo: (A) 8 week old IL-6Rα$^{fl/fl}$ and CD4-Cre-IL-6Rα$^{fl/fl}$ mice (n=3) were immunized s.c. with MOG-CFA. Mice were treated with either PC61 or HRPN. At d14, splenic T cells were restimulated with PMA, Ionomycin and Brefeldin A before staining with anti-IL-17A (Th17) and anti-IFN-γ (Th1). (B) Percentages of IFN-γ+ (Th1) and IL-17A+ (Th17) cells in IL-6Rα$^{fl/fl}$ and CD4-Cre-IL-6Rα$^{fl/fl}$ mice with indicated treatments are shown. Statistical significance was calculated using the student's t-test. Error bars represent +/-SD.

Given the restoration of Th17 responses in Treg-depleted CD4-Cre IL-6R$^{fl/fl}$ mice, we reasoned that the potential to induce EAE would return in the absence of peripheral tolerance. We therefore treated mice with PC61 or an isotype control antibody prior to immunization with MOG-CFA and pertussis toxin. Control antibody-treated CD4-Cre IL-6R$^{fl/fl}$ mice showed a strong resistance to EAE. However, T-reg-depleted CD4-Cre IL-6R$^{fl/fl}$ mice developed EAE with kinetics and severity similar to wild-type control animals (Fig. 31A). Despite the absence of IL-6 signaling, T-reg-depleted CD4-Cre IL-6R$^{fl/fl}$ mice not only developed EAE, but also mounted a Th17 response in the CNS (Fig. 31B), suggesting that IL-6 signaling is dispensable for the induction of pathogenic Th17 responses *in vivo*, at least under conditions of reduced T-reg levels. Collectively, these data illustrate why IL-6 is pivotal in dictating the balance between induced T-regs and Th17 cells *in vivo* and support data proposing that *de novo* generation of Foxp3^{+} T-regs occurs in the secondary lymphoid compartment in the absence of IL-6.

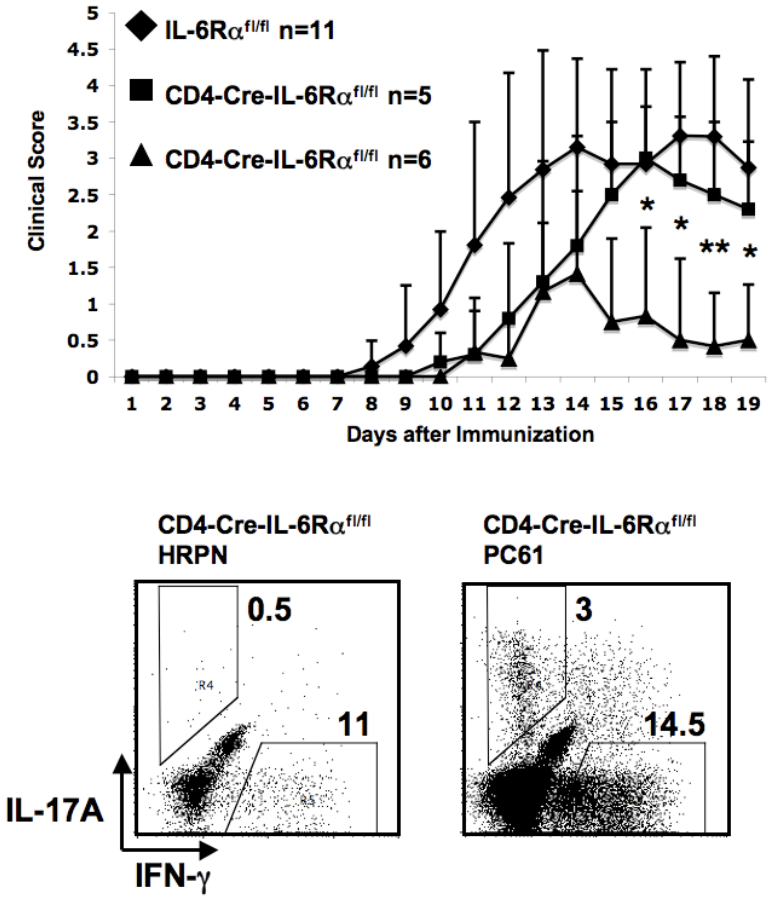

7

Fig. 31: Depletion of Tregs restores autoimmune neuroinflammation in the the absence of IL-6 signaling: (A)) 8 week old IL-6Rα$^{fl/fl}$ and CD4-Cre-IL-6Rα$^{fl/fl}$ mice were immunized s.c. with MOG-CFA and additional pertussis toxin. CD4-Cre-IL-6Rα$^{fl/fl}$ mice treated with either PC61 or HRPN. Group sizes are indicated on the daily clinical score. Statistical significance was calculated using the student's t-test and represents the difference between CD4-Cre-IL-6Rα$^{fl/fl}$ mice treated with either PC61 or HRPN. (B) On d14, CNS-isolated lymphocytes from 4 mice of indicated genotype and treatment were stained for expression of IL-17A and IFN-g. After pregating on CD4+ cells, percentages of IL-17A+ and IFNg+ cells are given.

6 EBI2 results section

6.1 $CD4^+$ T cells preferentially express EBI2

In the *ebi2*^{gfp} allele, EGFP expression is placed under the control of the *ebi2* promoter. In the homozygous state (*ebi2*$^{gfp/gfp}$), mice are deficient in EBI2. *ebi2*$^{gfp/+}$ mice express EBI2 from the wt allele, but retain the capability to report gene expression from the mutant *ebi2*^{gfp} allele. Thus, expression of EBI2 in different immune cell compartments is detectable using this reporter strain. This mouse strain was generated by Stefano Casola.

We wanted to understand the role of EBI2 in T cell function and immune responses *in vivo*. Mesenteric lymph nodes from *ebi2*$^{gfp/+}$ and *ebi2*$^{gfp/gfp}$ mice were isolated, and lymphocytes stained for expression of CD4 and CD8. A clear increase was observed in both percentage (Fig. 32A) and fluorescence intensity (Fig. 32B) of $CD4^+$ compared to $CD8^+$ T cells. EBI2 expression was markedly increased in *ebi2*$^{gfp/gfp}$ compared to *ebi2*$^{gfp/+}$ mice given the presence of two EGFP-expressing alleles. Tissue stainings from axilliary and mesenteric lymph nodes, Peyer's patches and spleens of *ebi2*$^{gfp/gfp}$ mice showed no overt differences in the organisation of T and B cell zones, or presence of $CD11c^+$ dendritic cells (Fig. 32C).

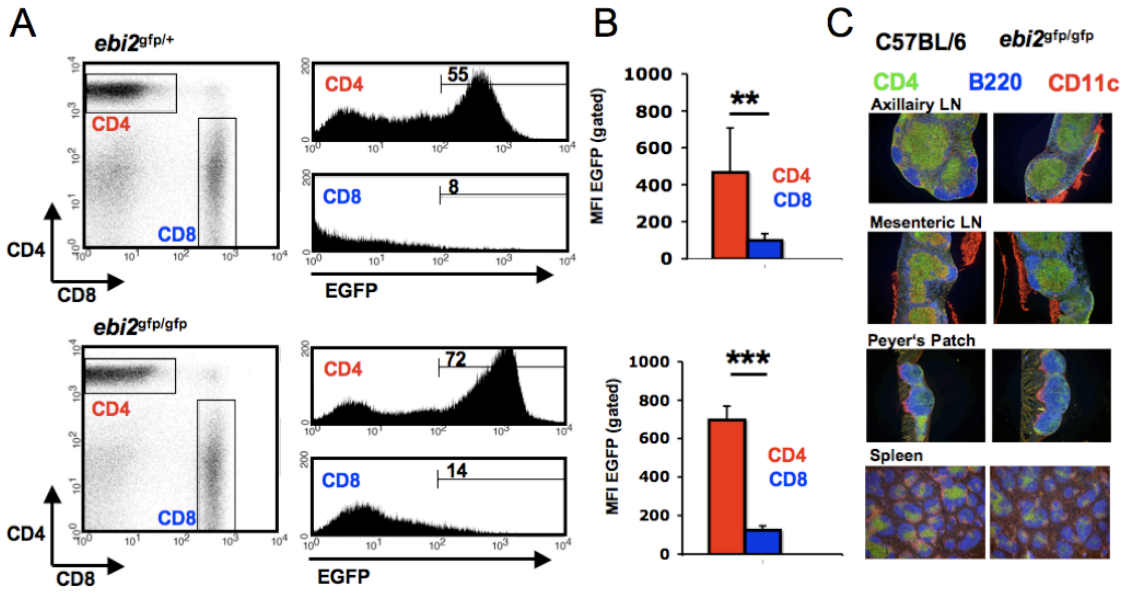

Fig. 32: CD4+ T cells express high levels of EBI2: (A) Mesenteric lymph nodes from *ebi2*$^{gfp/+}$ and *ebi2*$^{gfp/gfp}$ mice were isolated, and stained for CD4 and CD8. Histograms represent EGFP expression in the indicated gates. (B) Mean fluoresence intensity (MFI) vales are shown for the histograms in (A).

Statistical significance was calculated using the student's t-test. Error bars represent +/-SD. (C) Secondary lymphoind organs were isolated and immunostained for CD4, B220 and CD11c.

6.2 EBI2-deficient T cells produce cytokines and proliferate normally.

Despite normal organisation of secondary lymphoid organs, we wanted to examine the functionality of T cells deficient in EBI2. To this end, lymph nodes immunized *ebi2*$^{+/+}$, *ebi2*$^{gfp/+}$ and *ebi2*$^{gfp/gfp}$ mice were isolated ten days after s.c. injection of MOG-CFA. Whole LN cells were cultured with Concanavalin A (ConA) or MOG peptide for 72h. Deficiency of EBI2 had no effect either on ConA-induced proliferation or antigen-induced (MOG) proliferation (Fig. 33A). We reasoned however, that different expression levels of EBI2 might indeed have an effect on survival capabilities of T cells. FACS sorted EGFP^{high} or EGFP^{low} cells from *ebi2*$^{gfp/+}$ and *ebi2*$^{gfp/gfp}$ mice were placed in culture in the absence of stimulation. No significant differences were noted in the survival of EBI2-deficient T cells, or expression level in EBI2-competent T cells (Fig. 33B).

In a further experiment, spleens from MOG-CFA immunized *ebi2*$^{+/+}$, *ebi2*$^{gfp/+}$ and *ebi2*$^{gfp/gfp}$ mice were isolated after ten days and re-activated *in vitro* with MOG-peptide. Expression of IL-17A, IL-6 and GM-CSF in *ebi2*$^{+/+}$ mice was indistinguishable from *ebi2*$^{gfp/+}$ and *ebi2*$^{gfp/gfp}$ mice (Fig. 33C). These data indicate that EBI2-deficient T cells can express cytokines linked to autoimmune inflammation, and show no difference in their ability to proliferate or respond to antigen.

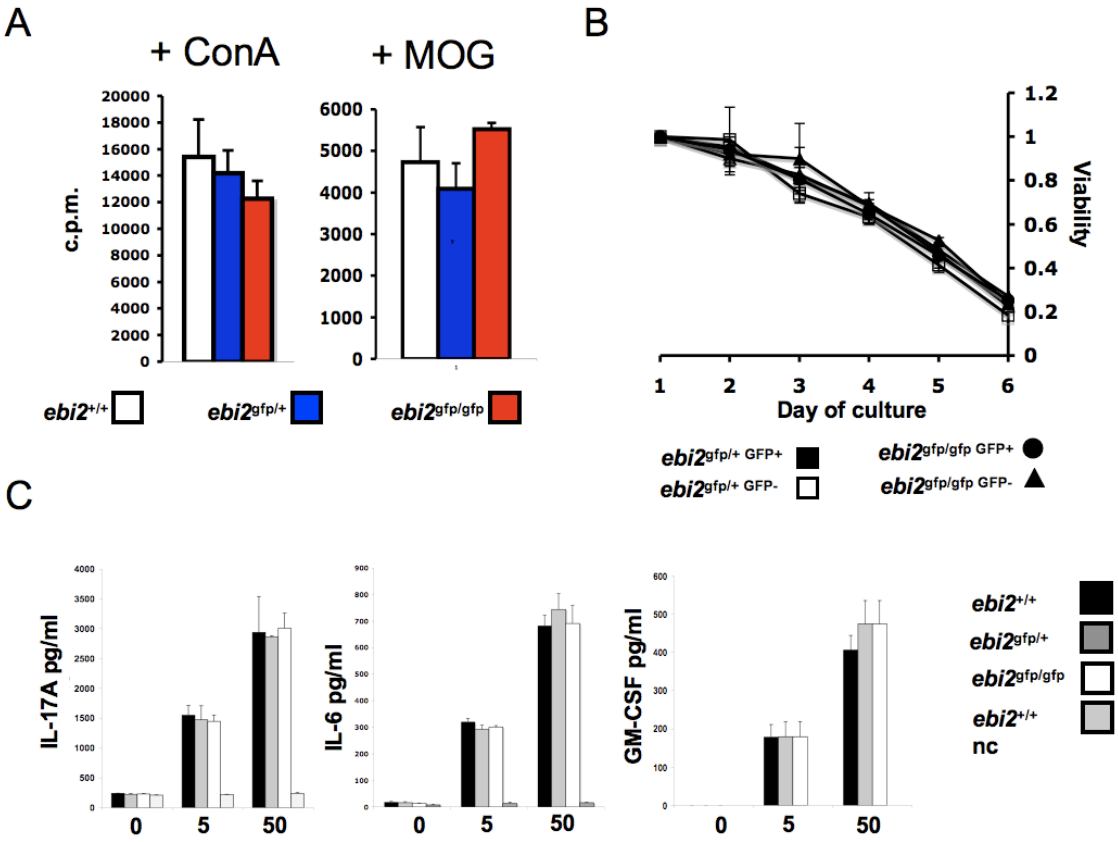

Fig. 33: EBI2 expression has no effect on T cell proliferation or cytokine production: (A) LN isolated from either naive or MOG-CFA-immunized *ebi2*$^{+/+}$, *ebi2*$^{gfp/+}$ or *ebi2*$^{gfp/gfp}$ mice were stimulated with ConA or MOG peptide, respectively. Thymidine incorporation was measured after 72h of proliferation. (B) T cells from *ebi2*$^{gfp/+}$ or *ebi2*$^{gfp/gfp}$ mice were sorted based on high or low EGFP expression. Cells were taken into culture. Daily measurements of Trypan Blue-positive T cells is shown relative to starting T cell numbers. (C) Splenocytes from MOG-CFA-immunized *ebi2*$^{+/+}$, *ebi2*$^{gfp/+}$ or *ebi2*$^{gfp/gfp}$ mice were stimulated with 0, 5 or 50ug MOG-peptide (n=3). After 48h, supernatants were assayed for expression of IL-17A, IL-6 and GM-CSF. Error bars represent +/-SD.

6.3 EBI2-deficient mice are resistant to EAE induction.

Having identified a stronger EBI2 expression in CD4 T cells compared to CD8 T cells, we hypothesized that EBI2 may have a function in CD4 T cells that is unique to these cells. Mice deficient for EBI2 have normal B and T cell development and homing of T cells to different immune organs (Fig. 32). However, many previous publications have demonstrated that G-protein-coupled receptors are involved also in T cell migration and homing after activation. We wanted to look at EBI2 expression with respect to proinflammatory T helper cells subsets, namely Th1 and Th17 cells. We immunized *ebi2*$^{gfp/+}$ and *ebi2*$^{gfp/gfp}$ mice with MOG-CFA and pertussis toxin. Spleens were isolated and assayed for expression of IFN-γ and IL-17A (Fig. 34A). All Th subsets were found to express EBI2. However, a significantly higher expression of EBI2 was observed in

Th1 cells of both *ebi2*$^{gfp/+}$ and *ebi2*$^{gfp/gfp}$ mice (Fig. 34B), suggesting that proinflammatory cells express EBI2, and in particular Th1 cells, in response to immunization with CFA.

In EAE, T cells are of critical importance, and their proper migration (Flugel et al., 2001) and homing to the central nervous system (CNS) (Reboldi et al., 2009) is essential for disease development. To test if in vivo inflammatory T cells are associated with EBI2 expression, we immunized *ebi2*$^{+/+}$, *ebi2*$^{gfp/+}$ and *ebi2*$^{gfp/gfp}$ mice with the MOG peptide p35-55 in CFA. Mice deficient for EBI2 develop significantly less disease compared to WT mice and to heterozygous mice (Fig. 34C). Interestingly, although all *ebi2*$^{gfp/+}$ mice developed EAE, their disease scores were significantly reduced compared to WT mice, indicating that expression levels of EBI2 influence disease susceptibility.

To test if the reason for this reduced disease score is due to inappropriate homing to T cells to the CNS, we analyzed the cell infiltrates in the CNS of these mice. Of the EBI2 KO mice, we chose mice that were afflicted with EAE, as otherwise one cannot find any cell infiltrates. Nevertheless, the EBI2-deficient mice accumulate drastically reduced cell infiltrates in the CNS. Both macrophages CD11b^{high}CD45^{high} less and cell in the lymphocyte gate are much reduced, compared to heterozygous and WT mice (Fig. 34D). Interestingly, in the *ebi2*$^{gfp/+}$ mice, about 93% of the CD4^{+} T cells express high levels of EBI2, which indicate the need to express this receptor in order to invade the CNS. When these cells are further analyzed for the expression of EAE-associated cytokines, we noticed that, similarly to our finding of the spleen of these mice, the vast majority of Th1 and Th17 cells express EBI2 (Fig. 34E). Taken together, EBI2 expression appears to correlate with EAE severity, and expression of proinflammatory cytokines by CNS-invading T cells correlates strongly with EBI2 expression.

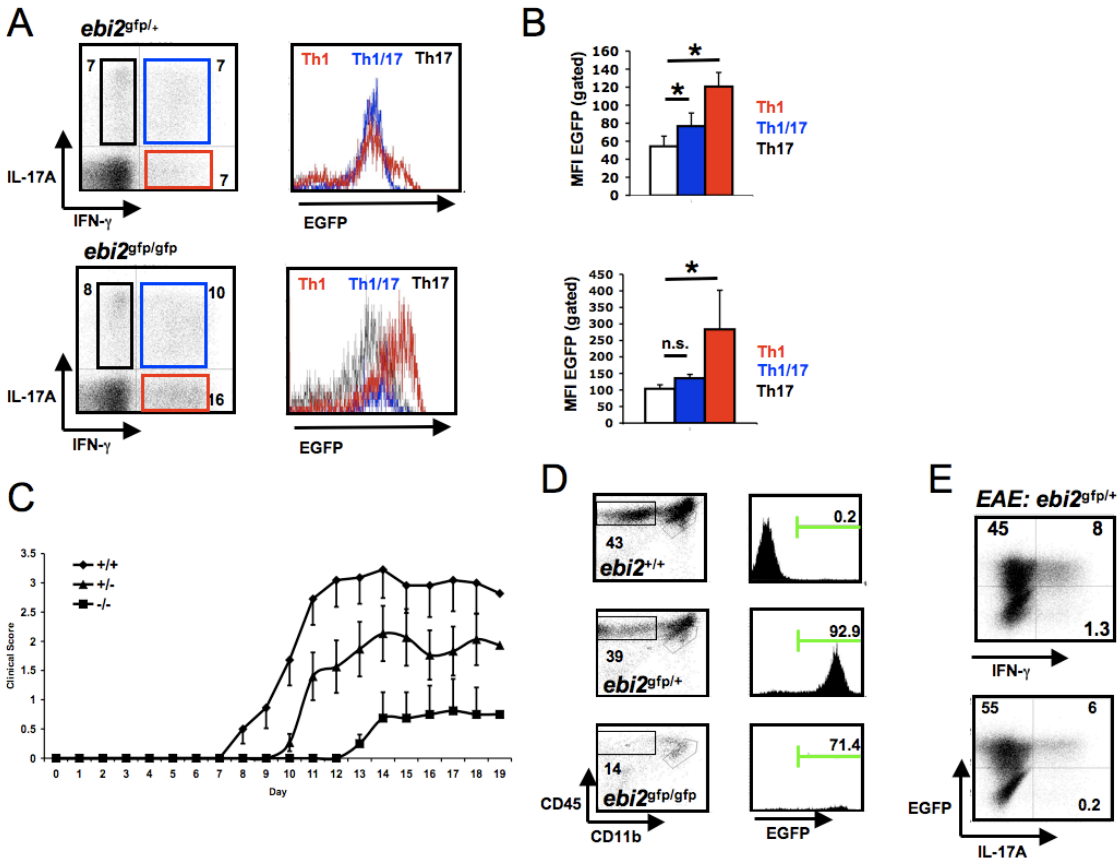

Fig. 34: EBI2-deficiency renders mice resistant to EAE: (A) Splenic T cells from MOG-CFA-immunized *ebi2*$^{gfp/+}$ or *ebi2*$^{gfp/gfp}$ mice were restimulated and stained for IL-17A and IFN-g, Percentages of cytokine-positive cells are given in the quadrants. (B) Mean fluoresence intensity (MFI) vales are shown for *ebi2*$^{gfp/+}$ or *ebi2*$^{gfp/gfp}$ Th1, Th1/17 and Th17 cells. (C) *ebi2*$^{gfp/+}$ or *ebi2*$^{gfp/gfp}$ T cells were activated with anti-CD3/28. After 36h, cells were stained with anti-CD69 and assayed for expression of EGFP. (D) MOG-CFA and pertussis toxin-immunized *ebi2*$^{+/+}$, *ebi2*$^{gfp/+}$ or *ebi2*$^{gfp/gfp}$ mice were scored daily for clinical signs of EAE. Error bars represent +/-SEM and represent at least three independent experiments. (E) CNS-isoalted lymphocytes were isolated at peak of EAE disease (d14) and stained for CD11b and CD45. Histograms represent EGFP expression in cells from the CD45+CD11b- gate. (F) CNS-isoalted lymphocytes were isolated at peak of EAE disease (d14) and stained for CD4, IL-17A and IFN-γ. Percentages shown are in the CD4+ gate.

6.4 EBI2-deficient mice are resistant to hapten induced ear swelling

The resistance of EBI2-deficient mice to induction of EAE encouraged the exploration of other models of T-cell mediated inflammation. Contact hypersensitivity (CHS) is elicited when chemical haptens bind proteins or peptides, after which these peptides become immunogenic. As previously discussed, CHS is a CD8 T cell-mediated disease, so we reasoned that the absence of EBI2 expression would have minimal impact given the strongly reduced expression of EBI2 in CD8^{+} T cells (Fig. 32A). To elicit a CHS response, the hapten dinitrofluorobenzene (DNFB) was appied to shave

skin on the belly of *ebi2*$^{+/+}$, *ebi2*$^{gfp/+}$ and *ebi2*$^{gfp/gfp}$ mice. Reapplication of DNFB to the ear after five days elicited inflammation in all genotypes, but the ear swelling induced in *ebi2*$^{gfp/gfp}$ mice was greatly reduced in comparison to *ebi2*$^{+/+}$and *ebi2*$^{gfp/+}$ mice (Fig. 35A). Tissue stainings of ear sections taken at 72h after DNFB-reapplication. Clearly

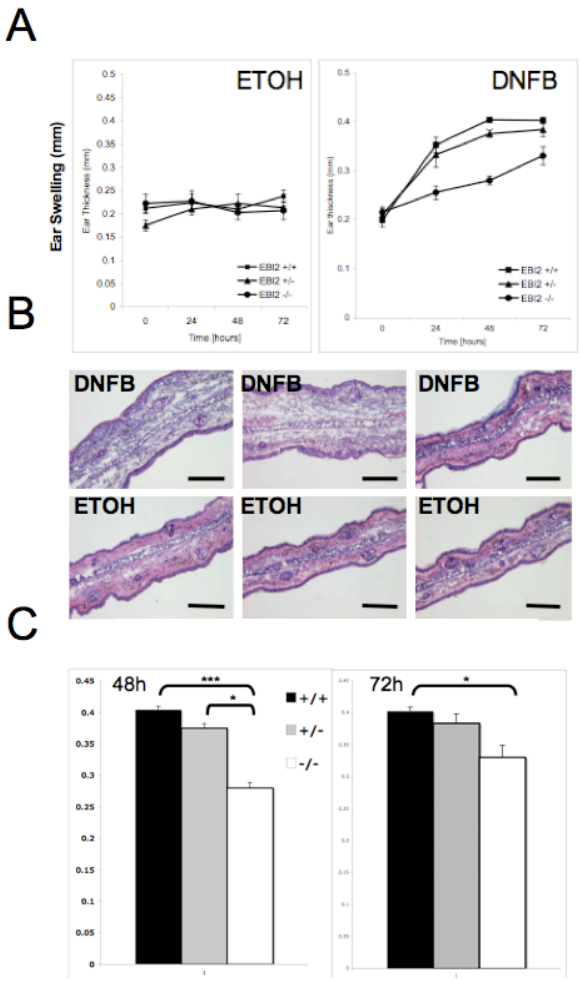

Fig. 35: EBI2 deficiency decreases hapten induce ear swelling: (A) *ebi2*$^{+/+}$, *ebi2*$^{gfp/+}$ or *ebi2*$^{gfp/gfp}$ mice were sensitized with DNFB (0.5% in ethanol) on the shaved belly. After 5d, DNFB was reapplied to the right ear of all sensitized mice. Ear swelling was measured over the following 72h. Control ears were treated with ethanol without DNFB. (B) H&E stainings of *ebi2*$^{+/+}$, *ebi2*$^{gfp/+}$ or *ebi2*$^{gfp/gfp}$ cryosections from DNFB-treated ears 72h after hapten readministration. Scale bars represent 100μm width. (C) Statistically significant differences at 48 and 72h were calculated using the student's t-test. Data shown represents two independent experiments.

reduced ear swelling was evident in the EBI2-deficient mice (Fig. 35B). These differences proved to be statistically significant between wt and EBI2-deficient mice at both 48 and 72h after hapten reapplication (Fig. 35C). Thus, both EAE and CHS immune responses are markedly reduced in EBI2-deificient mice.

6.5 EBI2-deficient T cells inefficiently migrate to secondary lymphoid organs.

In two T cell-mediated disease models, the inflammation induced was significantly reduced. We therefore reasoned that the defective immune responses would be derived from a lack of EBI2 on T cells, despite useage of a full knockout strain as opposed to a conditional allele. CD90.2^{+} cells were MACS-purified and intraveinously transferred into wt hosts mice. Shortly after transfer, hosts mice were sacrificed to view efficiency of T cell migration into secondary lymphoid organs. CD90.2^{+} *ebi2*$^{gfp/+}$ T cells migrated

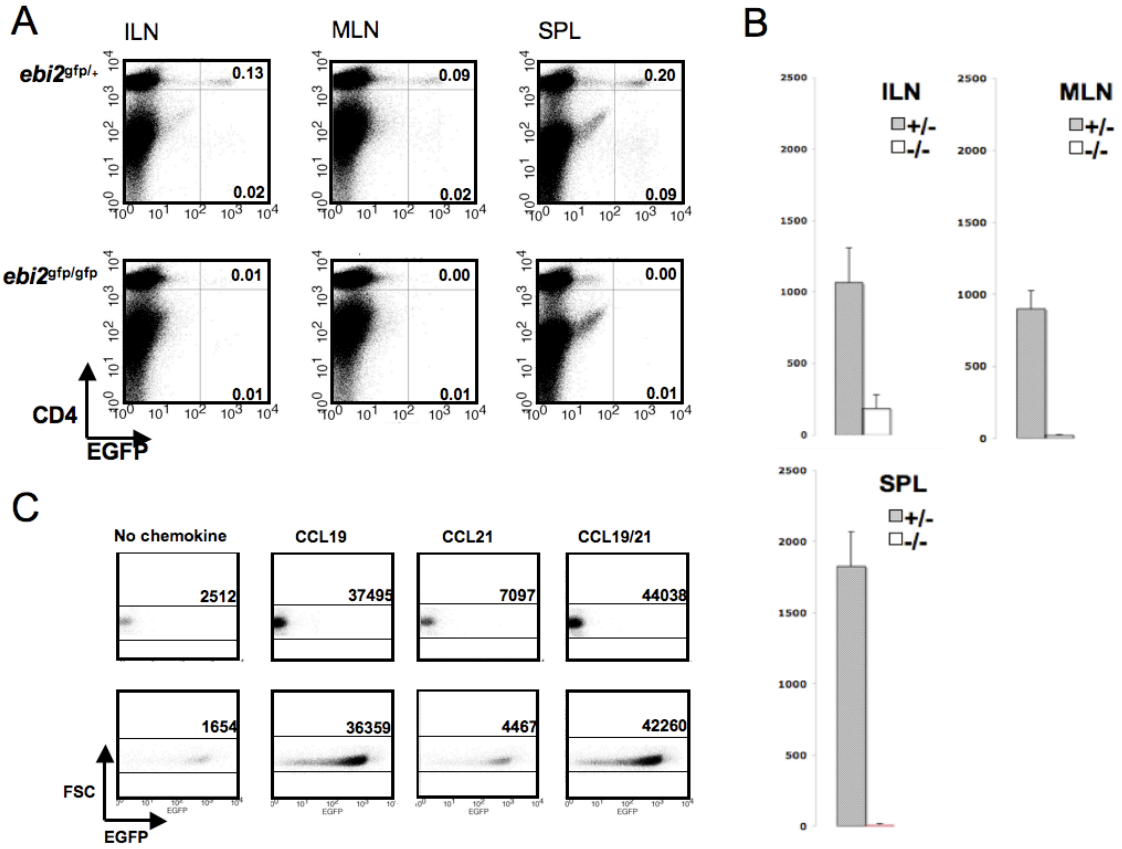

Fig. 36: EBI2-deficient T cells inefficiently migrate to secondary lymphoid tissue: (A) CD90.2 MACS-purified T cells from *ebi2*$^{gfp/+}$ or *ebi2*$^{gfp/gfp}$ mice were injected i.v. into the tail vein of wt recipient mice. After 3h, inguinal and mesenteric LN and spleens were isolated. CD4+EGFP+ and CD4-EGFP+ cells in the indicated organs are shown in the dot plots. (B) Total cell numbers of indicated genotypes in secondary lymphoid organs are shown (n=3). Error bars represent +/-SD. (C) *ebi2*$^{+/+}$ or *ebi2*$^{gfp/gfp}$ CD4+ T cells (n=2) were MACS-enriched and placed on transwells above T cell medium containing CCL19, CCL21 or both CCL19 and CCL21. Total cell numbers of viable cells migrated in response to indicated chemokines are shown in the dot plots.

rapidly into inguinal and mesenteric lymph nodes and spleens of wt mice (Fig. 36A). CD90.2+ *ebi2*$^{gfp/gfp}$ T cells did not appear in the secondary lymphoid organs with the

same efficency. This difference was witnessed both with percentage of $CD4^+EGFP^+$ cells arriving in the secondary lymphoid organs, and also the total number of transferred cells (Fig. 36B). The chemokines CCL19 and CCL21 are received by the chemokine receptor CCR7, a molecule essential for correct organisation of lymphocytes . EBI2 is still an orphan receptor, and we reasoned that a lack of migration may be due to an inherent inability of EBI2-deficient T cells to move from the blood stream and into the lymph nodes. EBI2-deficient T cells show no inherent lack of migratory capacity, as shown by an indisinguishable ability of EBI2-deficient and wt T cells to migrate in response to CCL19 and CCL21 gradients. Thus, EBI2-deficiency inhibits migration of T cells into secondary lymphoid organs, but this is not due to a lack of responsiveness to CCL19 and CCL21.

6.6 Low EBI2 expression correlates with a regulatory phenotype.

In the context of EAE, EBI2 expression correlated strongly with expression of proinflamatory cytokines, particularly IL-17A and IFN-γ. We reasoned that this molecule might indeed be necessary for effector cell function, and that within the $EBI2^{low}$ fraction of CD4 T cells, regulatory T cells may be overrepresented. To test this hypothesis, we sorted $CD4^{+}EGFP^{high}$ and $CD4^{+}EGFP^{low}$ T cells from *ebi2*$^{gfp/+}$ mice. After staining with anti-Foxp3 antibody, only 12% of $EGFP^{high}$ T cells expressed Foxp3. However, nearly 30% of $EGFP^{low}$ cells were $CD4^{+}Foxp3^{+}$, suggesting that a lower expression of EBI2 correlates with expression of Foxp3 *in vivo* (Fig. 37A). This finding was confirmed using RNA isolated from sorted $CD4^{+}EGFP^{high}$ and $CD4^{+}EGFP^{low}$ T cells (Fig. 37B), where $CD4^{+}EGFP^{low}$ T cells expressed higher levels of the transcription factor Foxp3.

We further sorted $CD4^{+}EGFP^{high}$ and $CD4^{+}EGFP^{low}$ T cells from pooled spleens and lymph nodes of *ebi2*$^{gfp/+}$ mice and transferred them into $RAG1^{-/-}$ hosts. After 4 weeks, it was apparent that host mice receiving $EBI2^{high}$ T cells had developed a mild form of colitis with increased granularity and translucency in the colon (Fig. 37C). To confirm that indeed EBI2 expression in these transferred cells correlated to EBI2 expression, RNA from $CD4^{+}EGFP^{high}$ and $CD4^{+}EGFP^{low}$ T cells from spleens and mesenteric lymph nodes of *ebi2*$^{gfp/+}$ mice was assayed for ebi2 expression by real time PCR. EBI2 expression was found to correlate with EGFP expression in this system (Fig.37D).

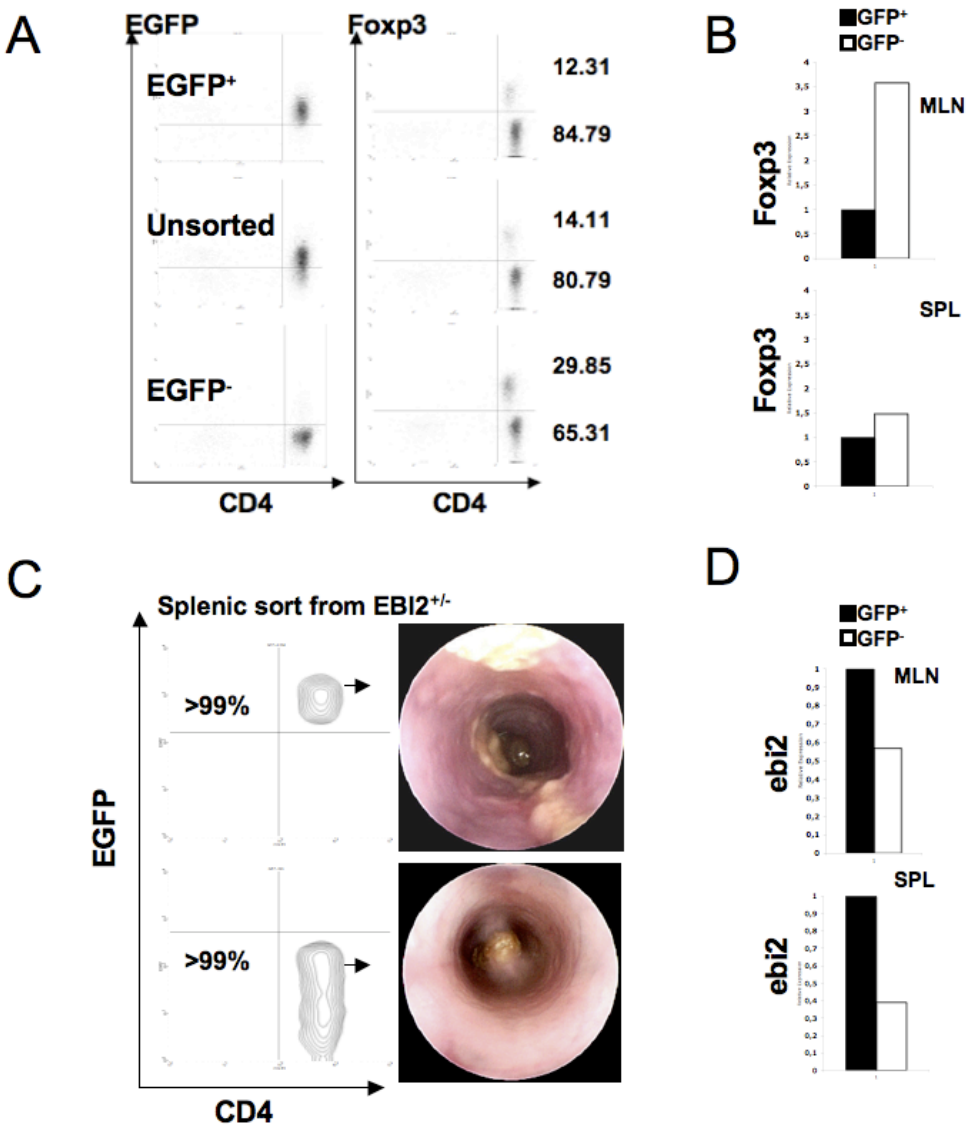

Fig. 37: Low EBI2-expression correlates to regulatory phenotype: (A) *ebi2*$^{gfp/+}$ T cells were FACS sorted (CD4$^+$EGFP$^+$ or CD4$^+$EGFP$^-$) and stained intracellularly for Foxp3. Percentages of Foxp3+ cells are shown in the indicated cell populations. (B) Real time expression for Foxp3 in FACS sorted (CD4$^+$EGFP$^+$ or CD4$^+$EGFP$^-$) CD4+ T cells. (C) *ebi2*$^{gfp/+}$ T cells were FACS sorted (CD4$^+$EGFP$^+$ or CD4$^+$EGFP$^-$) and 2x10^5 cells injected i.p. into RAG1-/- hosts. Colonoscopy was performed 4 weeks after transfer. (D) Real time expression for EBI2 expression in FACS-sorted (CD4$^+$EGFP$^+$ or CD4$^+$EGFP$^-$) CD4+ T cells.

6.7 EBI2-deficient T cells do not efficiently induce colitis in RAG1$^{-/-}$ hosts.

The finding that EBI2-low T cells were unable to induce colitis could be attributed to the fact that we effectively enriched the number of CD4$^+$Foxp3$^+$ T cells prior to transfer, or that lack of EBI2 expression was a major factor in the absence of colonic inflammation. CD4$^+$CD25$^-$ T cells were sorted from *ebi2*$^{+/+}$, *ebi2*$^{gfp/+}$ and *ebi2*$^{gfp/gfp}$

mice irrespective of EGFP intensity and transferred into the peritoneal cavity of RAG1$^{-/-}$ mice. 6 weeks after transfer, incidence of colitis and inflammation severity were recorded. EBI2-deficient T cells failed to increase clinical signs of colitis including vascularity, translucency and granularity compared to either wt or cells heterozygous for EBI2 (Fig. 38A). Colonic sections taken from mice 6 weeks after transfer also showed a strong reduction in CD4+ T cells migrating into the colon tissue (Fig. 38B). Thus, EBI2-deficiency renders T cells less able to induce inflammation in the context of transfer colitis.

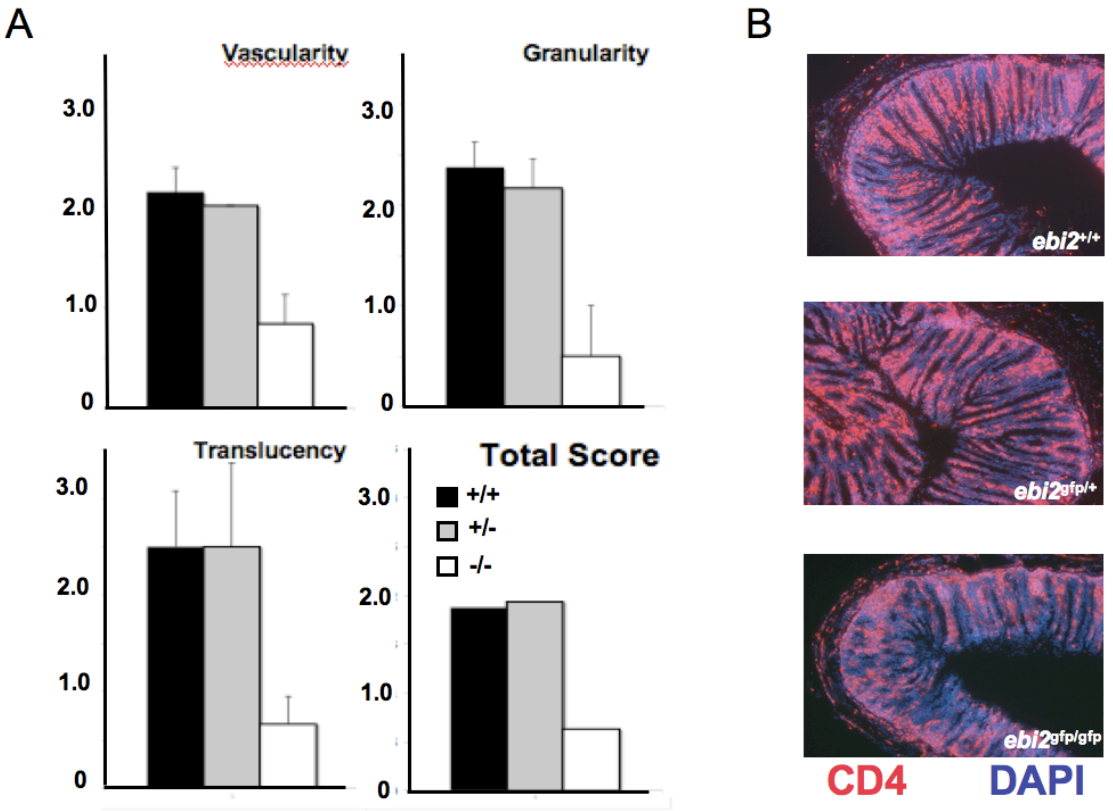

Fig. 38: EBI2-deficient T cells fail to induce transfer colitis: (A) *ebi2*$^{+/+}$, *ebi2*$^{gfp/+}$ or *ebi2*$^{gfp/gfp}$ CD4+CD25- T cells were FACS-sorted, and 2x10^5 cells injected i.p. into RAG1-/- hosts (n=3). After 4 weeks, vascularity, granularity and translucency of hosts colon tissue was analyzed. Error bars represent +/-SD. (B) Colons from RAG1-/- mice receiving either *ebi2*$^{+/+}$, *ebi2*$^{gfp/+}$ or *ebi2*$^{gfp/gfp}$ CD4+CD25- T cells were immunostained for CD4 and DAPI. Data shown represent three host mice per group.

7 Discussion

7.1 IL-17A$^{ind/+}$

7.1.1 K14 IL-17A$^{ind/+}$

Inflammatory processes of the skin have classically been segregated to either the cell-mediated Th1 or the humoral Th2 branch of the immune system. The recent addition of Th17 cells to current thinking in autoimmunity has created a marked paradigm shift. Indeed, the role of the IL-23/IL-17A axis has been studied intensively in recent years (McGeachy et al., 2009). Taken together, Th17 cytokines have been shown to stimulate cutaneous immune responses via activation of a wide range of downstream inflammatory mediators and the induction of immune cell and keratinocyte proliferation and angiogenesis. Hyperkeratosis was identified in K14-IL-17A^{ind} skin (personal communication, Dr. Esther von Stebut), which is characteristic of human psoriasis. Given the interest surrounding this issue and the lack of a generally accepted mouse model for human psoriasis, the purpose of the K14-IL-17A^{ind} strain was to provide a mouse model useful for sudying the effects of IL-17A in pathogenesis of psoriasis. In fact, newly developed treatment regimens for neutralizing IL-17A are proving to be excellent additions to the current therapeutic resources available for psoriasis.

Some previous findings strengthen the K14-IL-17A^{ind} strain as a useful model for the study of psoriasis. For example, subcutaneous injection with recombinant IL-17A led to upregulation of CCL20 and CCR6 expression in skin. This was accompanied by cutaneous T cell infiltration (Harper et al., 2009). These data therefore suggest that IL-17A stimulates CCL20 production *in vivo*, and provides a potential mechanism for CCR6-expressing Th17 cells maintain presence in psoriatic lesions through a chemotactic positive feedback loop. The expression of IL-17A from migrating Th17 cells would then result in neutrophil mobilization and propagation of the immune reaction. Thus, the K14-IL-17A^{ind} model would allow us to study how IL-17A-mediated CCL20 production attracts T cells to the site of inflammation.

The significant induction of granulocyte infiltration into the skin provides the opportunity to study how neutrophils behave once entering a site of inflammation.

Indeed, neutrophils themselves will produce their own signature chemokines (Scapini et al., 2000). The first chemokine shown to be produced by neutrophils, and certainly the most widely investigated in humans, is IL-8. Neutrophils are not only producers, but also the primary targets for IL-8, responding to this mediator by chemotaxis, release of granule enzymes, respiratory burst activity, upregulation of adhesion molecules expression on the surface, and increased adherence to unstimulated endothelial cells (Baggiolini, 1993; Baggiolini et al., 1994). Two receptors for IL-8 are expressed in neutrophils, namely CXCR1 and CXCR2. IL-8 is also chemotactic for basophils and T-lymphocyte subsets, although much less potently than for neutrophils. Therefore, expression of IL-8, and its murine homologues KC and MIP-2, would be worth investigating in the context of the K14-IL-17A^{ind} model. Interestingly, expression of IL-17F has been shown to have neutrophil attracting properties. Mouse skin intradermally injected with IL-17F expressed elevated levels of IL-8 (Watanabe et al., 2009). Histological examination showed that skin injected with IL-17F suffered from marked neutrophilia in dermis. This infiltration was significantly reduced by anti-IL-8 antibody administration. One might consider crossing the IL-17F-Cre to the iDTR or iDT strain (Buch et al., 2005) (Brockschnieder et al., 2004) to conditionally delete IL-17F-expressing cell types in inflamed skin. Addition of Imiquimod is sufficient to induce a psoriasis-like phenotype (van der Fits et al., 2009). The contribution of IL-17F to psoriasis development could be assessed in this model after administration of Imiquimod. Or additionaly, IL-17FCre^{EYFP} mice could be used to report on the activity of IL-17F expression in Imiquimod-induced psoriasis. Or indeed, K14-IL-17A^{ind} mice could host bone marrow from IL-17FCre^{EYFP} mice to study if indeed IL-17A expression in the skin caused a positive feedback loop resulting in Th17 migration into the skin.

7.1.2 CD4-IL-17A$^{ind/+}$

It was believed for more than a decade that Th1 cells are the main encephalitogenic population in CNS inflammatory diseases such as MS and EAE. As a consequence of this, the expression of IFN-γ in the CNS was a prime suspect for the major pathogenic molecule in EAE. In addition, Th1-promoting factors such as IL-12 and IL-18 were considered indispensable for the initiation of autoimmune disease in mice. This simplistic paradigm had to be revised when it was discovered that mice deficient in IFN-γ, TNF-α, IL-12p35, and IL-18 are either fully susceptible to EAE or hypersusceptible. While IL-12 is dispensable for the induction of EAE, its close relative IL-23 has been demonstrated to be absolutely essential. It was shown that IL-23 was able to stimulate the expression of IL-17A by effector T cells (Langrish et al., 2005). Furthermore, the obvious overlap between Th17 cells and autoimmune diseases such as rheumatoid arthritis, MS, and psoriasis has clearly marked this population as pathogenic. While IL-17A is now considered to be the main driving force behind tissue inflammation, it is surprising that the majority of claims are based on correlative relationships between Th17 cells and their presence in an inflammatory lesion. Assuming that IL-17A drives the inflammatory process and could contribute to blood brain barrier breakdown and increased neutrophil activity, we generated transgenic mice, in which T cells produce high levels of IL-17A. This was obtained by crossing the IL-17A^{ind} allele described in this thesis to the CD4-Cre transgene. Much to our surprise, highly increased levels of T cell–derived IL-17A did not worsen, accelerate or prolong the development of EAE or impact detectably on the inflammation in the CNS. This finding was published earlier this year (Haak et al., 2009).

Attempts to neutralize IL-17A in EAE had previously yielded only minimal reductions in disease severity, Blocking IL-17A alone with an antagonistic mAb or IL-17A and IL-17F combined using a soluble IL-17 receptor both failed to completely abrogate disease progression (Hofstetter et al., 2005). Komiyama et al addressed the role of IL-17A in EAE using a genetic approach, generating an *il17a*-deficient mouse strain (Komiyama et al., 2006). Unlike the deficiencies in IL-23 (p19) and IL-6, which render mice completely resistant to EAE, loss of IL-17A does not fully interrupt EAE development. Therapeutic targeting of IL-17A using a vaccination strategy showed a more robust efficacy but did not lead to complete resistance to EAE (Rohn et al., 2006). The far more critical role of IL-23 and IL-6 in the development of autoimmune

inflammation indicates that the associated disruption of IL-17A and IL-17F production is a contributing factor, but not the main cause of the complete EAE resistance observed in IL-23– and IL-6–deficient mice. With respect to Th17 cells in EAE, much progress has been made in unravelling the transcription factors and cytokine requirements for their development (Korn et al., 2007a; Veldhoen et al., 2006), and more recently, effector maintenance (Chung et al., 2009; McGeachy et al., 2009). Given the already pre-existing link between MS lesions and IL-17 production (Lock et al., 2002), the immunological community believed that a major breakthrough in MS treatment was on the horizon. While the pathogenic role of Th17 cells has been described in a number of disease models (CIA, EAE, UAE), the molecular explanation behind the pathogenicity of Th17 cells is now undoubtedly more complex than this single hallmark cytokine. For example, IL-17A-deficient or anti-IL-17A-treated mice are indeed able to develop EAE, though the kinetic and severity of disease is reduced, albeit to varying degrees (Haak et al., 2009) (Komiyama et al., 2006) (Hofstetter et al., 2005). When one contrasts this milder phenotype with the absolute and reproducible resistance of IL-23p19-deficient or IL-6 deficient mice (ref Cua, ref Korn), it is clear that IL-23 and IL-6 signaling on T cells results in more than just Th17 development. Indeed, TGF-β and IL-6-polarized Th17 cells per se are not able to induce EAE, even if they are myelin-specific (Yang et al., 2009). In contrast IL-23-driven myelin-specific Th17 cells were able to induce EAE (McGeachy et al., 2007). However, the results from a clinical trial using anti-p40 to treat MS patients was unsuccessful, showing that IL-23 in humans may indeed not be the major player in the human condition, and as such highlight possible differences in the molecular requirements for EAE and MS pathogenesis. The clinical trial was, however, conducted on patients with wide ranging MS pathogenesis, and in part after years of suffering with MS. As IL-23 has been shown to be essential in induction of EAE, it was conversely shown to be dispensible for maintenance of disease (Thakker et al., 2007). Thus, IL-12/23 p40 treatment may function better when administered much earlier in the disease development. IL-17-producing CD4+ and CD8+ T-cells are nonetheless detectable in active and chronic MS, and consist of both CD4 and CD8 T-cells (Tzartos et al., 2008). Thus, elucidating a role for Th17 cells in MS is indeed a worthwhile endeavour, but accumulating evidence from both EAE and clinical trials suggests that the causes of MS are more complex. One must not rule out the current theory that Th17 cells are highly flexible in their cytokine repertoire (Ivanov et al., 2007a) (Zhou et al., 2009), and although IL-17A

expression is indeed linked to Th17 cells, the ‚Th17' phenotype may only represent a stage in the life of an effector cell, and subsequently expressed cytokines are the true pathogenic molecules.

In agreement with our conclusions, in other models of autoimmunity such as experimental autoimmune uveitis (EAU), the function of IL-17A appears to be redundant (Yoshimura et al., 2008). In the context of contact hypersensitivity, IL-17A was also purported to play a role by promoting various proinflammatory cytokines and chemokines, recruiting neutrophils, enhancing antibody production, and activating T cells (Iwakura et al., 2008). In spite of this finding, we can cleary show that significantly increased amounts of IL-17A delivered into hapten-challenged ears did not intensify the inflammation. The concept that IL-17A itself is not likely the only pathogenic molecule generated by Th17 cells was further supported after the demonstration that IL-23–driven Th cells but not TGF-β and IL-6–driven Th cells were encephalitogenic, regardless of their secretion of IL-17A, and this was performed in SJL/J mice, where IL-17A is considered to play a more significant role (McGeachy and Cua, 2007). Indeed, the strains of mice used appear to determine the therapeutic potential of anti–IL-17A therapy. While IL-17A blockade has hardly any effect in C57BL/6 mice (Hofstetter et al., 2005), SJL/J mice show more pronounced disease alleviation after anti–IL-17A treatment (Langrish et al., 2005). Bearing this in mind, it will be useful to backcross the CD4-Cre and the IL-17A^{ind} allele to the SJL background. In this setting, it may be observed that IL-17A will have a more important role in disease progression. Nevertheless, neutralization of IL-17A has not been demonstrated to completely prevent EAE development in the SJL/J strain (Toy et al., 2006).

The fact that *Il17f*$^{-/-}$ mice treated with anti–IL-17A mAbs developed only a slightly ameliorated disease course with a similar incidence and severity as untreated mice or WT mice supports the notion that neither IL-17A nor IL-17F, either individually or in combination, are essential for the development of autoimmune CNS inflammation (Haak et al., 2009). In addition, the fact that mice in which transgenic overexpression of IL-17A is directed toward T cells also displayed an unaltered EAE phenotype further distances IL-17 from key players in CNS autoimmunity (Haak et al., 2009). Integrating all current data generated by deletion of IL-17A as well as IL-17F or induced overexpression of IL-17A, it can safely be concluded that, unlike IL-23 and IL-6, neither of these Th17 cytokines are key players in EAE. It is likely that the tissue

distribution of IL-17RA and IL-17RC, the receptor complex for IL-17A and IL-17F (Toy et al., 2006; Wright et al., 2008), determines the pathogenic capacity of Th17 cells. The CNS expresses low levels of IL-17R in comparison to the skin or lung (Haudenschild et al., 2002; Yao et al., 1995), thus explaining the severe impact of total IL-17A overexpression on the skin but not the CNS. Translating these findings into the clinic for therapeutic targeting of this pathway in MS is even more complicated considering the data obtained in a recent clinical trial in MS patients. MS patients were treated with mAb specific to IL-12/IL-23p40, which surprisingly had no beneficial effect, indicating that in MS patients, these Th1- and Th17-inducing cytokines may not play an essential role in disease progression (Segal et al., 2008). On the other hand, targeting of the IL-23 pathway has a profound efficacious impact on psoriasis, again supporting the notion that the tissue distribution of cytokine receptors such as IL-17R determines the impact of Th17 cells on inflammation. While IL-17 family member molecules currently function as markers for pathogenic T cells, we conclude that unidentified factors or mechanisms employed by Th17 cells must convey their pathogenic capacity in the context of EAE.

7.1.3 Deleter IL-17A$^{ind/+}$

Peripheral blood neutrophil numbers are tightly regulated in both mice and humans. Homeostatic regulatory mechanisms have been proposed (Demetri and Griffin, 1991) and debated (Horwitz et al., 2001) but never demonstrated. Enormous numbers of neutrophils (10^{11} polymorphonuclear neutrophils (PMN)/day in humans) which circulate for a few hours and undergo apoptosis, are produced every day. Older neutrophils in the blood start expressing CXCR4 and home back to the bone marrow (Martin et al., 2003); however, this process is unlikely to occur in neutrophils that have left the bloodstream and have migrated into tissues. It is clear that this homeostasis is clearly imbalanced in the Deleter IL-17A^{ind} strain.

Some drawbacks are apparent when using the Deleter IL-17A^{ind} strain for studying the immune system and immune responses. The early death of these mice render them of limited use for longer term experiments. In addition, the significant growth retardation, the artificially high levels of neutrophils in the blood and organs and the overt anemia indicate that these mice will be physiologically unable to provide accurate results. Interestingly, the Deleter IL-17A^{ind} strain might prove useful in the study of some malignancies. Chronic myeloid leukaemia (CML) is a disease in which white blood cells proliferate out of control. In the case of chronic neutrophil leukaemia (CNL), a rare myeloproliferative disorder in which neutrophils proliferate out of control (Hasle et al., 1996), parallels can be drawn between the phenotype shown in the Deleter IL-17A^{ind} strain and patients with CNL. The underlying causes of the neutrophilia observed may be completely different, but pathogenesis created as a result of neutrophilia can indeed be studied in this model.

7.2 IL-17F-Cre

7.2.1 IL-17A$^+$IFN-γ$^+$ T cells

Th17 cells were thought to be distinct from Th1 on the basis of RORγt expression, which appears specific to Th17 cells. In addition, they can arise in the absence of T-bet or Stat4 (Ivanov et al., 2006) (Weaver et al., 2007; Weaver and Murphy, 2007). However, we can show that under homeostatic or inflammatory conditions, IL-17A$^+$IFN-γ$^+$ double-producing cells can be found, suggesting that there may be a relationship between the Th1 and Th17 cells and their differentiation regimen, at least in a later stage. Whether these cells arise from Th17 cells or Th1 cells was an open question. Our data go some way to showing that these IL-17A$^+$IFN-γ$^+$ double-producing cells can, at least in part, arise from Th17 cells.

Some recent publications support our data on the instability of Th17 cytokine expression. Lexberg et al. demonstrated that constant exposure to TGF-β and IL-6 was essential for maintenance of IL-17A and IL-17F expression (Lexberg et al., 2008). Indeed, the presence of TGF-β alone was shown to sustain expression of IL-17 and IL-17F (Lee et al., 2009). It is possible that IL-21 produced by Th17 cells in this setting could act in concert with exogenous TGF-β to maintain a cytokine environment necessary to retain IL-17A and IL-17F expression. It is feasible that the availability of these molecules in RAG1-deficient hosts might indeed be altered and result in the downregulation of Th17 cytokines from both Th17 and Tc17 cells. Also the excessive IL-7R signalling in RAG1-deficient mice and pressure to homeostatically expand may also play a role in Th17 cells losing their cytokine signatures and perhaps even the observed upregulation of IFN-γ. This possibility could easily be tested *in vitro*.

In vitro-polarized Th17 cells also failed to maintain IL-17A and IL-17F expression and were readily made to express IFN-γ and IL-4 in response to IL-12 or IL-4 signaling, respectively (Lee et al., 2009). IFN-γ expression from these cells was induced by IL-23. Whether or not this is the reason for conversion we see in RAG1-deficient hosts remains to be clarified. In contrast to *in vitro*-differentiated Th17 cells, in vivo memory CD4+CD62L^{low} Th17 cells appear more resistant to conversion (Lexberg et al., 2008). Thus, these results suggest that there may be epigenetic differences between *in vitro*- and *in vivo*-generated Th17 cells (discussed below). The possibility exists using the IL-17FCre^{EYFP} mice to analyse egigenetic modifications

from *ex vivo* or *in vitro*-generated Th17 cells, and as such would be well placed to answer this question.

The basis of our understanding of the cell types and molecular effectors which mediate the pathogenesis of EAE has escalated dramatically. However, it is important to question some basic principles on which current EAE research has been founded. For example, the observation that myelin-specific Th1 cells were sufficient to induce EAE in mice directed the field of MS research toward IFN-γ, the hallmark cytokine of these pathogenic effector cells. It was clearly demonstrated however that both healthy individuals and MS patients harbor myelin-specific CD4+ T cells, but these cells are more likely to have a Th1 phenotype in MS patients. It was therefore surprising that numerous reports illustrate a protective effect of IFN-γ with respect to EAE pathogenesis. Both IFN-γ-deficient mice and mice treated with neutralizing antibodies against IFN-γ were still susceptible, or hyper susceptible to EAE. Despite efforts to uncover the mechanism behind a protective role for IFN-γ, answers have remined elusive. It was recently shown that IFN-γ signaling downregulates expression of IL-1R on macrophages (Hu et al., 2005). Chen Dong and colleagues were able to describe a crucial role for the IL-1/IL-1R axis in the development of EAE and early generation of Th17 cells. IL-1 receptor expression in T cells, which was induced by IL-6, was necessary for the induction of experimental autoimmune encephalomyelitis and for early Th17 cell differentiation *in vivo* (Chung et al., 2009). Moreover, IL-1 signaling in T cells was required in dendritic cell-mediated Th17 cell differentiation from naive or regulatory precursors and IL-1 synergized with IL-6 and IL-23 to regulate Th17 cell differentiation and maintain cytokine expression in effector Th17 cells. Importantly, IL-1 regulated the expression of the transcription factors IRF4 and RORγt during Th17 cell differentiation; overexpression of these two factors resulted in IL-1-independent Th17 cell polarization (Chung et al., 2009). Thus, IFN-γ may downregulate IL-1R expression on immune cell types and ultimately diminishing the potential to mount an inflammatory response.

7.2.2 Th17 and Foxp3 expression

TGF-β is profoundly important for the establishment of tolerance. It is required for the differentiation iTregs and for peripheral maintenance of nTreg cells after thymic

emigration (Chen et al., 2003) (Li et al., 2006). For this reason, it was surprising for the immunological community in 2006, when a string of publications showed that TGF-β is also essential for the differentiation of proinflammatory Th17 cells (Bettelli et al., 2006; Mangan et al., 2006; Veldhoen et al., 2006). Mice lacking TGF-β lack both Foxp3+ Tregs and Th17 cells, which results in lethal autoimmunity caused by unregulated Th1 aggression (Li et al., 2006; Veldhoen et al., 2006). These findings again highlight the link between Treg and Th17 differentiation (Beriou et al., 2009), and also point to the obvious suppression of Th1 cells by Tregs under normal conditions. We sought to investigate the plasticity of fully mature Th17 cells (as defined by strong expression of IL-17A and IL-17F) with respect to Foxp3 upregulation. The recent data of iTreg and nTreg converting towards Th17 cells indicate that Tregs may represent a dynamic population capable of deciding whether to switch from suppression to inflammation. Our data was published and indicates that this switch is unidirectional (Croxford et al., 2009).

The exposure of antigen-activated naive CD4+ T cells to TGF-β results in transcriptional upregulation of both Foxp3+ and RORγt+, transcription factors that direct distinct CD4+ T cell differentiation programs (Zhou et al., 2008). IL-6 signaling is then necessary to inhibit Foxp3 expression such that the equilibrium in the nucleus shifts toward a RORγt-dominant environment to permit Th17 differentiation. Several transcription factors have been implicated in modulating the RORγt-Foxp3 balance during T helper cell differentiation. IRF4 is essential for Th17 cell differentiation both *in vitro* and *in vivo* (Brustle et al., 2007). Its absence in mice resulted in reduced RORγt expression, increased Foxp3 expression, loss of IL-17 production, and protection from experimental autoimmune encephalomyelitis (EAE). IRF4 was also identified as a direct target of Foxp3, and its targeted loss to Tregs selectively impaired suppression of Th2 cell responses (Zheng et al., 2009). Runx1 was recently shown to form a complex with RORγt and to cooperate with it to promote Th17 cell differentiation (Zhang et al., 2008). In Treg cells, an interaction between Runx1 and Foxp3 was reported to be required for suppression of IL-2 and IFN-γ production, upregulation of Treg cell-associated molecules, and suppressive activity (Ono et al., 2007).

T cells that coexpress RORγt and Foxp3 have been identified *in vivo* in both mice and humans (Voo et al., 2009; Zhou et al., 2008). Foxp3+RORγt+ cells from the small intestine produce less IL-17A compared to Foxp3-RORγt+ cells (Zhou et al., 2008) (Zhou et al., 2008), whereas Foxp3 deficiency results in a marked increase in IL-

17 but not RORγt expression (Gavin et al., 2007). These observations suggest that Foxp3 may antagonize RORγt-induced IL-17 expression in a cell-intrinsic manner. One should consider that Foxp3+RORγt+ cells may also exist as a transient population that can give rise to either Treg or Th17 cells. A plausible explanation for the reduced amount of IL-17A in cells that coexpress RORγt and Foxp3 is provided by the finding that these two transcription factors can interact with each other, perhaps in the context of larger nuclear complexes. A similar physical interaction was first demonstrated between Foxp3 and RORα, which is closely related to RORγt and is similarly sufficient for inducing IL-17 expression but has only a minor redundant role in Th17 cell differentiation. Whereas transduction of naive CD4+ T cells with RORγt induces IL-17 expression, cotransduction with Foxp3 abrogates induction as long as Foxp3 contains its exon-2-encoded domain that is required for binding to RORγt (Zhou et al., 2008). After *in vitro* induction of RORγt and Foxp3 by TGF-β, cells do not express IL-17 but have the dual potential to differentiate into either the Th17 or Treg cell lineage depending on the cytokine environment. In the presence of proinflammatory cytokines (IL-6, IL-21, or IL-23) and low concentrations of TGF-β, RORγt expression is further upregulated, whereas Foxp3 expression and function are inhibited. This relieves repression of RORγt activity by Foxp3 in favor of Th17 cell lineage specification. In contrast, in the absence of proinflammatory cytokines, high concentrations of TGF-β are optimal for Foxp3 expression and thus tip the balance toward Treg cell differentiation (Zhou et al., 2008). This shift toward Treg cells is enhanced by IL-2 and retinoic acid (RA). Both inhibit Th17 cell differentiation by reducing RORγt expression and enhancing TGF-β-induced Foxp3 expression, thus influencing Th17-Treg cell specification (Coombes et al., 2007) (Mucida and Cheroutre, 2007; Mucida et al., 2007).

Stat3, a transcription factor common to the IL-6, IL-21, and IL-23 signaling pathways, is also essential for Th17 cell differentiation. Stat3 binds to the *il17a* locus to direct its transcription, presumably through cooperative activity with RORγt (Chen et al., 2006). TGF-β-induced Foxp3 expression is inhibited by proinflammatory cytokines in a Stat3-dependent manner. Forced expression of an active form of Stat3 enhanced IL-17A expression in the presence of TGF-β, presumably by upregulation of RORγt expression and suppression of Foxp3 expression (Zhou et al., 2007) (Yang et al., 2007). It remains to be determined whether the coordinated activity of Stat3 and RORγt in induction of IL-17A is due to a physical interaction between these two factors and

whether relief of Foxp3 inhibition by proinflammatory cytokines is mediated by perturbation of RORγt-Foxp3 interaction through the activity of Stat3.

7.3 CD4-IL-6R$^{fl/fl}$

In this section I investigated the role of IL-6 in the development of pathogenic CD4+ T cells during an autoimmune response *in vivo*. We found that CD4+ T cell-restricted unresponsiveness to IL-6 results in an overt T-reg response *in vivo* which inhibits the induction of Th1 and Th17 effector cells and results in full resistance to EAE. However, the failure to induce Th17 cells in CD4-IL-6R$^{fl/fl}$ mice is not due to an intrinsic inability of CD4-IL-6R$^{fl/fl}$ CD4+ T cells to become Th17 cells, since the combination of TGF-β plus IL-21 induced the expression of IL-17A from naive CD4-IL-6R$^{fl/fl}$ T cells. Also, T-reg-depleted CD4-IL-6R$^{fl/fl}$ mice were able to mount a pathogenic Th1 and Th17 response upon immunization with MOG/CFA and pertussis toxin. Thus, alternative pathways exist to induce Th17 cells in the absence of IL-6 signaling. This pathway is likely to be the IL-21 pathway, but more experiments would be needed to confirm this hypothesis. A neutralizing antibody against IL-21 in T-reg-depleted CD4-IL-6R$^{fl/fl}$ mice should again render these mice resistant to EAE. We are also in the process of procuring IL-21R-deficient mice to cross to the CD4-IL-6R$^{fl/fl}$ mice. One could deplete Tregs in CD4-IL-6R$^{fl/fl}$ IL-21R$^{-/-}$ mice, and see if the absence of both IL-21 and IL-6 signaling is enough to render mice resistant to EAE induction, even in the absence of Tregs.

IL-21 also, however, suppresses the induction of Foxp3 (Korn et al., 2007a). These findings suggest that the IL-6/IL-6R signaling in CD4+ T cells constitutes a dominant pathway since in the absence of IL-6R signaling but in the presence of an intact IL-21/IL-21R system, the induction of Foxp3 was still not suppressed and the mice developed an overwhelming T-reg response. We must therefore conclude from this data that the IL-21-mediated inhibition of Foxp3 and induction of Th17 cells respresents only a minor pathway in wild type mice.

IL-6 is a potent factor to switch immune responses from the induction of Foxp3+ T-regs to pathogenic Th17 cells *in vivo*. There is accumulating molecular evidence that a single naive T cell can develop into both a functional T-reg and an IL-17A-producing T cell (Coquet et al., 2008). TGF-β is necessary to induce the expression of both Foxp3, the master transcription factor of T-regs, and ROR-γt, the essential transcription factor of Th17 cells (Serada S, PNAS, 2008). Although necessary for the expression of both Foxp3 and ROR-γt, TGF-β enhances the function

of Foxp3, but inhibits the function of ROR-γt (Serada et al., 2008b). Only when additional signaling of 'pro-inflammatory' cytokines like IL-6 or IL-21 is operational, the TGF-β-mediated functional inhibition of ROR-γt is relieved and Th17 cells are induced. Here, we show that after T-reg depletion, the development of Th17 cells is possible in the absence of IL-6 signaling suggesting that other factors can compensate for IL-6 effects in inducing Th17 cells. It has recently been shown that STAT-3, ROR-γt, and ROR-α are required to induce IL-17 in T cells (Dong, 2008). Although IL-6 and IL-21 use totally unrelated receptors, both recruit STAT-3 as downstream signaling molecule (Spolski and Leonard, 2008). Thus, IL-21 signaling can circumvent IL-6R signaling defects and induce Th17 cells. STAT-3 is also necessary and might even be sufficient to inhibit Foxp3 (Yang et al., 2008c). However, in case of a deficient IL-6R system, the induction of Foxp3 cannot be suppressed suggesting that activation of STAT-3 by other factors such as IL-21 is qualitatively or quantitatively insufficient to compensate for IL-6 in the inhibition of Foxp3 induction and the generation of functional T-regs *in vivo*. We conclude that IL-6/IL-6R signaling has a dominant function in the suppression of Foxp3+ *in vivo*. This idea is supported by the fact that under conditions of high availability of IL-6, IL-21R KO mice do not exhibit enhanced induction of T-regs and are susceptible to EAE (Coquet et al., 2008; Sonderegger et al., 2008).

These data illustrate the pivotal role of IL-6 in dictating the balance between iT-regs and Th17 cells *in vivo* and show that the *de novo* generation of Foxp3+ T-regs is the default pathway in the absence of IL-6. This supports data previously generated by us and others (Korn et al., 2008). Blockade of IL-6 signaling might therefore represent an appealing strategy to control antigen-specific autoimmune responses. A recent report confirmed that administration of a neutralizing anti-IL-6R antibody abrogates the initiation of inflammation in EAE due to a reduced Th17 response (Serada et al., 2008a). In conclusion, these findings have an important impact on the attempts to generate antigen-specific Foxp3+ T-regs and controlling the direction of immune responses for therapy *in vivo*. Indeed, as soon as IL-6 production or signaling is blocked, immunogenic vaccination is likely to be result in an overwhelming collection of antigen specific Foxp3+ T-regs. It may then perhaps be possible to immunize an individual against a specific autoantigen in combination with IL-6 neutralization to reduce the likelihood of an autoimmune response to this antigen.

7.4 EBI2

A reporter mouse generated by Stefano Casola was made available to our group on a collaborative basis, with our role to study the effect of EBI2 deficiency on T cell function. Despite efforts by numerous groups, EBI2 remains an orphan GPCR and the identity of its ligand and potential cellular sources are still unknown. Molecular studies of EBI2 have predicted that this receptor may have constitutive activity, similar to that observed for many herpesvirus-encoded 7TM receptors (Rosenkilde et al., 2008). The group of Robert Brink hypothesized that heterodimerization of EBI2 with other chemokine receptors could positively or negatively regulate its activity (Gatto et al., 2009). EBI2 deficiency might therefore be expected to affect the in vitro chemotaxis of T cells. Thus, our working hypothesis was that migration of T cells would be altered by loss of EBI2, and that this change may affect the development of inflammation via reduced T cell homing into sites of inflammation.

Initial observations of these mice showed strong expression of EBI2 in CD4 T cells, but a weaker expression in CD8 T cells. This early observation hinted at a role for EBI2 in CD4-mediated immune regulation in which cytotoxic T cells were not required. In line with this, EBI2-deficient mice proved to be resistant to EAE, a primarily T cell-mediated autoimmune disease. It was also therefore interesting to find that Th1 and Th17 cells both express EBI2 in the CNS, which implies a need to express EBI2 to enter into a site of inflammation. Although we hypothesited that EBI2 may share ligand specificity with CCR7, no differences in chemoattraction to the chemokine ligand CCL19 and CCL21 were observed, showing that EBI2 did not share ligand specificity with CCR7. One can also assume from this finding that pathogenic Th1 and Th17 cells in the context of EAE, which highly express EBI2, may rely on the ligand to enter into the inflamed CNS.

Although publications speculating a role for EBI2 are limiting, two recent studies have defined a role for EBI2 ‚fine-tuning' the position of B cells in the germinal centre. Both publications, however, fell short of providing the ligand for EBI2. Firstly, and similarly to our targeting approach, the group of Jason Cyster placed a GFP reporter cassette downstream of the EBI2 promoter and used fluorescence intensity to demonstrate the levels of EBI2 expression in their analysis of B cell migration. They established that EBI2 is upregulated in B cells after activation through the BCR or via CD40 engagement. It was unfortunately not discussed that an activation of B cells will

result in an increase in cellular size, and as such will increase the amount of GFP signal without necessarily being the result of increased gene expression. This process was, however, hypothesized to be necessary for the directing of activated B cells to interfollicular regions and the outer follicle (Pereira et al., 2009). Defects in these processes are probably responsible for the EBI2-deficient mice displaying limited ability to mount an early T-dependent IgG antibody response. Their findings suggest that EBI2 is needed within B cells to orchestrate these events. The authors did not exclude that EBI2 may have a role in positioning activated CD4 helper T cells within these regions. Although the ligand for EBI2 remains undefined, Cyster speculated that concentrations of the ligand would be more concentrated in the outer follicle compared to centre follicle as well as in interfollicular regions. The final proposal was that cells expressing EBI2 are more strongly attracted to the outer follicle compared to cells lacking this receptor. Although B cell-deficient mice are not at all resistant to EAE induction (Wolf et al., 1996) (and personal observations), one might conclude that an impaired immune response might result in resistance to EAE, particularly if motion of CD4+ T cells in secondary lymphoid tissue is compromised.

A second group were able to reach similar conclusions, demonstrating that EBI2-mediated positioning of B cells represents a critical step in directing activated B cells into the extrafollicular versus GC compartments. Their data additionally suggest that downregulation of EBI2 by Bcl-6 is a critical event in mediating GC B cell differentiation. Although both publications fell short of providing the ligand for EBI2 in vivo, the migratory behavior of both naive and activated EBI2-deficient B cells indicated that these B cells failed to be attracted to the periphery of B cell follicles and extrafollicular regions. These findings therefore logically suggest that the ligand will be in high concentrations in these sites, and the search fort he ligand for EBI2 should continue in the B cell follicle.

8 Bibliography

Afkarian, M., Sedy, J.R., Yang, J., Jacobson, N.G., Cereb, N., Yang, S.Y., Murphy, T.L., and Murphy, K.M. (2002). T-bet is a STAT1-induced regulator of IL-12R expression in naive CD4+ T cells. Nature immunology *3*, 549-557.

Aggarwal, S., Ghilardi, N., Xie, M.H., de Sauvage, F.J., and Gurney, A.L. (2003). Interleukin-23 promotes a distinct CD4 T cell activation state characterized by the production of interleukin-17. The Journal of biological chemistry *278*, 1910-1914.

Akiba, H., Kehren, J., Ducluzeau, M.T., Krasteva, M., Horand, F., Kaiserlian, D., Kaneko, F., and Nicolas, J.F. (2002). Skin inflammation during contact hypersensitivity is mediated by early recruitment of CD8+ T cytotoxic 1 cells inducing keratinocyte apoptosis. J Immunol *168*, 3079-3087.

Alexander, W.S., Starr, R., Fenner, J.E., Scott, C.L., Handman, E., Sprigg, N.S., Corbin, J.E., Cornish, A.L., Darwiche, R., Owczarek, C.M.*, et al.* (1999). SOCS1 is a critical inhibitor of interferon gamma signaling and prevents the potentially fatal neonatal actions of this cytokine. Cell *98*, 597-608.

Appelberg, R. (2007). Neutrophils and intracellular pathogens: beyond phagocytosis and killing. Trends in microbiology *15*, 87-92.

Asensi, V., Valle, E., Meana, A., Fierer, J., Celada, A., Alvarez, V., Paz, J., Coto, E., Carton, J.A., Maradona, J.A.*, et al.* (2004). In vivo interleukin-6 protects neutrophils from apoptosis in osteomyelitis. Infection and immunity *72*, 3823-3828.

Awasthi, A., Carrier, Y., Peron, J.P., Bettelli, E., Kamanaka, M., Flavell, R.A., Kuchroo, V.K., Oukka, M., and Weiner, H.L. (2007). A dominant function for interleukin 27 in generating interleukin 10-producing anti-inflammatory T cells. Nature immunology *8*, 1380-1389.

Baggiolini, M. (1993). Chemotactic and inflammatory cytokines--CXC and CC proteins. Advances in experimental medicine and biology *351*, 1-11.

Baggiolini, M. (1998). Chemokines and leukocyte traffic. Nature *392*, 565-568.

Baggiolini, M., Dewald, B., and Moser, B. (1994). Interleukin-8 and related chemotactic cytokines--CXC and CC chemokines. Advances in immunology *55*, 97-179.

Baxter, A.G. (2007). The origin and application of experimental autoimmune encephalomyelitis. Nature reviews *7*, 904-912.

Beauvillain, C., Delneste, Y., Scotet, M., Peres, A., Gascan, H., Guermonprez, P., Barnaba, V., and Jeannin, P. (2007). Neutrophils efficiently cross-prime naive T cells in vivo. Blood *110*, 2965-2973.

Bennouna, S., Bliss, S.K., Curiel, T.J., and Denkers, E.Y. (2003). Cross-talk in the innate immune system: neutrophils instruct recruitment and activation of dendritic cells during microbial infection. J Immunol *171*, 6052-6058.

Beriou, G., Costantino, C.M., Ashley, C.W., Yang, L., Kuchroo, V.K., Baecher-Allan, C., and Hafler, D.A. (2009). IL-17-producing human peripheral regulatory T cells retain suppressive function. Blood *113*, 4240-4249.

Bettelli, E., Carrier, Y., Gao, W., Korn, T., Strom, T.B., Oukka, M., Weiner, H.L., and Kuchroo, V.K. (2006). Reciprocal developmental pathways for the generation of pathogenic effector TH17 and regulatory T cells. Nature *441*, 235-238.

Bettelli, E., Pagany, M., Weiner, H.L., Linington, C., Sobel, R.A., and Kuchroo, V.K. (2003). Myelin oligodendrocyte glycoprotein-specific T cell receptor transgenic mice develop spontaneous autoimmune optic neuritis. The Journal of experimental medicine *197*, 1073-1081.

Bliss, S.K., Gavrilescu, L.C., Alcaraz, A., and Denkers, E.Y. (2001). Neutrophil depletion during Toxoplasma gondii infection leads to impaired immunity and lethal systemic pathology. Infection and immunity *69*, 4898-4905.
Bluestone, J.A., and Abbas, A.K. (2003). Natural versus adaptive regulatory T cells. Nature reviews *3*, 253-257.
Bour, H., Demidem, A., Garrigue, J.L., Krasteva, M., Schmitt, D., Claudy, A., and Nicolas, J.F. (1995). In vitro T cell response to staphylococcal enterotoxin B superantigen in chronic plaque type psoriasis. Acta dermato-venereologica *75*, 218-221.
Brockschnieder, D., Lappe-Siefke, C., Goebbels, S., Boesl, M.R., Nave, K.A., and Riethmacher, D. (2004). Cell depletion due to diphtheria toxin fragment A after Cre-mediated recombination. Molecular and cellular biology *24*, 7636-7642.
Brown, D.A., and Sawchenko, P.E. (2007). Time course and distribution of inflammatory and neurodegenerative events suggest structural bases for the pathogenesis of experimental autoimmune encephalomyelitis. J Comp Neurol *502*, 236-260.
Brustle, A., Heink, S., Huber, M., Rosenplanter, C., Stadelmann, C., Yu, P., Arpaia, E., Mak, T.W., Kamradt, T., and Lohoff, M. (2007). The development of inflammatory T(H)-17 cells requires interferon-regulatory factor 4. Nature immunology *8*, 958-966.
Buch, T., Heppner, F.L., Tertilt, C., Heinen, T.J., Kremer, M., Wunderlich, F.T., Jung, S., and Waisman, A. (2005). A Cre-inducible diphtheria toxin receptor mediates cell lineage ablation after toxin administration. Nature methods *2*, 419-426.
Chabaud, M., Garnero, P., Dayer, J.M., Guerne, P.A., Fossiez, F., and Miossec, P. (2000). Contribution of interleukin 17 to synovium matrix destruction in rheumatoid arthritis. Cytokine *12*, 1092-1099.
Chang, S.H., and Dong, C. (2007). A novel heterodimeric cytokine consisting of IL-17 and IL-17F regulates inflammatory responses. Cell research *17*, 435-440.
Chang, S.H., Park, H., and Dong, C. (2006). Act1 adaptor protein is an immediate and essential signaling component of interleukin-17 receptor. The Journal of biological chemistry *281*, 35603-35607.
Channon, J.Y., Seguin, R.M., and Kasper, L.H. (2000). Differential infectivity and division of Toxoplasma gondii in human peripheral blood leukocytes. Infection and immunity *68*, 4822-4826.
Chen, S.C., Chang, Y.L., Wang, D.L., and Cheng, J.J. (2006). Herbal remedy magnolol suppresses IL-6-induced STAT3 activation and gene expression in endothelial cells. British journal of pharmacology *148*, 226-232.
Chen, W., Jin, W., Hardegen, N., Lei, K.J., Li, L., Marinos, N., McGrady, G., and Wahl, S.M. (2003). Conversion of peripheral CD4+CD25- naive T cells to CD4+CD25+ regulatory T cells by TGF-beta induction of transcription factor Foxp3. The Journal of experimental medicine *198*, 1875-1886.
Chung, Y., Chang, S.H., Martinez, G.J., Yang, X.O., Nurieva, R., Kang, H.S., Ma, L., Watowich, S.S., Jetten, A.M., Tian, Q., and Dong, C. (2009). Critical regulation of early Th17 cell differentiation by interleukin-1 signaling. Immunity *30*, 576-587.
Coombes, J.L., Siddiqui, K.R., Arancibia-Carcamo, C.V., Hall, J., Sun, C.M., Belkaid, Y., and Powrie, F. (2007). A functionally specialized population of mucosal CD103+ DCs induces Foxp3+ regulatory T cells via a TGF-beta and retinoic acid-dependent mechanism. The Journal of experimental medicine *204*, 1757-1764.
Coquet, J.M., Chakravarti, S., Smyth, M.J., and Godfrey, D.I. (2008). Cutting edge: IL-21 is not essential for Th17 differentiation or experimental autoimmune encephalomyelitis. J Immunol *180*, 7097-7101.

Croxford, A.L., Kurschus, F.C., and Waisman, A. (2009). Cutting edge: an IL-17F-CreEYFP reporter mouse allows fate mapping of Th17 cells. J Immunol *182*, 1237-1241.
Cua, D.J., Sherlock, J., Chen, Y., Murphy, C.A., Joyce, B., Seymour, B., Lucian, L., To, W., Kwan, S., Churakova, T.*, et al.* (2003). Interleukin-23 rather than interleukin-12 is the critical cytokine for autoimmune inflammation of the brain. Nature *421*, 744-748.
De Blasi, A., Parruti, G., and Sallese, M. (1995). Regulation of G protein-coupled receptor kinase subtypes in activated T lymphocytes. Selective increase of beta-adrenergic receptor kinase 1 and 2. The Journal of clinical investigation *95*, 203-210.
Demetri, G.D., and Griffin, J.D. (1991). Granulocyte colony-stimulating factor and its receptor. Blood *78*, 2791-2808.
Denkers, E.Y., Butcher, B.A., Del Rio, L., and Bennouna, S. (2004). Neutrophils, dendritic cells and Toxoplasma. International journal for parasitology *34*, 411-421.
Desvignes, C., Esteves, F., Etchart, N., Bella, C., Czerkinsky, C., and Kaiserlian, D. (1998). The murine buccal mucosa is an inductive site for priming class I-restricted CD8+ effector T cells in vivo. Clinical and experimental immunology *113*, 386-393.
Di Cesare, A., Di Meglio, P., and Nestle, F.O. (2009). The IL-23/Th17 axis in the immunopathogenesis of psoriasis. The Journal of investigative dermatology *129*, 1339-1350.
Dilulio, N.A., Engeman, T., Armstrong, D., Tannenbaum, C., Hamilton, T.A., and Fairchild, R.L. (1999). Groalpha-mediated recruitment of neutrophils is required for elicitation of contact hypersensitivity. European journal of immunology *29*, 3485-3495.
Dong, C. (2008). TH17 cells in development: an updated view of their molecular identity and genetic programming. Nature reviews *8*, 337-348.
Dutt, S., Ermann, J., Tseng, D., Liu, Y.P., George, T.I., Fathman, C.G., and Strober, S. (2005). L-selectin and beta7 integrin on donor CD4 T cells are required for the early migration to host mesenteric lymph nodes and acute colitis of graft-versus-host disease. Blood *106*, 4009-4015.
Eberl, G., and Littman, D.R. (2003). The role of the nuclear hormone receptor RORgammat in the development of lymph nodes and Peyer's patches. Immunological reviews *195*, 81-90.
Eijkelkamp, N., Heijnen, C.J., Lucas, A., Premont, R.T., Elsenbruch, S., Schedlowski, M., and Kavelaars, A. (2007a). G protein-coupled receptor kinase 6 controls chronicity and severity of dextran sodium sulphate-induced colitis in mice. Gut *56*, 847-854.
Eijkelkamp, N., Kavelaars, A., Elsenbruch, S., Schedlowski, M., Holtmann, G., and Heijnen, C.J. (2007b). Increased visceral sensitivity to capsaicin after DSS-induced colitis in mice: spinal cord c-Fos expression and behavior. American journal of physiology *293*, G749-757.
Fenner, J.E., Starr, R., Cornish, A.L., Zhang, J.G., Metcalf, D., Schreiber, R.D., Sheehan, K., Hilton, D.J., Alexander, W.S., and Hertzog, P.J. (2006). Suppressor of cytokine signaling 1 regulates the immune response to infection by a unique inhibition of type I interferon activity. Nature immunology *7*, 33-39.
Ferguson, S.S. (2001). Evolving concepts in G protein-coupled receptor endocytosis: the role in receptor desensitization and signaling. Pharmacological reviews *53*, 1-24.
Ferretti, S., Bonneau, O., Dubois, G.R., Jones, C.E., and Trifilieff, A. (2003). IL-17, produced by lymphocytes and neutrophils, is necessary for lipopolysaccharide-induced airway neutrophilia: IL-15 as a possible trigger. J Immunol *170*, 2106-2112.
Flugel, A., Berkowicz, T., Ritter, T., Labeur, M., Jenne, D.E., Li, Z., Ellwart, J.W., Willem, M., Lassmann, H., and Wekerle, H. (2001). Migratory activity and functional

changes of green fluorescent effector cells before and during experimental autoimmune encephalomyelitis. Immunity *14*, 547-560.
Fontenot, J.D., Rasmussen, J.P., Williams, L.M., Dooley, J.L., Farr, A.G., and Rudensky, A.Y. (2005). Regulatory T cell lineage specification by the forkhead transcription factor foxp3. Immunity *22*, 329-341.
Fujino, S., Andoh, A., Bamba, S., Ogawa, A., Hata, K., Araki, Y., Bamba, T., and Fujiyama, Y. (2003). Increased expression of interleukin 17 in inflammatory bowel disease. Gut *52*, 65-70.
Gatto, D., Paus, D., Basten, A., Mackay, C.R., and Brink, R. (2009). Guidance of B cells by the orphan G protein-coupled receptor EBI2 shapes humoral immune responses. Immunity *31*, 259-269.
Gavin, M.A., Rasmussen, J.P., Fontenot, J.D., Vasta, V., Manganiello, V.C., Beavo, J.A., and Rudensky, A.Y. (2007). Foxp3-dependent programme of regulatory T-cell differentiation. Nature *445*, 771-775.
Gyulveszi, G., Haak, S., and Becher, B. (2009). IL-23-driven encephalo-tropism and Th17 polarization during CNS-inflammation in vivo. European journal of immunology *39*, 1864-1869.
Haak, S., Croxford, A.L., Kreymborg, K., Heppner, F.L., Pouly, S., Becher, B., and Waisman, A. (2009). IL-17A and IL-17F do not contribute vitally to autoimmune neuro-inflammation in mice. The Journal of clinical investigation *119*, 61-69.
Happel, K.I., Zheng, M., Young, E., Quinton, L.J., Lockhart, E., Ramsay, A.J., Shellito, J.E., Schurr, J.R., Bagby, G.J., Nelson, S., and Kolls, J.K. (2003). Cutting edge: roles of Toll-like receptor 4 and IL-23 in IL-17 expression in response to Klebsiella pneumoniae infection. J Immunol *170*, 4432-4436.
Harper, E.G., Guo, C., Rizzo, H., Lillis, J.V., Kurtz, S.E., Skorcheva, I., Purdy, D., Fitch, E., Iordanov, M., and Blauvelt, A. (2009). Th17 cytokines stimulate CCL20 expression in keratinocytes in vitro and in vivo: implications for psoriasis pathogenesis. The Journal of investigative dermatology *129*, 2175-2183.
Harrington, L.E., Hatton, R.D., Mangan, P.R., Turner, H., Murphy, T.L., Murphy, K.M., and Weaver, C.T. (2005). Interleukin 17-producing CD4+ effector T cells develop via a lineage distinct from the T helper type 1 and 2 lineages. Nature immunology *6*, 1123-1132.
Hasle, H., Olesen, G., Kerndrup, G., Philip, P., and Jacobsen, N. (1996). Chronic neutrophil leukaemia in adolescence and young adulthood. British journal of haematology *94*, 628-630.
Haudenschild, D., Moseley, T., Rose, L., and Reddi, A.H. (2002). Soluble and transmembrane isoforms of novel interleukin-17 receptor-like protein by RNA splicing and expression in prostate cancer. The Journal of biological chemistry *277*, 4309-4316.
Hirano, T., Yasukawa, K., Harada, H., Taga, T., Watanabe, Y., Matsuda, T., Kashiwamura, S., Nakajima, K., Koyama, K., Iwamatsu, A., and et al. (1986). Complementary DNA for a novel human interleukin (BSF-2) that induces B lymphocytes to produce immunoglobulin. Nature *324*, 73-76.
Hofstetter, H.H., Ibrahim, S.M., Koczan, D., Kruse, N., Weishaupt, A., Toyka, K.V., and Gold, R. (2005). Therapeutic efficacy of IL-17 neutralization in murine experimental autoimmune encephalomyelitis. Cellular immunology *237*, 123-130.
Horwitz, B.H., Mizgerd, J.P., Scott, M.L., and Doerschuk, C.M. (2001). Mechanisms of granulocytosis in the absence of CD18. Blood *97*, 1578-1583.
Hu, X., Ho, H.H., Lou, O., Hidaka, C., and Ivashkiv, L.B. (2005). Homeostatic role of interferons conferred by inhibition of IL-1-mediated inflammation and tissue destruction. J Immunol *175*, 131-138.

Inoue, H., Nojima, H., and Okayama, H. (1990). High efficiency transformation of Escherichia coli with plasmids. Gene *96*, 23-28.
Ivanov, II, McKenzie, B.S., Zhou, L., Tadokoro, C.E., Lepelley, A., Lafaille, J.J., Cua, D.J., and Littman, D.R. (2006). The orphan nuclear receptor RORgammat directs the differentiation program of proinflammatory IL-17+ T helper cells. Cell *126*, 1121-1133.
Ivanov, II, Zhou, L., and Littman, D.R. (2007a). Transcriptional regulation of Th17 cell differentiation. Seminars in immunology *19*, 409-417.
Ivanov, S., Bozinovski, S., Bossios, A., Valadi, H., Vlahos, R., Malmhall, C., Sjostrand, M., Kolls, J.K., Anderson, G.P., and Linden, A. (2007b). Functional relevance of the IL-23-IL-17 axis in lungs in vivo. American journal of respiratory cell and molecular biology *36*, 442-451.
Iwakura, Y., Nakae, S., Saijo, S., and Ishigame, H. (2008). The roles of IL-17A in inflammatory immune responses and host defense against pathogens. Immunological reviews *226*, 57-79.
Jetten, A.M. (2004). Recent advances in the mechanisms of action and physiological functions of the retinoid-related orphan receptors (RORs). Curr Drug Targets Inflamm Allergy *3*, 395-412.
Johnson, J.L., Moore, E.E., Tamura, D.Y., Zallen, G., Biffl, W.L., and Silliman, C.C. (1998). Interleukin-6 augments neutrophil cytotoxic potential via selective enhancement of elastase release. The Journal of surgical research *76*, 91-94.
Kamanaka, M., Kim, S.T., Wan, Y.Y., Sutterwala, F.S., Lara-Tejero, M., Galan, J.E., Harhaj, E., and Flavell, R.A. (2006). Expression of interleukin-10 in intestinal lymphocytes detected by an interleukin-10 reporter knockin tiger mouse. Immunity *25*, 941-952.
Kamimura, D., Ishihara, K., and Hirano, T. (2003). IL-6 signal transduction and its physiological roles: the signal orchestration model. Reviews of physiology, biochemistry and pharmacology *149*, 1-38.
Kehren, J., Desvignes, C., Krasteva, M., Ducluzeau, M.T., Assossou, O., Horand, F., Hahne, M., Kagi, D., Kaiserlian, D., and Nicolas, J.F. (1999). Cytotoxicity is mandatory for CD8(+) T cell-mediated contact hypersensitivity. The Journal of experimental medicine *189*, 779-786.
Kim, J.M., Rasmussen, J.P., and Rudensky, A.Y. (2007). Regulatory T cells prevent catastrophic autoimmunity throughout the lifespan of mice. Nature immunology *8*, 191-197.
Kivisakk, P., Imitola, J., Rasmussen, S., Elyaman, W., Zhu, B., Ransohoff, R.M., and Khoury, S.J. (2009). Localizing central nervous system immune surveillance: meningeal antigen-presenting cells activate T cells during experimental autoimmune encephalomyelitis. Ann Neurol *65*, 457-469.
Knoechel, B., Lohr, J., Kahn, E., Bluestone, J.A., and Abbas, A.K. (2005). Sequential development of interleukin 2-dependent effector and regulatory T cells in response to endogenous systemic antigen. The Journal of experimental medicine *202*, 1375-1386.
Kolls, J.K., Kanaly, S.T., and Ramsay, A.J. (2003). Interleukin-17: an emerging role in lung inflammation. American journal of respiratory cell and molecular biology *28*, 9-11.
Kolls, J.K., and Linden, A. (2004). Interleukin-17 family members and inflammation. Immunity *21*, 467-476.
Komiyama, Y., Nakae, S., Matsuki, T., Nambu, A., Ishigame, H., Kakuta, S., Sudo, K., and Iwakura, Y. (2006). IL-17 plays an important role in the development of experimental autoimmune encephalomyelitis. J Immunol *177*, 566-573.

Korn, T., Bettelli, E., Gao, W., Awasthi, A., Jager, A., Strom, T.B., Oukka, M., and Kuchroo, V.K. (2007a). IL-21 initiates an alternative pathway to induce proinflammatory T(H)17 cells. Nature *448*, 484-487.
Korn, T., Mitsdoerffer, M., Croxford, A.L., Awasthi, A., Dardalhon, V.A., Galileos, G., Vollmar, P., Stritesky, G.L., Kaplan, M.H., Waisman, A.*, et al.* (2008). IL-6 controls Th17 immunity in vivo by inhibiting the conversion of conventional T cells into Foxp3+ regulatory T cells. Proceedings of the National Academy of Sciences of the United States of America *105*, 18460-18465.
Korn, T., Oukka, M., Kuchroo, V., and Bettelli, E. (2007b). Th17 cells: effector T cells with inflammatory properties. Seminars in immunology *19*, 362-371.
Kuestner, R.E., Taft, D.W., Haran, A., Brandt, C.S., Brender, T., Lum, K., Harder, B., Okada, S., Ostrander, C.D., Kreindler, J.L.*, et al.* (2007). Identification of the IL-17 receptor related molecule IL-17RC as the receptor for IL-17F. J Immunol *179*, 5462-5473.
Lahl, K., Loddenkemper, C., Drouin, C., Freyer, J., Arnason, J., Eberl, G., Hamann, A., Wagner, H., Huehn, J., and Sparwasser, T. (2007). Selective depletion of Foxp3+ regulatory T cells induces a scurfy-like disease. The Journal of experimental medicine *204*, 57-63.
Langrish, C.L., Chen, Y., Blumenschein, W.M., Mattson, J., Basham, B., Sedgwick, J.D., McClanahan, T., Kastelein, R.A., and Cua, D.J. (2005). IL-23 drives a pathogenic T cell population that induces autoimmune inflammation. The Journal of experimental medicine *201*, 233-240.
Lee, Y.K., Turner, H., Maynard, C.L., Oliver, J.R., Chen, D., Elson, C.O., and Weaver, C.T. (2009). Late developmental plasticity in the T helper 17 lineage. Immunity *30*, 92-107.
Lexberg, M.H., Taubner, A., Forster, A., Albrecht, I., Richter, A., Kamradt, T., Radbruch, A., and Chang, H.D. (2008). Th memory for interleukin-17 expression is stable in vivo. European journal of immunology *38*, 2654-2664.
lexSanger, F., Air, G.M., Barrell, B.G., Brown, N.L., Coulson, A.R., Fiddes, C.A., Hutchison, C.A., Slocombe, P.M., and Smith, M. (1977). Nucleotide sequence of bacteriophage phi X174 DNA. Nature *265*, 687-695.
Li, W., Carper, K., Zheng, X.X., Kuhr, C.S., Reyes, J.D., Liang, Y., Perkins, D.L., Thomson, A.W., and Perkins, J.D. (2006). The role of Foxp3+ regulatory T cells in liver transplant tolerance. Transplantation proceedings *38*, 3205-3206.
Lock, C., Hermans, G., Pedotti, R., Brendolan, A., Schadt, E., Garren, H., Langer-Gould, A., Strober, S., Cannella, B., Allard, J.*, et al.* (2002). Gene-microarray analysis of multiple sclerosis lesions yields new targets validated in autoimmune encephalomyelitis. Nature medicine *8*, 500-508.
Lombardi, M.S., Kavelaars, A., and Heijnen, C.J. (2002). Role and modulation of G protein-coupled receptor signaling in inflammatory processes. Critical reviews in immunology *22*, 141-163.
Lombardi, M.S., Kavelaars, A., Schedlowski, M., Bijlsma, J.W., Okihara, K.L., Van de Pol, M., Ochsmann, S., Pawlak, C., Schmidt, R.E., and Heijnen, C.J. (1999). Decreased expression and activity of G-protein-coupled receptor kinases in peripheral blood mononuclear cells of patients with rheumatoid arthritis. Faseb J *13*, 715-725.
Luche, H., Weber, O., Nageswara Rao, T., Blum, C., and Fehling, H.J. (2007). Faithful activation of an extra-bright red fluorescent protein in "knock-in" Cre-reporter mice ideally suited for lineage tracing studies. European journal of immunology *37*, 43-53.
Manel, N., Unutmaz, D., and Littman, D.R. (2008). The differentiation of human T(H)-17 cells requires transforming growth factor-beta and induction of the nuclear receptor RORgammat. Nature immunology *9*, 641-649.

Mangan, P.R., Harrington, L.E., O'Quinn, D.B., Helms, W.S., Bullard, D.C., Elson, C.O., Hatton, R.D., Wahl, S.M., Schoeb, T.R., and Weaver, C.T. (2006). Transforming growth factor-beta induces development of the T(H)17 lineage. Nature *441*, 231-234.
Martin, C., Burdon, P.C., Bridger, G., Gutierrez-Ramos, J.C., Williams, T.J., and Rankin, S.M. (2003). Chemokines acting via CXCR2 and CXCR4 control the release of neutrophils from the bone marrow and their return following senescence. Immunity *19*, 583-593.
Mayer, K.D., Mohrs, K., Crowe, S.R., Johnson, L.L., Rhyne, P., Woodland, D.L., and Mohrs, M. (2005). The functional heterogeneity of type 1 effector T cells in response to infection is related to the potential for IFN-gamma production. J Immunol *174*, 7732-7739.
McGeachy, M.J., Bak-Jensen, K.S., Chen, Y., Tato, C.M., Blumenschein, W., McClanahan, T., and Cua, D.J. (2007). TGF-beta and IL-6 drive the production of IL-17 and IL-10 by T cells and restrain T(H)-17 cell-mediated pathology. Nature immunology *8*, 1390-1397.
McGeachy, M.J., Chen, Y., Tato, C.M., Laurence, A., Joyce-Shaikh, B., Blumenschein, W.M., McClanahan, T.K., O'Shea, J.J., and Cua, D.J. (2009). The interleukin 23 receptor is essential for the terminal differentiation of interleukin 17-producing effector T helper cells in vivo. Nature immunology *10*, 314-324.
McGeachy, M.J., and Cua, D.J. (2007). The link between IL-23 and Th17 cell-mediated immune pathologies. Seminars in immunology *19*, 372-376.
Megiovanni, A.M., Sanchez, F., Robledo-Sarmiento, M., Morel, C., Gluckman, J.C., and Boudaly, S. (2006). Polymorphonuclear neutrophils deliver activation signals and antigenic molecules to dendritic cells: a new link between leukocytes upstream of T lymphocytes. Journal of leukocyte biology *79*, 977-988.
Miltenyi, S., Muller, W., Weichel, W., and Radbruch, A. (1990). High gradient magnetic cell separation with MACS. Cytometry *11*, 231-238.
Miyamoto, M., Prause, O., Sjostrand, M., Laan, M., Lotvall, J., and Linden, A. (2003). Endogenous IL-17 as a mediator of neutrophil recruitment caused by endotoxin exposure in mouse airways. J Immunol *170*, 4665-4672.
Mohrs, K., Harris, D.P., Lund, F.E., and Mohrs, M. (2005). Systemic dissemination and persistence of Th2 and type 2 cells in response to infection with a strictly enteric nematode parasite. J Immunol *175*, 5306-5313.
Mosmann, T.R., Cherwinski, H., Bond, M.W., Giedlin, M.A., and Coffman, R.L. (1986). Two types of murine helper T cell clone. I. Definition according to profiles of lymphokine activities and secreted proteins. J Immunol *136*, 2348-2357.
Mucida, D., and Cheroutre, H. (2007). TGFbeta and retinoic acid intersect in immune-regulation. Cell adhesion & migration *1*, 142-144.
Mucida, D., Park, Y., Kim, G., Turovskaya, O., Scott, I., Kronenberg, M., and Cheroutre, H. (2007). Reciprocal TH17 and regulatory T cell differentiation mediated by retinoic acid. Science (New York, N.Y *317*, 256-260.
Mullis, K.B., and Faloona, F.A. (1987). Specific synthesis of DNA in vitro via a polymerase-catalyzed chain reaction. Methods in enzymology *155*, 335-350.
Murphy, C.A., Langrish, C.L., Chen, Y., Blumenschein, W., McClanahan, T., Kastelein, R.A., Sedgwick, J.D., and Cua, D.J. (2003). Divergent pro- and antiinflammatory roles for IL-23 and IL-12 in joint autoimmune inflammation. The Journal of experimental medicine *198*, 1951-1957.
Nakae, S., Komiyama, Y., Nambu, A., Sudo, K., Iwase, M., Homma, I., Sekikawa, K., Asano, M., and Iwakura, Y. (2002). Antigen-specific T cell sensitization is impaired in IL-17-deficient mice, causing suppression of allergic cellular and humoral responses. Immunity *17*, 375-387.

Nathan, C. (2006). Neutrophils and immunity: challenges and opportunities. Nature reviews *6*, 173-182.
Nau, K.C., and Lewis, W.D. (2008). Multiple myeloma: diagnosis and treatment. American family physician *78*, 853-859.
Nurieva, R., Yang, X.O., Martinez, G., Zhang, Y., Panopoulos, A.D., Ma, L., Schluns, K., Tian, Q., Watowich, S.S., Jetten, A.M., and Dong, C. (2007). Essential autocrine regulation by IL-21 in the generation of inflammatory T cells. Nature *448*, 480-483.
O'Connor, W., Jr., Kamanaka, M., Booth, C.J., Town, T., Nakae, S., Iwakura, Y., Kolls, J.K., and Flavell, R.A. (2009). A protective function for interleukin 17A in T cell-mediated intestinal inflammation. Nature immunology *10*, 603-609.
Okada, T., and Cyster, J.G. (2007). CC chemokine receptor 7 contributes to Gi-dependent T cell motility in the lymph node. J Immunol *178*, 2973-2978.
Ono, M., Yaguchi, H., Ohkura, N., Kitabayashi, I., Nagamura, Y., Nomura, T., Miyachi, Y., Tsukada, T., and Sakaguchi, S. (2007). Foxp3 controls regulatory T-cell function by interacting with AML1/Runx1. Nature *446*, 685-689.
Park, H., Li, Z., Yang, X.O., Chang, S.H., Nurieva, R., Wang, Y.H., Wang, Y., Hood, L., Zhu, Z., Tian, Q., and Dong, C. (2005). A distinct lineage of CD4 T cells regulates tissue inflammation by producing interleukin 17. Nature immunology *6*, 1133-1141.
Pereira, J.P., Kelly, L.M., Xu, Y., and Cyster, J.G. (2009). EBI2 mediates B cell segregation between the outer and centre follicle. Nature *460*, 1122-1126.
Pesce, J.T., Liu, Z., Hamed, H., Alem, F., Whitmire, J., Lin, H., Liu, Q., Urban, J.F., Jr., and Gause, W.C. (2008). Neutrophils clear bacteria associated with parasitic nematodes augmenting the development of an effective Th2-type response. J Immunol *180*, 464-474.
Ramos, C.D., Canetti, C., Souto, J.T., Silva, J.S., Hogaboam, C.M., Ferreira, S.H., and Cunha, F.Q. (2005). MIP-1alpha[CCL3] acting on the CCR1 receptor mediates neutrophil migration in immune inflammation via sequential release of TNF-alpha and LTB4. Journal of leukocyte biology *78*, 167-177.
Ransohoff, R.M., Kivisakk, P., and Kidd, G. (2003). Three or more routes for leukocyte migration into the central nervous system. Nature reviews *3*, 569-581.
Reboldi, A., Coisne, C., Baumjohann, D., Benvenuto, F., Bottinelli, D., Lira, S., Uccelli, A., Lanzavecchia, A., Engelhardt, B., and Sallusto, F. (2009). C-C chemokine receptor 6-regulated entry of TH-17 cells into the CNS through the choroid plexus is required for the initiation of EAE. Nature immunology *10*, 514-523.
Rohn, T.A., Jennings, G.T., Hernandez, M., Grest, P., Beck, M., Zou, Y., Kopf, M., and Bachmann, M.F. (2006). Vaccination against IL-17 suppresses autoimmune arthritis and encephalomyelitis. European journal of immunology *36*, 2857-2867.
Rosenkilde, M.M., Smit, M.J., and Waldhoer, M. (2008). Structure, function and physiological consequences of virally encoded chemokine seven transmembrane receptors. British journal of pharmacology *153 Suppl 1*, S154-166.
Rouvier, E., Luciani, M.F., Mattei, M.G., Denizot, F., and Golstein, P. (1993). CTLA-8, cloned from an activated T cell, bearing AU-rich messenger RNA instability sequences, and homologous to a herpesvirus saimiri gene. J Immunol *150*, 5445-5456.
Ruddy, M.J., Shen, F., Smith, J.B., Sharma, A., and Gaffen, S.L. (2004). Interleukin-17 regulates expression of the CXC chemokine LIX/CXCL5 in osteoblasts: implications for inflammation and neutrophil recruitment. Journal of leukocyte biology *76*, 135-144.
Sambrook, J. (1989). Molecular cloning. A laboratory manual, (2nd edition).
Scapini, P., Lapinet-Vera, J.A., Gasperini, S., Calzetti, F., Bazzoni, F., and Cassatella, M.A. (2000). The neutrophil as a cellular source of chemokines. Immunological reviews *177*, 195-203.

Schwenk, F., Baron, U., and Rajewsky, K. (1995). A cre-transgenic mouse strain for the ubiquitous deletion of loxP-flanked gene segments including deletion in germ cells. Nucleic acids research *23*, 5080-5081.
Segal, B.M., Constantinescu, C.S., Raychaudhuri, A., Kim, L., Fidelus-Gort, R., and Kasper, L.H. (2008). Repeated subcutaneous injections of IL12/23 p40 neutralising antibody, ustekinumab, in patients with relapsing-remitting multiple sclerosis: a phase II, double-blind, placebo-controlled, randomised, dose-ranging study. Lancet neurology *7*, 796-804.
Serada, S., Fujimoto, M., Mihara, M., Koike, N., Ohsugi, Y., Nomura, S., Yoshida, H., Nishikawa, T., Terabe, F., Ohkawara, T.*, et al.* (2008a). IL-6 blockade inhibits the induction of myelin antigen-specific Th17 cells and Th1 cells in experimental autoimmune encephalomyelitis. Proc Natl Acad Sci U S A.
Serada, S., Fujimoto, M., Mihara, M., Koike, N., Ohsugi, Y., Nomura, S., Yoshida, H., Nishikawa, T., Terabe, F., Ohkawara, T.*, et al.* (2008b). IL-6 blockade inhibits the induction of myelin antigen-specific Th17 cells and Th1 cells in experimental autoimmune encephalomyelitis. Proceedings of the National Academy of Sciences of the United States of America *105*, 9041-9046.
Shalom-Barak, T., Quach, J., and Lotz, M. (1998). Interleukin-17-induced gene expression in articular chondrocytes is associated with activation of mitogen-activated protein kinases and NF-kappaB. The Journal of biological chemistry *273*, 27467-27473.
Sonderegger, I., Kisielow, J., Meier, R., King, C., and Kopf, M. (2008). IL-21 and IL-21R are not required for development of Th17 cells and autoimmunity in vivo. Eur J Immunol.
Spolski, R., and Leonard, W.J. (2008). Interleukin-21: basic biology and implications for cancer and autoimmunity *. Annu Rev Immunol *26*, 57-79.
Srinivas, S., Watanabe, T., Lin, C.S., William, C.M., Tanabe, Y., Jessell, T.M., and Costantini, F. (2001). Cre reporter strains produced by targeted insertion of EYFP and ECFP into the ROSA26 locus. BMC developmental biology *1*, 4.
Taga, T., Hibi, M., Hirata, Y., Yamasaki, K., Yasukawa, K., Matsuda, T., Hirano, T., and Kishimoto, T. (1989). Interleukin-6 triggers the association of its receptor with a possible signal transducer, gp130. Cell *58*, 573-581.
Thakker, P., Leach, M.W., Kuang, W., Benoit, S.E., Leonard, J.P., and Marusic, S. (2007). IL-23 is critical in the induction but not in the effector phase of experimental autoimmune encephalomyelitis. J Immunol *178*, 2589-2598.
Toy, D., Kugler, D., Wolfson, M., Vanden Bos, T., Gurgel, J., Derry, J., Tocker, J., and Peschon, J. (2006). Cutting edge: interleukin 17 signals through a heteromeric receptor complex. J Immunol *177*, 36-39.
Tvinnereim, A.R., Hamilton, S.E., and Harty, J.T. (2004). Neutrophil involvement in cross-priming CD8+ T cell responses to bacterial antigens. J Immunol *173*, 1994-2002.
Tzartos, J.S., Friese, M.A., Craner, M.J., Palace, J., Newcombe, J., Esiri, M.M., and Fugger, L. (2008). Interleukin-17 production in central nervous system-infiltrating T cells and glial cells is associated with active disease in multiple sclerosis. The American journal of pathology *172*, 146-155.
van der Fits, L., Mourits, S., Voerman, J.S., Kant, M., Boon, L., Laman, J.D., Cornelissen, F., Mus, A.M., Florencia, E., Prens, E.P., and Lubberts, E. (2009). Imiquimod-induced psoriasis-like skin inflammation in mice is mediated via the IL-23/IL-17 axis. J Immunol *182*, 5836-5845.
Vasioukhin, V., Degenstein, L., Wise, B., and Fuchs, E. (1999). The magical touch: genome targeting in epidermal stem cells induced by tamoxifen application to mouse

skin. Proceedings of the National Academy of Sciences of the United States of America *96*, 8551-8556.
Veldhoen, M., Hocking, R.J., Atkins, C.J., Locksley, R.M., and Stockinger, B. (2006). TGFbeta in the context of an inflammatory cytokine milieu supports de novo differentiation of IL-17-producing T cells. Immunity *24*, 179-189.
Voo, K.S., Wang, Y.H., Santori, F.R., Boggiano, C., Wang, Y.H., Arima, K., Bover, L., Hanabuchi, S., Khalili, J., Marinova, E.*, et al.* (2009). Identification of IL-17-producing FOXP3+ regulatory T cells in humans. Proceedings of the National Academy of Sciences of the United States of America *106*, 4793-4798.
Vroon, A., Kavelaars, A., Limmroth, V., Lombardi, M.S., Goebel, M.U., Van Dam, A.M., Caron, M.G., Schedlowski, M., and Heijnen, C.J. (2005). G protein-coupled receptor kinase 2 in multiple sclerosis and experimental autoimmune encephalomyelitis. J Immunol *174*, 4400-4406.
Wagner, N., Lohler, J., Tedder, T.F., Rajewsky, K., Muller, W., and Steeber, D.A. (1998). L-selectin and beta7 integrin synergistically mediate lymphocyte migration to mesenteric lymph nodes. European journal of immunology *28*, 3832-3839.
Wang, J., Lin, W., Popko, B., and Campbell, I.L. (2004). Inducible production of interferon-gamma in the developing brain causes cerebellar dysplasia with activation of the Sonic hedgehog pathway. Molecular and cellular neurosciences *27*, 489-496.
Watanabe, H., Kawaguchi, M., Fujishima, S., Ogura, M., Matsukura, S., Takeuchi, H., Ohba, M., Sueki, H., Kokubu, F., Hizawa, N.*, et al.* (2009). Functional characterization of IL-17F as a selective neutrophil attractant in psoriasis. The Journal of investigative dermatology *129*, 650-656.
Weaver, C.T., Hatton, R.D., Mangan, P.R., and Harrington, L.E. (2007). IL-17 family cytokines and the expanding diversity of effector T cell lineages. Annual review of immunology *25*, 821-852.
Weaver, C.T., and Murphy, K.M. (2007). The central role of the Th17 lineage in regulating the inflammatory/autoimmune axis. Seminars in immunology *19*, 351-352.
Wolf, S.D., Dittel, B.N., Hardardottir, F., and Janeway, C.A., Jr. (1996). Experimental autoimmune encephalomyelitis induction in genetically B cell-deficient mice. The Journal of experimental medicine *184*, 2271-2278.
Wright, J.F., Bennett, F., Li, B., Brooks, J., Luxenberg, D.P., Whitters, M.J., Tomkinson, K.N., Fitz, L.J., Wolfman, N.M., Collins, M.*, et al.* (2008). The human IL-17F/IL-17A heterodimeric cytokine signals through the IL-17RA/IL-17RC receptor complex. J Immunol *181*, 2799-2805.
Wright, J.F., Guo, Y., Quazi, A., Luxenberg, D.P., Bennett, F., Ross, J.F., Qiu, Y., Whitters, M.J., Tomkinson, K.N., Dunussi-Joannopoulos, K.*, et al.* (2007). Identification of an interleukin 17F/17A heterodimer in activated human CD4+ T cells. The Journal of biological chemistry *282*, 13447-13455.
Yang, L., Anderson, D.E., Baecher-Allan, C., Hastings, W.D., Bettelli, E., Oukka, M., Kuchroo, V.K., and Hafler, D.A. (2008a). IL-21 and TGF-beta are required for differentiation of human T(H)17 cells. Nature *454*, 350-352.
Yang, X.O., Nurieva, R., Martinez, G.J., Kang, H.S., Chung, Y., Pappu, B.P., Shah, B., Chang, S.H., Schluns, K.S., Watowich, S.S.*, et al.* (2008b). Molecular antagonism and plasticity of regulatory and inflammatory T cell programs. Immunity *29*, 44-56.
Yang, X.O., Nurieva, R., Martinez, G.J., Kang, H.S., Chung, Y., Pappu, B.P., Shah, B., Chang, S.H., Schluns, K.S., Watowich, S.S.*, et al.* (2008c). Molecular Antagonism and Plasticity of Regulatory and Inflammatory T Cell Programs. Immunity.
Yang, X.O., Panopoulos, A.D., Nurieva, R., Chang, S.H., Wang, D., Watowich, S.S., and Dong, C. (2007). STAT3 regulates cytokine-mediated generation of inflammatory helper T cells. The Journal of biological chemistry *282*, 9358-9363.

Yang, X.O., Pappu, B.P., Nurieva, R., Akimzhanov, A., Kang, H.S., Chung, Y., Ma, L., Shah, B., Panopoulos, A.D., Schluns, K.S*., et al.* (2008d). T helper 17 lineage differentiation is programmed by orphan nuclear receptors ROR alpha and ROR gamma. Immunity *28*, 29-39.
Yang, Y., Weiner, J., Liu, Y., Smith, A.J., Huss, D.J., Winger, R., Peng, H., Cravens, P.D., Racke, M.K., and Lovett-Racke, A.E. (2009). T-bet is essential for encephalitogenicity of both Th1 and Th17 cells. The Journal of experimental medicine *206*, 1549-1564.
Yao, Z., Fanslow, W.C., Seldin, M.F., Rousseau, A.M., Painter, S.L., Comeau, M.R., Cohen, J.I., and Spriggs, M.K. (1995). Herpesvirus Saimiri encodes a new cytokine, IL-17, which binds to a novel cytokine receptor. Immunity *3*, 811-821.
Ye, P., Garvey, P.B., Zhang, P., Nelson, S., Bagby, G., Summer, W.R., Schwarzenberger, P., Shellito, J.E., and Kolls, J.K. (2001a). Interleukin-17 and lung host defense against Klebsiella pneumoniae infection. American journal of respiratory cell and molecular biology *25*, 335-340.
Ye, P., Rodriguez, F.H., Kanaly, S., Stocking, K.L., Schurr, J., Schwarzenberger, P., Oliver, P., Huang, W., Zhang, P., Zhang, J*., et al.* (2001b). Requirement of interleukin 17 receptor signaling for lung CXC chemokine and granulocyte colony-stimulating factor expression, neutrophil recruitment, and host defense. The Journal of experimental medicine *194*, 519-527.
Yoshida, K., Taga, T., Saito, M., Suematsu, S., Kumanogoh, A., Tanaka, T., Fujiwara, H., Hirata, M., Yamagami, T., Nakahata, T*., et al.* (1996). Targeted disruption of gp130, a common signal transducer for the interleukin 6 family of cytokines, leads to myocardial and hematological disorders. Proceedings of the National Academy of Sciences of the United States of America *93*, 407-411.
Yoshimura, T., Sonoda, K.H., Miyazaki, Y., Iwakura, Y., Ishibashi, T., Yoshimura, A., and Yoshida, H. (2008). Differential roles for IFN-gamma and IL-17 in experimental autoimmune uveoretinitis. International immunology *20*, 209-214.
Zheng, Y., Chaudhry, A., Kas, A., deRoos, P., Kim, J.M., Chu, T.T., Corcoran, L., Treuting, P., Klein, U., and Rudensky, A.Y. (2009). Regulatory T-cell suppressor program co-opts transcription factor IRF4 to control T(H)2 responses. Nature *458*, 351-356.
Zhou, L., Chong, M.M., and Littman, D.R. (2009). Plasticity of CD4+ T cell lineage differentiation. Immunity *30*, 646-655.
Zhou, L., Ivanov, II, Spolski, R., Min, R., Shenderov, K., Egawa, T., Levy, D.E., Leonard, W.J., and Littman, D.R. (2007). IL-6 programs T(H)-17 cell differentiation by promoting sequential engagement of the IL-21 and IL-23 pathways. Nature immunology *8*, 967-974.
Zhou, L., Lopes, J.E., Chong, M.M., Ivanov, II, Min, R., Victora, G.D., Shen, Y., Du, J., Rubtsov, Y.P., Rudensky, A.Y*., et al.* (2008). TGF-beta-induced Foxp3 inhibits T(H)17 cell differentiation by antagonizing RORgammat function. Nature *453*, 236-240.

9 Versicherung

Ich versichere, daß ich die von mir vorgelegte Dissertation selbständig angefertigt, die benutzten Quellen und Hilfsmittel vollständig angegeben und die Stellen der Arbeit - einschließlich Tabellen, Karten und Abbildungen -, die anderen Werken im Wortlaut oder dem Sinn nach entnommen sind, in jedem Einzelfall als Entlehnung kenntlich gemacht habe; daß diese Dissertation noch keiner anderen Fakultät oder Universität zur Prüfung vorgelegen hat; daß sie - abgesehen von unten angegebenen Teilpublikationen - noch nicht veröffentlicht worden ist sowie, daß ich eine solche Veröffentlichung vor Abschluß des Promotionsverfahrens nicht vornehmen werde. Die Bestimmungen dieser Promotionsordnung sind mir bekannt. Die von mir vorgelegte Dissertation ist von Prof. Dr. Ari Waisman betreut worden.

10 Lebenslauf

Persönliche Daten

Name	Andrew Lewis Croxford
Geburtsdatum	04.01.1981
Geburtsort	New York, USA
Adresse	Boppstr. 46 55118 Mainz croxfora@uni-mainz.de

Familienstand	ledig
Nationalität	Britisch

Schulische Ausbildung

1989- 1993	Blackthorns Primary School
1993- 1997	Oathall Community College
1997-1998	Haywards Heath College
1998-1999	Duff Miller College

Studium

2000-2004	BSc in Genetics with German, Victoria University of Manchester
2004-2005	MSc Immunology and Immunogenetics, Victoria University of Manchester

Promotion

Seit Januar 2006 „Novel Mouse Models for Use in IL-17A and Th17 Research“, am 1. Med Klinik und Polyklinik, University of Mainz.

Publications

Cellular Mechanisms of Interleukin-17-Induced Blood-Brain Barrier Disruption
Jula Huppert*, Dorothea Closhen*, Andrew Croxford*, Robin White, Paulina Kulig, Eweline Pietrowski, Ingo Bechmann, Burkhard Becher, Heiko J. Luhmann, Ari Waisman#, Christoph R. W. Kuhlmann#
FASEB. 2009 Nov 25 (Epub ahead of print)

Cutting edge: an IL-17F-Cre^{EYFP} reporter mouse allows fate mapping of Th17 cells.
Croxford AL, Kurschus FC, Waisman A.
J Immunol. 2009 Feb 1;182(3):1237-41.

IL-17A and IL-17F do not contribute vitally to autoimmune neuro-inflammation in mice.
Haak S*, Croxford AL*, Kreymborg K, Heppner FL, Pouly S, Becher B#, Waisman A#.
J Clin Invest. 2009 Jan;119(1):61-9. doi: 10.1172/JCI35997.

IL-6 controls Th17 immunity in vivo by inhibiting the conversion of conventional T cells into Foxp3+ regulatory T cells.
Korn T*, Mitsdoerffer M*, Croxford AL, Awasthi A, Dardalhon VA, Galileos G, Vollmar P, Stritesky GL, Kaplan MH, Waisman A, Kuchroo VK, Oukka M.
Proc Natl Acad Sci U S A. 2008 Nov 25;105(47):18460-5.

New tools to study the role of B cells in cytomegalovirus infections.
Waisman A, Croxford AL, Demircik F.
Med Microbiol Immunol. 2008 Jun;197(2):145-9. Review.

MHC-restricted T cell receptor signaling is required for alpha beta TCR replacement of the pre T cell receptor.
Croxford AL, Akilli-Ozturk O, Rieux-Laucat F, Förster I, Waisman A, Buch T.
Eur J Immunol. 2008 Feb;38(2):391-9

Five cases of de novo inflammatory bowel disease after orthotopic liver transplantation.
Wörns MA, Lohse AW, Neurath MF, Croxford AL, Otto G, Kreft A, Galle PR, Kanzler S.
Am J Gastroenterol. 2006 Aug;101(8):1931-7.

In Press

IL-23 receptor regulates unconventional IL-17-producing T cells that control early stages of infection

Lorena Riol-Blanco, Vanja Lazarevic, Amit Awasthi, Meike Mitsdoerffer, Andrew L. Croxford, Brian S Wilson, Ari Waisman|, Vijay K Kuchroo, Laurie H Glimcher, Mohamed
Oukka